REPORT DOCUMENTATION PAGE

Form Approved
OMB No. 0704-0188

1. REPORT DATE *(DD-MM-YYYY)*	2. REPORT TYPE	3. DATES COVERED *(From - To)*
24-05-2011	Journal Article	

4. TITLE AND SUBTITLE

Preparation and Characterization of the Binary Group 13 Azides $M(N_3)_3$ and $M(N_3)_3 \cdot CH_3CN$ (M=Ga, In, Tl), $[Ga(N_3)_5]^{2-}$, and $[M(N_3)_6]^{3-}$ (M = In, Tl) (Preprint)

5a. CONTRACT NUMBER

5b. GRANT NUMBER

5c. PROGRAM ELEMENT NUMBER

6. AUTHOR(S)
Ralf Haiges, Jerry A. Boatz, Jodi M. Williams, and Karl O. Christe

5d. PROJECT NUMBER

5f. WORK UNIT NUMBER
50260541

7. PERFORMING ORGANIZATION NAME(S) AND ADDRESS(ES)

Air Force Research Laboratory (AFMC)
AFRL/RZSP
10 E. Saturn Blvd.
Edwards AFB CA 93524-7680

8. PERFORMING ORGANIZATION REPORT NUMBER

AFRL-RZ-ED-JA-2011-179

9. SPONSORING / MONITORING AGENCY NAME(S) AND ADDRESS(ES)

Air Force Research Laboratory (AFMC)
AFRL/RZS
5 Pollux Drive
Edwards AFB CA 93524-7048

10. SPONSOR/MONITOR'S ACRONYM(S)

11. SPONSOR/MONITOR'S NUMBER(S)
AFRL-RZ-ED- JA-2011-179

12. DISTRIBUTION / AVAILABILITY STATEMENT

Approved for public release; distribution unlimited (PA #11178).

13. SUPPLEMENTARY NOTES
For publication in Angewandte Chemie.

14. ABSTRACT

There has been much interest in polyazido compounds during the last two decades. In particular, the potential of group 13 azides as precursors for the synthesis of the corresponding nitrides has been studied in great detail due to their usefulness for semiconductor and optoelectronic applications. Although most of these efforts were devoted to gallium azides, aluminium and indium azides were also explored. For thallium, the monoazide is well known and is an impact and highly friction sensitive compound, similar in properties to silver azide and lead diazide. However, little is known about the triazide. To our knowledge, the only previous report deals with the formation of a highly explosive yellow solid, formed by the reaction of Tl(OH)3 with HN3. Based on its elemental analysis, it had the composition Tl(N3)2 and was proposed to be the mixed Tl(I)/Tl(III) salt, Tl[Tl(N3)4], but this interpretation was subsequently questioned. The syntheses and characterisation of molecules with a high number of azido groups is very challenging due to the high energy content of the azido group which is responsible for their frequently encountered explosive and shock-sensitive nature. In this paper, we wish to communicate the syntheses of Ga(N3)3, In(N3)3, and Tl(N3)3 in SO2 and CH3CN solutions, their 1:1 adducts with CH3CN, and the first examples of multiply charged group 13 polyazido anions, [Ga(N3)5]2-, [In(N3)6]3- and [Tl(N3)6]3-. We also report the crystal structures of the tetraphenylphosphonium salts of the [Ga(N3)5]2-, [In(N3)6]3- and [Tl(N3)6]3 anions, and the vibrational spectra and electronic structure calculations for all the compounds.
.

15. SUBJECT TERMS

16. SECURITY CLASSIFICATION OF:			17. LIMITATION OF ABSTRACT	18. NUMBER OF PAGES	19a. NAME OF RESPONSIBLE PERSON
					Mr. Wayne Kalliomaa
a. REPORT	b. ABSTRACT	c. THIS PAGE	SAR	90	19b. TELEPHONE NUMBER *(include area code)*
Unclassified	**Unclassified**	**Unclassified**			N/A

DOI: 10.1002/anie.200((will be filled in by the editorial staff))

Preparation and Characterization of the Binary Group 13 Azides $M(N_3)_3$ and $M(N_3)_3 \cdot CH_3CN$ (M = Ga, In, Tl), $[Ga(N_3)_5]^{2-}$, and $[M(N_3)_6]^{3-}$ (M = In, Tl) (PREPRINT)

Ralf Haiges, Jerry A. Boatz, Jodi M. Williams, and Karl O. Christe**

Dedicated to the memory of Prof. Kurt Dehnicke, an old friend and pioneer of azide chemistry

There has been much interest in polyazido compounds during the last two decades.[1-19] In particular, the potential of group 13 azides as precursors for the synthesis of the corresponding nitrides has been studied in great detail due to their usefulness for semiconductor and optoelectronic applications. Although most of these efforts were devoted to gallium azides,[20,21] aluminium and indium azides were also explored.[20,22] For thallium, the monoazide is well known and is an impact and highly friction sensitive compound, similar in properties to silver azide and lead diazide.[23] However, little is known about the triazide. To our knowledge, the only previous report deals with the formation of a highly explosive yellow solid, formed by the reaction of $Tl(OH)_3$ with HN_3.[24 24] Based on its elemental analysis, it had the composition $Tl(N_3)_2$ and was proposed to be the mixed Tl(I)/Tl(III) salt, $Tl[Tl(N_3)_4]$, but this interpretation was subsequently questioned.[23]

The syntheses and characterisation of molecules with a high number of azido groups is very challenging due to the high energy content of the azido group which is responsible for their frequently encountered explosive and shock-sensitive nature. In this paper, we wish to communicate the syntheses of $Ga(N_3)_3$, $In(N_3)_3$, and $Tl(N_3)_3$ in SO_2 and CH_3CN solutions, their 1:1 adducts with CH_3CN, and the first examples of multiply charged group 13 polyazido anions, $[Ga(N_3)_5]^{2-}$, $[In(N_3)_6]^{3-}$ and $[Tl(N_3)_6]^{3-}$. We also report the crystal structures of the tetraphenylphosphonium salts of the $[Ga(N_3)_5]^{2-}$, $[In(N_3)_6]^{3-}$ and $[Tl(N_3)_6]^{3}$ anions, and the vibrational spectra and electronic structure calculations for all the compounds.

In analogy to our previously reported syntheses of inorganic polyazides,[14] the trifluorides GaF_3, InF_3 and TlF_3 were reacted with an excess of trimethylsilyl azide in SO_2 solution. This resulted in rapid and complete fluoride-azide exchange [Eq. (1) (M = Ga, In, Tl)].

$$MF_3 + 3\ Me_3SiN_3 \xrightarrow{SO_2} M(N_3)_3 + 3\ Me_3SiF \quad (1)$$

Pumping off the volatile compounds SO_2, Me_3SiF, and excess Me_3SiN_3) at -20 °C produces the neat triazides as colorless to orange solids. The azides $Ga(N_3)_3$, $In(N_3)_3$, and $Tl(N_3)_3$ are stable at room-temperature but very shock-sensitive. While $Ga(N_3)_3$ is the least sensitive of the three compounds, it is still dangerous and we encountered several explosions while handling small samples. $In(N_3)_3$ and especially $Tl(N_3)_3$ are more treacherous and tend to explode violently upon the slightest provocation (agitation, rapid change in temperature and/or pressure). The physical properties of $Ga(N_3)_3$ and $In(N_3)_3$ are in excellent agreement with previous literature reports.[20]

By using CH_3CN instead of SO_2 as solvent for the reactions of GaF_3, InF_3, and TlF_3 with excess Me_3SiN_3, colourless to orange solutions were obtained. Removal of all volatile materials (Me_3SiF, CH_3CN and excess Me_3SiN_3) resulted in the isolation of the acetonitrile adducts of the triazides as pale yellow to orange solids [Eq. (2) (M = Ga, In, Tl)].

$$MF_3 + 3\ Me_3SiN_3 \xrightarrow{CH_3CN} M(N_3)_3 \cdot CH_3CN + 3\ Me_3SiF \quad (2)$$

It was not possible to remove the acetonitrile by continued pumping at ambient temperature. Even after pumping for 24 hours, samples of $M(N_3)_3 \cdot CH_3CN$ showed virtually no mass-loss.

The neat acetonitrile adducts of the triazides $M(N_3)_3 \cdot CH_3CN$ are less dangerous than the donor-free triazides but are still shock-sensitive and can explode violently upon provocation (e.g. agitation). The stabilization of these triazides by adduct formation with CH_3CN is in accord with previous reports that $Ga(N_3)_3$ is a strong Lewis acid and can form stable, structurally characterized adducts with either one molecule of trialkylamine[20] or three molecules of pyridine,[20,21] yielding pseudo-tetrahedral or pseudo-octahedral *mer*-configuration adducts, respectively.

All attempts to grow single crystals of the triazides or their acetonitrile adducts by recrystallization were unsuccessful. The identity of the compounds $M(N_3)_3$ and $M(N_3)_3 \cdot CH_3CN$ was established by the observed material balances, vibrational spectra, and by their conversions with tetraphenyphosphonium azide, PPh_4N_3 into compounds of the previously unknown anions $[Ga(N_3)_5]^{2-}$, $[In(N_3)_6]^{3-}$, and $[Tl(N_3)_6]^{3-}$ which were characterized by their crystal structures.

[*] Prof. Dr. R. Haiges, Prof. Dr. K. O. Christe
Loker Research Institute and Department of Chemistry
University of Southern California
Los Angeles, CA 90089-1661 (USA)
Fax: (+1) 213-740-6679
E-mail: haiges@usc.edu, kchriste@usc.edu

Dr. J. A. Boatz
Space and Missile Propulsion Division
Air Force Research Laboratory (AFRL/RZSP)
10 East Saturn Boulevard
Edwards Air Force Base, CA 93524 (USA)

J. M. Williams
Strike Officer
USS Hue City (CG 66)

[**] This work was funded by the Air Force Office of Scientific Research, the Office of Naval Research, the Defense Threat Reduction Agency, and the National Science Foundation. We thank Profs. G. Olah and S. Prakash for their steady support, and Drs. W. Wilson and R. Wagner for their help and stimulating discussions. Grants of computer time from the Department of Defense High Performance Computing Modernization Program at the Engineer Research and Development (ERDC) and Navy Department of Defense Supercomputing Centers are gratefully acknowledged.

Supporting information for this article is available on the WWW under http://www.angewandte.org or from the author.

The recording of the vibrational spectrum of the neat triazides was very challenging due to their extreme shock-sensitivity. In spite of these difficulties, we succeeded to record Raman spectra of amorphous samples of all three neat triazides as well as an IR spectrum of $Ga(N_3)_3$.

The vibrational frequencies and intensities observed for amorphous $M(N_3)_3$ and $M(N_3)_3 \cdot CH_3CN$ (M = Ga, In, Tl) are compared with those calculated for the free molecular species at the MP2/SBKJ+(d) and B3LYP/SBKJ+(d) levels of theory in Tables S6 – S7 of the Supplementary Material.

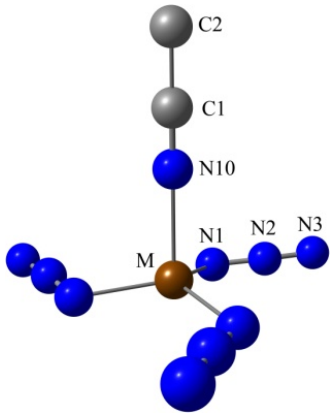

Figure 1. Calculated C_3 structure of the acetonitrile adducts $M(N_3)_3 \cdot CH_3CN$ (M = Ga, In). Bond lengths and angles are listed in the Supplementary Material.

The MP2 and B3LYP calculations result in minimum energy structures of C_{3h} symmetry for all three neat planar triazides $M(N_3)_3$. However, another isomer of C_s symmetry and only slightly higher energy is also found for the three compounds. At the B3LYP/SBKJ+(d) level, the C_s isomer of $Ga(N_3)_3$ is only 1.3 kcal/mol (MP2: 2.5 kcal/mol) higher in energy, the one of $In(N_3)_3$ is only 0.7 kcal/mol (MP2: 1.1 kcal/mol) higher in energy and the one of $Tl(N_3)_3$ was found to be only 0.7 kcal/mol (MP2: 0.6 kcal/mol) higher in energy. The two structures are very similar (see Table S1 Supplementary Material) and deviate from each other only in the orientation of one azido group. The small energy differences of less than 3 kcal/mol between the C_{3h} and C_s structures demonstrate the general floppiness of the azido ligands. The agreement between the predicted and observed vibrational spectra is only fair and indicates that the neat triazides are strongly associated in the solid state, in accord with their low solubilities and volatilities.

For $Ga(N_3)_3 \cdot CH_3CN$ and $In(N_3)_3 \cdot CH_3CN$ (Figure 1), the MP2/SBKJ+(d) and B3LYP/SBKJ+(d) calculations result in a minimum energy structures of C_3 symmetry, resembling the crystal structure known for the $Ga(N_3)_3 \cdot NR_3$ adducts.[20] The predicted minimum energy structure of $Tl(N_3)_3 \cdot CH_3CN$ is of C_s symmetry at the B3LYP/SBKJ+(d) level and of C_1 symmetry at the MP2/SBKJ+(d) level of theory (see Supplementary Material).

As found for other binary polyazides,[8-15,20-22] the neutral polyazides can be stabilized either by the formation of donor-acceptor adducts with Lewis bases or by anion formation which increases the ionicity of the azido groups. Because an ionic azide group possesses two double bonds while a covalent azido group has a single and a triple bond, increasing the ionicity of the existing azido ligands by further azide addition makes the breaking of an N-N bond more difficult and enhances the activation energy barrier toward catastrophic N_2 elimination. The group 13 $M(N_3)_3$ molecules are all strong Lewis acids and, in principle, could add one, two or three azide ions to form the $[M(N_3)_4]^-$, $[M(N_3)_5]^{2-}$ and $[M(N_3)_6]^{3-}$ anions, respectively. In the case of boron, the maximum coordination number (CN) is 4 and, therefore, only the $[B(N_3)_4]^-$ anion is formed.[1a,25] In contrast, Al, Ga, In, and Tl prefer CNs larger than 4, preferably 6, and cases of CN 4 are only known for $[Al(N_3)_4]^-$[23] and $[Ga(N_3)_4]^-$.[20] Since the azido ligand, unlike the nitrato ligand,[26] is only monodentate, in $[M(N_3)_4]^-$ an increase of CN 4 to 6 requires the addition of two extra donor molecules. Two well characterized examples for the latter case are $[Al(N_3)_4(THF)_2]^-$ and $[In(N_3)_4(Pyr)_2]^-$.[20]

To examine the stabilization of the very explosive triazides $M(N_3)_3$ (M = Ga, In, Tl) by azide addition, these compounds were reacted with one equivalent of tetraphenyl phosphonium azide, $[PPh_4][N_3]$ in acetonitrile solution. Under these conditions, no evidence for the formation of tetraazido anions, $[M(N_3)_4]^-$, was found. Instead, a 1:1 mixture of a $[PPh_4]_2[Ga(N_3)_5]$ and the unreacted triazide was obtained for $Ga(N_3)_3$. In case of $In(N_3)_3$ and $Tl(N_3)_3$, 1:2 mixtures of the corresponding hexaazido compounds $[PPh_4]_3[M(N_3)_6]$ and the triazides were obtained.

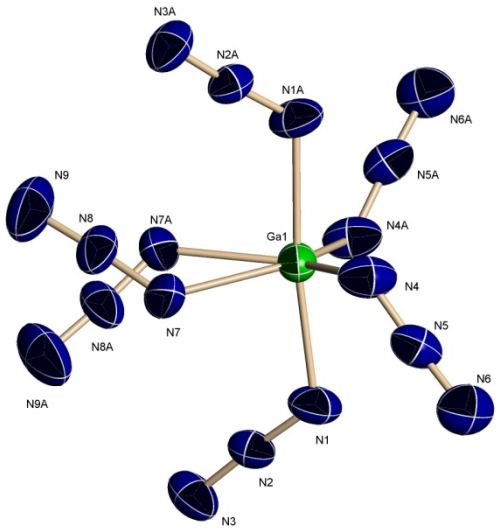

Figure 2. The anion in $[PPh_4]_2[Ga(N_3)_5]$. The two azido groups at N7 and N7A show a positional disorder and have site occupancy factor of 0.5. Thermal ellipsoids are shown at the 50% probability level. Selected bond lengths [Å] and angles [°]: Ga1-N1 2.049(2), Ga1-N4 1.937(2), Ga1-N7 1.948(4), N1-N2 1.191(2), N2-N3 1.152(2), N1-Ga1-N1A 173.42(11), N1-Ga1-N4 89.70(8), N1-Ga1-N4A 87.31(8), N1-Ga1-N7 85.14(14), N1-Ga1-N7A 101.34(14), N4-Ga1-N4A 125.88(13), N4-Ga1-N7 107.11(17), N4-Ga1-N7A 126.38(18).

The triazides were then reacted with three equivalents of $[PPh_4][N_3]$ in acetonitrile solution. While in the case of $In(N_3)_3$ and $Tl(N_3)_3$ the pure hexaaxido salts $[PPh_4]_3[M(N_3)_6]$ were formed [Eq. (3) (M = In, Tl)], in the case of $Ga(N_3)_3$ only 1:1 mixtures of the pentaazide $[PPh_4]_2[Ga(N_3)_5]$ and unreacted $[PPh_4N_3]$ were obtained [Eq. (4)].

$$M(N_3)_3 + 3\,[PPh_4][N_3] \xrightarrow{CH_3CN} [PPh_4]_3[M(N_3)_6] \quad (3)$$

$$Ga(N_3)_3 + 2\,[PPh_4][N_3] \xrightarrow{CH_3CN} [PPh_4]_2[Ga(N_3)_5] \quad (4)$$

$[PPh_4]_3[In(N_3)_6]$ and $[PPh_4]_3[Tl(N_3)_6]$ were isolated as room-temperature stable, crystalline solids of yellow and orange color, respectively. $[PPh_4]_2[Ga(N_3)_5]$ was isolated as colorless crystals that are stable at room-temperature. Because of the increased ionicity of their azido ligands and the presence of two or even three large counter-ions per anion which diminishes shock propagation, all three compounds are much less sensitive and explosive than their parent compounds, $M(N_3)_3$ (M = Ga, In, Tl) and could be manipulated in our study at room temperature without explosion. The $[PPh_4]_2[Ga(N_3)_5]$, $[PPh_4]_3[In(N_3)_6]$, and $[PPh_4]_3[Tl(N_3)_6]$ salts were characterized by the observed material balances, their IR and Raman spectra (see Supplementary Material), and their crystal structures

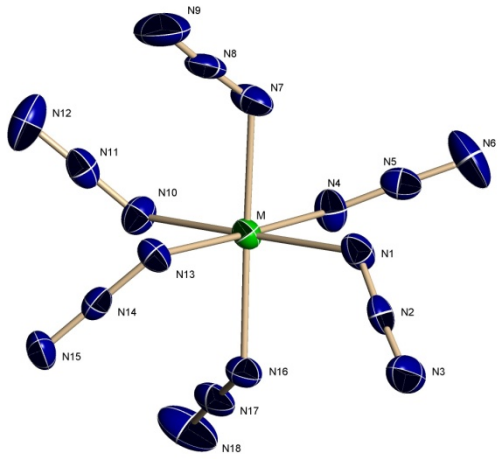

Figure 3. The hexaazido anion in $[PPh_4]_3[M(N_3)_6]$ (M = In, Tl). Thermal ellipsoids are shown at the 50% probability level. Selected bond lengths [Å] and angles [°] for M = In [M = Tl]: M-N1 2.217(2) [2.322(3)], M-N4 2.193(2) [2.278(3)], M-N13 2.238(2) [2.328(3)], N1-N2 1.183(3) [1.182(5)], N2-N3 1.160(3) [1.156(5)], N1-M-N4 90.14(8) [89.61(13)], N1-M-N7 86.27(8) [91.92(14)], N1-M-N10 177.44(8) [176.57(13)], N1-M-N13 93.38(8) [94.51(13)], N1-M-N16 90.27(8) [90.71(13)], N7-M-N16 175.44(8) [174.90(14)].

The structures of $[PPh_4]_2[Ga(N_3)_5]$, $[PPh_4]_3[In(N_3)_6]$, and $[PPh_4]_3[Tl(N_3)_6]$ were established by single crystal X-ray diffraction studies (Figures 2-3 and Supplementary Material). The crystal structure of $[PPh_4]_2[Ga(N_3)_5]$[27] revealed the presence of well separated $[PPh_4]^+$ and $[Ga(N_3)_5]^{2-}$ ions. The closest Ga···N and N···N contacts between neighboring anions are 7.9 Å and 5.6 Å, respectively. The observed geometry of the $[Ga(N_3)_5]^{2-}$ anion (Figure 3) is derived from a trigonal-bipyramidal GaN_5 skeleton and in good general agreement with the propeller-type C_s structure predicted by our theoretical calculations. This structure is in good agreement with the ones calculated for $As(N_3)_5$,[6,11] $Sb(N_3)_5$,[6,11] and $[Fe(N_3)_5]^{2-}$[30] but contrary to the structure observed for $[Bi(N_3)_5]^{2-}$[19] or the one calculated for $[Se(N_3)_5]^{-}$[31] for which the free valence electron pair on its central atom becomes sterically active, and also in contrast to the theoretically predicted structures of $Nb(N_3)_5$[14] and $Ta(N_3)_5$.[14] While the axial M-N-N bonds in $Nb(N_3)_5$ and $Ta(N_3)_5$ are almost linear and the M-N distances are essentially the same, the five Ga-N-N bonds in $[Ga(N_3)_5]^{2-}$ are strongly bent with angles of about 120° and, as expected from VSEPR arguments,[32] the axial Ga-N bonds are significantly longer than the equatorial ones.

$[PPh_4]_3[In(N_3)_6]$ crystallizes in the monoclinic space group $P2_1/n$. The X-ray crystal structure[28] showed the presence of well separated $[PPh_4]^+$ cations and $[In(N_3)_6]^{3-}$ anions without significant cation-anion interaction. Between neighboring anions, the closest In···N and N···N contacts were found to be 8.4 Å and 6.4 Å, respectively. $[PPh_4]_3[Tl(N_3)_6]$ crystallizes in the monoclinic space group $P2_1/n$ and is isostructural to $[PPh_4]_3[In(N_3)_6]$. Again, well separated cations and anions without significant cation-anion interaction were observed in the X-ray crystal structure.[29] Between neighboring anions, the closest Tl···N and N···N contacts were found to be 8.4 Å and 6.4 Å, respectively. The observed structures of the $[In(N_3)_6]^{3-}$ and $[Tl(N_3)_6]^{3-}$ anions (Figure 4) are only slightly distorted from perfect S_6 symmetry and are analogous to other hexaazido species such as $[As(N_3)_6]^-$,[6] $[Si(N_3)_6]^-$,[4] $[Ge(N_3)_6]^-$,[3] $W(N_3)_6$,[13] and $[Ti(N_3)_6]^{2-}$,[12] and contrary to that of $[Te(N_3)_6]^{2-}$.[8]

Theoretical calculations were carried out for all the different polyazide species of this study. For the tetraazido anions $[M(N_3)_4]^-$ (M = Ga, In, Tl) (Figure 4 and Supplementary Material), the B3LYP/SBKJ+(d) level of theory predicts a minimum energy structure of D_{2d} symmetry. At the MP2/SBKJ+(d) level of theory, the structures of $[Ga(N_3)_4]^-$ and $[In(N_3)_4]^-$ are predicted to be of D_{2d} symmetry, the one of $[Tl(N_3)_4]^-$ is calculated to be of C_2 symmetry. For the pentaazido anions $[M(N_3)_5]^{2-}$ (M = Ga, In, Tl) minimum energy structures of C_s symmetry were found (see Supplementary Material).

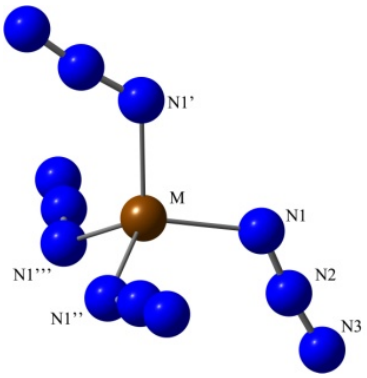

Figure 4. Calculated D_{2d} structure of the tetraazido anions $[M(N_3)_4]^-$ (M = Ga, In, Tl). Bond lengths and angles are given in the Supplementary Material.

In summary, the extremely shock-sensitive group 13 triazides $Ga(N_3)_3$, $In(N_3)_3$, and $Tl(N_3)_3$ have been prepared in SO_2 and CH_3CN solutions. The use of the corresponding fluoride starting materials and SO_2 as a solvent provides a convenient synthesis for the neat free triazides and firmly established the existence of thallium triazide. In CH_3CN solution, the new $M(N_3)_3 \cdot CH_3CN$ donor-acceptor adducts were obtained. Reactions of the triazides with either stoichiometric amounts or an excess of tetraphenyl-phosphonium azide in CH_3CN solution yield exclusively the novel $[Ga(N_3)_5]^{2-}$, $[In(N_3)_6]^{3-}$ and $[Tl(N_3)_6]^{3-}$ anions, the first examples of multiply charged group 13 polyazido anions. Furthermore, the series $M(N_3)_3$, $M(N_3)_3 \cdot CH_3CN$, $[M(N_3)_4]^-$, $[M(N_3)_5]^{2-}$, and $[M(N_3)_6]^{3-}$ (M = Ga, In, Tl) has been studied by theoretical calculations.

Experimental Section

Caution! The polyazides of this work are extremely shock-sensitive and can explode violently upon the slightest provocation. They should be handled only on a scale of less than 1 mmol using appropriate safety precautions.[15] In addition, thallium and its compounds are very poisonous. **Ignoring safety precautions can lead to serious injuries!**

Materials and Apparatus: All reactions were carried out in Teflon-FEP ampules that were closed by stainless steel valves. Volatile materials were handled in a Pyrex glass vacuum line. Non-volatile materials were handled in the dry nitrogen atmosphere of a glove box. Raman spectra were recorded in the Teflon reactors in the range 4000–80 cm^{-1} on a Bruker Equinox 55 FT-RA spectrophotometer using a Nd-YAG laser at 1064 nm with power levels less than 50 mW! Infrared spectra were recorded in the range 4000-400 cm^{-1} on a Midac, M Series, FT-IR spectrometer using KBr pellets. The pellets were carefully prepared inside the glove box using an Econo mini-press (Barnes Engineering Co.). The starting materials GaF_3, InF_3 (both Aldrich), and TlF_3 (Ozark Mahoning) were used without further purification. Me_3SiN_3 (Aldrich) was purified by fractional condensation prior to use. Solvents were dried by standard methods and freshly distilled prior to use. PPh_4N_3 was prepared by a literature method.[33]

Preparation of $M(N_3)_3$ (M = Ga, In, Tl): A sample of MF_3 (0.2 mmol) was loaded into a Teflon-FEP ampule, followed by the addition of SO_2 (40 mmol) and Me_3SiN_3 (1.0 mmol) *in vacuo* at -196 °C. The mixture was allowed to warm to ambient temperature. After 10 hours at ambient temperature, white to orange precipitates were obtained. The temperature was lowered to -20 °C, and all volatile material was pumped off. After additional pumping for 4 hours at ambient temperature, off-white to orange solids were obtained.

Preparation of $M(N_3)_3 \cdot xCH_3CN$ (M = Ga, In Tl): A sample of MF_3 (0.4 mmol) was loaded into a Teflon-FEP ampule, followed by the addition of acetonitrile (60 mmol) and Me_3SiN_3 (2.0 mmol) *in vacuo* at -196 °C. The mixture was allowed to warm to ambient temperature. After 6 hours at ambient temperature, colorless to orange solutions were obtained. The temperature was lowered to -20 °C, and all volatile material was pumped off. After additional pumping for 4 hours at ambient temperature, off-white to orange solids were obtained.

Preparation of $[Ga(N_3)_5]^{2-}$ and $[M(N_3)_6]^{3-}$ (M = In, Tl) salts: Under a stream of dry nitrogen, a stoichiometric amount of PPh_4N_3 (0.60 mmol for $[Ga(N_3)_5]^{2-}$ and 0.9 mmol for $[M(N_3)_6]^{3-}$) was added to a frozen solution of the corresponding triazide (0.30 mmol) in CH_3CN (40 mmol) at -64 °C. The reaction mixture was kept at -25 °C for 30 min, occasionally agitated and then warmed to ambient temperature. After 30 min, all volatiles were removed at -20 °C in a dynamic vacuum, leaving behind crystalline solids; weights expected for 0.30 mmol of $[PPh_4]_2[Ga(N_3)_5]$, $[PPh_4]_3[In(N_3)_6]$, and $[PPh_4]_3[Tl(N_3)_6]$: 0.288 g, 0.416 g, and 0.442 g weights found: 0.280 g, 0.430 g and 0.453 g, respectively.

Theoretical Methods: The molecular structures, harmonic vibrational frequencies, and IR and Raman vibrational intensities were calculated using second-order perturbation theory (MP2, also known as MBPT(2)[34] and also at the DFT level using the B3LYP hybrid functional[35a-c] which included the VWN5 correlation functional[35d] The Stevens, Basch, Krauss, and Jasien (SBKJ) effective core potentials and the corresponding valence-only basis sets were used.[36] The SBKJ valence basis sets were augmented with a d-polarization function[37] and a diffuse s+p shell[38] on each heavy atom,denoted as SBKJ+(d). Hessians (energy second derivatives) were calculated for the final equilibrium structures to verify them as local minima, that is, having a positive definite Hessian. All calculations were performed by using the electronic structure code GAMESS.[39]

Received: ((will be filled in by the editorial staff))
Published online on ((will be filled in by the editorial staff))

Keywords: Polyazides · Group 13 Azides · Crystal Structures · Vibrational Spectra · Electronic Structure Calculations

[1] a) E. Wiberg, H. Michaud, *Z. Naturforsch. B* **1954,** *9,* 495, 496, 497, 499, 500, 501, 502; b) Z. Dori, R. F. Ziolo, *Chem. Rev*. **1973**, *73*, 247-254; c) I. C. Tornieporth-Oetting, T. M. Klapötke, *Angew. Chem.* **1995**, *107*, 559-568; *Angew. Chem. Int. Ed.* **1995**, *34*, 511-520; d) T. M. Klapötke, *Chem. Ber.* **1997**, *130*, 443-452; e) A. Kornath, *Angew. Chem.* **2001**, *113*, 3231-3232; *Angew. Chem. Int. Ed.* **2001**, *113*, 3135-3136; f) W. Fraenk, T. M. Klapötke in *Inorganic Chemistry Highlights* (Eds.: G. Meyer, D. Naumann, L. Wesemann), Wiley-VCH, Weinheim, **2002**; g) J. Müller, *Coord. Chem. Rev.* **2002**, *235*, 105-119; h) C. Knapp, J. Passmore, *Angew. Chem.* **2004**, *116*, 4938-4941; *Angew. Chem. Int. Ed.* **2004**, *43*, 4834-4836.

[2] B. Neumüller, F. Schmock, K. Dehnicke, *Z. Anorg. Allg. Chem.* **1999**, *625*, 1243-1245.

[3] A. C. Filippou, P. Portius, D. U. Neumann, K.-D. Wehrstedt, *Angew. Chem.* **2000**, *112*, 4524-4527; *Angew. Chem. Int. Ed*. **2000**, *39*, 4333-4336.

[4] C. Filippou, P. Portius, G. Schnakenburg, *J. Am. Chem. Soc.* **2002**, *124*, 12396-12397.

[5] T. M. Klapötke, B. Krumm, P. Mayer, H. Pietrowski, O. P. Ruscitti, A. Schiller, *Inorg. Chem*. **2002**, *41*, 1184-1193.

[6] a) T. M. Klapötke, H. Nöth, T. Schütt, M. Warchhold, *Angew. Chem.* **2000**, *112*, 2197—2199; *Angew. Chem. Int. Ed*. **2000**, *39*, 2108--2109; b) K. Karaghiosoff, T. M. Klapötke, B. Krumm, H. Nöth, T. Schütt, M. Suter, *Inorg. Chem.* **2002**, *41*, 170-179.

[7] T. M. Klapötke, B. Krumm, P. Mayer, I. Schwab, *Angew. Chem.* **2003**, *115*, 6024-6026; *Angew. Chem. Int. Ed.* **2003**, *42*, 5843-5846.

[8] R. Haiges, J. A. Boatz, A. Vij, M. Gerken, S. Schneider, T. Schroer, K. O. Christe, *Angew. Chem.* **2003**, *115*, 6027-6031; *Angew. Chem. Int. Ed.* **2003**, *42*, 5847-5851.

[9] R. Haiges, A. Vij, J. A. Boatz, S. Schneider, T. Schroer, M. Gerken, K. O. Christe, *Chem. Eur. J*. **2004**, *10*, 508-517.

[10] R. Haiges, S. Schneider, T. Schroer, K. O. Christe, *Angew. Chem.* **2004**, *116*, 5027-5032; *Angew. Chem. Int. Ed*. **2004**, *43*, 4919-4924.

[11] R. Haiges, J. A. Boatz, A. Vij, V. Vij, M. Gerken, S. Schneider, T. Schroer, M. Yousufuddin, K. O. Christe, *Angew. Chem.* **2004**, *116*, 6844; *Angew. Chem. Int. Ed.* **2004**, *43*, 6676-6680.

[12] R. Haiges, J. A. Boatz, S. Schneider, T. Schroer, M. Yousufuddin, K. O. Christe, *Angew. Chem.* **2004**, *116*, 3210-3214; *Angew. Chem. Int. Ed*. **2004**, *43*, 3148-3152.

[13] R. Haiges, J. A. Boatz, R. Bau, S. Schneider, T. Schroer, M. Yousufuddin, K. O. Christe, *Angew. Chem.* **2005**, *117*, 1894-1899; *Angew. Chem. Int. Ed*. **2005**, *44*, 1860-1865.

[14] R. Haiges, J. A. Boatz, T. Schroer, M. Yousufuddin, K. O. Christe, *Angew. Chem.* **2006**, *118*, 4948-4953; *Angew. Chem. Int. Ed*. **2006**, *45*, 4830-4835.

[15] R. Haiges, J. A. Boatz, M. Yousufuddin, K. O. Christe, *Angew. Chem.* **2007**, *119*, 2927-2932; *Angew. Chem. Int. Ed*. **2007**, *46*, 2869-2874.

[16] a) J. P. Johnson, G. K. MacLean, J. Passmore, P. S. White, *Can. J. Chem.* **1989**, *67*, 1687-1692; b) M. J. Crawford, A. Ellern, P. Mayer, *Angew. Chem.* **2005**, *117*, 8086-8090; *Angew. Chem. Int. Ed.* **2005**, *44*, 7874-7878.

[17] A. Villinger, A. Schulz, *Angew. Chem. Int. Ed.* **2010**, *49*, 8017-8020.

[18] R. Haiges, J. A. Boatz, K. O. Christe, *Angew. Chem.* **2010**, *122*, 8180-8184; *Angew. Chem. Int. Ed.* **2010**, *49*, 8008-8012.

[19] R. Haiges, D. A. Dixon, K. O. Christe, in preparation.

[20] a) R. A. Fischer, A. Miehr, H. Sussek, H. Pritzkow, E. Herdtweck, J. Mueller, O. Ambacher, T. Metzger, *Chem. Commun.* **1996**, *2685*; b) R. A. Fischer, A. Miehr, E. Herdtweck, M. R. Mattner, O. Ambacher, T. Metzger, E. Born, S. Weinkauf, C. R. Pulham, S. Parsons, *Chem. Eur. J.* **1996**, *2,*1353; c) A. C. Frank, F. Stowasser, H. Sussek, H. Pritzkow, C. R. Miskys, O. Ambacher, M. Giersig, R. A. Fischer, *J. Am. Chem. Soc.* **1998**, *120*, 3512; d) A. Devi, H.sussek, H. Pritzkow, M. Winter, R.A, Fischer, *Eur. J. Inorg. Chem.* ***1999,*** 2127; e) R. A. Fischer, H. Sussek, H. Parala, H. Pritzkow, *J. Organomet. Chem.* **1999**, *592,* 205*;* f) H. Sussek, F. Stowasser, H. Pritzkow, R. A. Fischer, *Eur. J. Inorg. Chem.* ***2000,*** 455.

[21] a) D. A. Neumayer, A. H. Cowley, A. Decken, R. A. Jones, V. Lakhotia, J. G. Ekerdt, *J. Am. Chem. Soc.* **1995**, *117*, 5893; b) C. J. Carmalt, A. H. Cowley, R. D. Culp, R. A. Jones, *Chem. Commun.* **1996**, 1543.

[22] C. J. Linnen, D. E. Macks, R. D. Coombe, *J. Phys. Chem. B* **1997**, *101,* 1602.

[23] H. D. Fair, R. F. Walker, *Energetic Materials, Volume 1, Physics and Chemistry of the Inorganic Azides,* Plenum Press, New York and London, **1977**.

[24] L. M. Dennis, M. Doan, A. C. Gill, *J. Am. Chem. Soc.* **1896**, *18,* 97.

[25] W. Fraenk, T. Habereder, A. Hammerl, T. M. Klapoetke, B. Krumm, P. Mayer, H. Noeth, M. Warchhold, *Inorg. Chem.* **2001***, 40,* 1334.

[26] C. B. Jones, R. Haiges, T. Schroer, K. O. Christe, *Angew. Chem.* **2006,** *45,* 4981.

[27] Crystal data for $C_{48}H_{40}GaN_{15}P_2$: M_r = 958.61, monoclinic, space group C2/c, a = 11.771(4), b = 18.031(6), c = 21.793(7) Å, α = 90, β = 91.974(5), γ = 90 °, V = 4622(2) Å^3, $F(000)$ = 1976, $\rho_{calcd.}$ (Z = 4) = 1.377 g·cm^{-3}, μ = 0.717 mm^{-1}, approximate crystal dimensions 0.23 x 0.15 x 0.09 mm^3, θ range = 1.87 to 27.53°, $Mo_{K\alpha}$ (λ = 0.71073 Å), T = 140(2) K, 19912 measured data (Bruker 3-circle, SMART APEX CCD with χ-axis fixed at 54.74°, using the SMART V 5.630 program, Bruker AXS: Madison, WI, 2003), of which 5242 (R_{int} = 0.0369) unique. Lorentz and polarization correction (SAINT V 6.45 program, Bruker AXS: Madison, WI, 2003), absorption correction (SADABS program, Bruker AXS: Madison, WI, 2003). Structure solution by Direct methods (SHELXTL 6.14, Bruker AXS: Madison, WI, 2003), full-matrix least-squares refinement on F^2, data to parameters ratio: 16.8 : 1, final R indices [$I>2\sigma(I)$]: $R1$ = 0.0383, $wR2$ = 0.0889, R indices (all data): $R1$ = 0.0530, $wR2$ = 0.0971, GOF on F^2 = 1.029. Further crystallographic details can be obtained from the Cambridge Crystallographic Data Centre (CCDC, 12 Union Road, Cambridge CB21EZ, UK (Fax: (+44) 1223-336-033; e-mail: deposit@ccdc.cam.ac.uk) on quoting the deposition no. CCDC 811062.

[28] Crystal data for $C_{72}H_{60}InN_{18}P_3$: M_r = 1385.11, monoclinic, space group P2(1)/n, a = 13.1599(14), b = 22.704(2), c = 22.032(2) Å, α = 90, β = 96.707(2), γ = 90 °, V = 6537.6(12) Å^3, $F(000)$ = 2848, $\rho_{calcd.}$ (Z = 4) = 1.407 g·cm^{-3}, μ = 0.494 mm^{-1}, approximate crystal dimensions 0.23 x 0.16 x 0.10 mm^3, θ range = 1.29 to 27.52°, $Mo_{K\alpha}$ (λ = 0.71073 Å), T = 163(2) K, 40351 measured data (Bruker 3-circle, SMART APEX CCD with χ-axis fixed at 54.74°, using the SMART V 5.630 program, Bruker AXS: Madison, WI, 2003), of which 14707 (R_{int} = 0.0649) unique. Lorentz and polarization correction (SAINT V 6.45 program, Bruker AXS: Madison, WI, 2003), absorption correction (SADABS program, Bruker AXS: Madison, WI, 2003). Structure solution by Patterson method (SHELXTL 6.14, Bruker AXS: Madison, WI, 2003), full-matrix least-squares refinement on F^2, data to parameters ratio: 17.4 : 1, final R indices [$I>2\sigma(I)$]: $R1$ = 0.0382, $wR2$ = 0.0609, R indices (all data): $R1$ = 0.0626, $wR2$ = 0.064, GOF on F^2 = 0.892. Further crystallographic details can be obtained from the Cambridge Crystallographic Data Centre (CCDC, 12 Union Road, Cambridge CB21EZ, UK (Fax: (+44) 1223-336-033; e-mail: deposit@ccdc.cam.ac.uk) on quoting the deposition no. CCDC 811063.

[29] Crystal data for $C_{72}H_{60}N_{18}P_3Tl$: M_r = 1474.66, monoclinic, space group P2(1)/n, a = 13.1409(11), b = 22.8133(19), c = 22.0468(19) Å, α = 90, β = 96.685(2), γ = 90 °, V = 6564.4(10) Å^3, $F(000)$ = 2976, $\rho_{calcd.}$ (Z = 4) = 1.492 g·cm^{-3}, μ = 2.593 mm^{-1}, approximate crystal dimensions 0.45 x 0.19 x 0.18 mm^3, θ range = 1.29 to 27.53°, $Mo_{K\alpha}$ (λ = 0.71073 Å), T = 142(2) K, 40264 measured data (Bruker 3-circle, SMART APEX CCD with χ-axis fixed at 54.74°, using the SMART V 5.630 program, Bruker AXS: Madison, WI, 2003), of which 14611 (R_{int} = 0.0305) unique. Lorentz and polarization correction (SAINT V 6.45 program, Bruker AXS: Madison, WI, 2003), absorption correction (SADABS program, Bruker AXS: Madison, WI, 2003). Structure solution by Patterson method (SHELXTL 6.14, Bruker AXS: Madison, WI, 2003), full-matrix least-squares refinement on F^2, data to parameters ratio: 17.3 : 1, final R indices [$I>2\sigma(I)$]: $R1$ = 0.0309, $wR2$ = 0.0729, R indices (all data): $R1$ = 0.0422, $wR2$ = 0.0775, GOF on F^2 = 1.050. Further crystallographic details can be obtained from the Cambridge Crystallographic Data Centre (CCDC, 12 Union Road, Cambridge CB21EZ, UK (Fax: (+44) 1223-336-033; e-mail: deposit@ccdc.cam.ac.uk) on quoting the deposition no. CCDC 811064.

[30] J. Drummond, J. S. Wood, *Chem. Commun*. **1969**, 1373.

[31] T. M. Klapötke, B. Krumm, M. Scherr, R. Haiges, K. O. Christe, *Angew. Chem. Int. Ed.* **2007**, *46*, 8686-8690.

[32] a) R. J. Gillespie, I. Hargittai, *The VSEPR Model of Molecular Geometry,* Allyn and Bacon, A Division of Simon & Schuster, Inc.: Needham Heights, MA, **1991**; b) R. J. Gillespie, P. L. A. Popelier, *Chemical Bonding and Molecular Geometry: from Lewis to Electron Densities,* Oxford University Press, **2001**.

[33] R. Haiges, T. Schroer, M. Yousufuddin, K. O. Christe, *Z. Anorg. Allg. Chem*., **2005,** *631,* 2691-2695.

[34] a) C. Moller, M. S. Plesset, *Phys. Rev.* 1934, **46**, 618; b) J. A. Pople, J. S. Binkley, R. Seeger, *Int. J. Quantum Chem. Symp.* 1976, **10**, 1; c) M. J. Frisch, M. Head-Gordon, J. A. Pople, *Chem. Phys. Lett.* 1990, **166**, 275; d) R. J. Bartlett, D. M. Silver, *Int. J. Quantum Chem. Symp.* 1975, **9**, 1927.

[35] a) A. D. Becke, *J. Chem. Phys.* 1993, **98**, 5648; b) P. J. Stephens, F. J. Devlin, C. F. Chablowski, M. J. Frisch, *J. Phys. Chem.* 1994, **98**, 11623; c) R. H. Hertwig, W. Koch, *Chem. Phys. Lett.* 1997, **268**, 345; d) S. H. Vosko, L. Wilk, M. Nusair, *Can. J. Phys.* 1980, **58**, 1200.

[36] a) W. J. Stevens, H. Basch, M. Krauss, *J. Chem. Phys.* 1984, **81**, 6026; b) W. J. Stevens, M. Krauss, H. Basch, P. G. Jasien, *Can. J. Chem.* 1992, **70**, 612.

[37] a) P. C. Hariharan, J. A. Pople, *Theor. Chim. Acta* 1973, **28**, 213; b) "Gaussian Basis Sets for Molecular Calculations" S.Huzinaga, J.Andzelm, M.Klobukowski, E.Radzio-Andzelm, Y.Sakai, H.Tatewaki Elsevier, Amsterdam, 1984.

[38] T. Clark, J. Chandrasekhar, G. W. Spitznagel, P. von R. Schleyer, *J. Comput. Chem.* 1983, **4**, 294.

[39] a) M.W.Schmidt, K.K.Baldridge, J.A.Boatz, S.T.Elbert, M.S.Gordon, J.H.Jensen, S.Koseki, N.Matsunaga, K.A.Nguyen, S.Su, T.L.Windus, M.Dupuis, J.A.Montgomery *J. Comput. Chem*., 1993, **14**, 1347; b) M.S.Gordon, M.W.Schmidt pp. 1167-1189, in "Theory and Applications of Computational Chemistry: the first forty years" C.E.Dykstra, G.Frenking, K.S.Kim, G.E.Scuseria (editors), Elsevier, Amsterdam, 2005.

Entry for the Table of Contents

Layout 1:

Polyazide Chemistry

Ralf Haiges*, Jerry A. Boatz, Jodi M. Williams, Karl O. Christe* _____
Page – Page

Preparation and Characterization of the Binary Group 13 Azides $M(N_3)_3$ and $M(N_3)_3 \cdot CH_3CN$ (M = Ga, In, Tl), $[Ga(N_3)_5]^{2-}$, and $[M(N_3)_6]^{3-}$ (M = In, Tl)

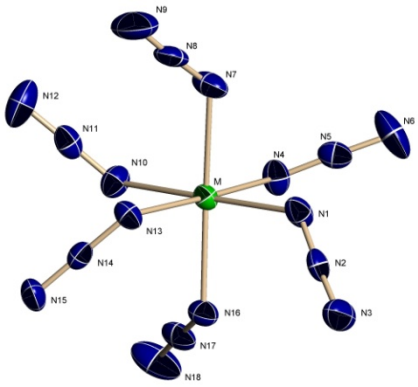

The use of the corresponding fluoride starting materials and SO_2 as a solvent provides a convenient synthesis for the neat group 13 triazides $Ga(N_3)_3$, $In(N_3)_3$, and $Tl(N_3)_3$ and firmly establishes the existence of thallium triazide. In CH_3CN solution, the new $M(N_3)_3 \cdot CH_3CN$ donor-acceptor adducts were obtained. Reactions of the triazides with tetraphenyl-phosphonium azide in CH_3CN solution yield exclusively the novel $[Ga(N_3)_5]^{2-}$, $[In(N_3)_6]^{3-}$ and $[Tl(N_3)_6]^{3-}$ anions.

Preparation and Characterization of the Binary Group 13 Azides $M(N_3)_3$ and $M(N_3)_3 \cdot CH_3CN$ (M = Ga, In, Tl), $[Ga(N_3)_5]^{2-}$, and $[M(N_3)_6]^{3-}$ (M = In, Tl)

Ralf Haiges, Jerry A. Boatz, Jodi M. Williams, and Karl O. Christe**

Supporting Information

Table S1. Calculated structures[a] for $Ga(N_3)_3$, $In(N_3)_3$ and $Tl(N_3)_3$

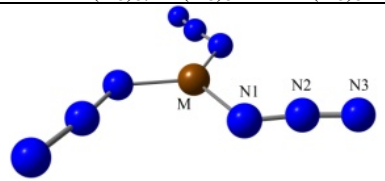

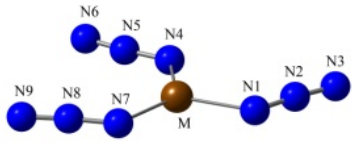

	$Ga(N_3)_3$ C_{3h}		$In(N_3)_3$ C_{3h}		$Tl(N_3)_3$ C_{3h}		$Ga(N_3)_3$ C_s		$In(N_3)_3$ C_s		$Tl(N_3)_3$ C_s	
	B3LYP	MP2	B3LYP	MP2	B3LYP	MP2	B3LYP	MP2	B3LYP	MP2	B3LYP	MP2
M-N1	1.853	1.839	2.080	2.059	2.210	2.154	1.847	1.833	2.071	2.052	2.195	2.143
M-N4	-	-	-	-	-	-	1.862	1.845	2.091	2.068	2.206	2.150
M-N7	-	-	-	-	-	-	1.853	1.839	2.079	2.061	2.230	2.169
N1-N2	1.256	1.263	1.255	1.264	1.257	1.271	1.256	1.264	1.254	1.264	1.257	1.272
N2-N3	1.159	1.198	1.163	1.202	1.166	1.202	1.159	1.198	1.163	1.203	1.166	1.202
N4-N5	-	-	-	-	-	-	1.254	1.263	1.254	1.264	1.257	1.273
N5-N6	-	-	-	-	-	-	1.160	1.200	1.164	1.204	1.166	1.203
N7-N8	-	-	-	-	-	-	1.255	1.264	1.254	1.266	1.255	1.271
N8-N9	-	-	-	-	-	-	1.160	1.200	1.164	1.203	1.167	1.204
M-N1-N2	120.6	119.2	120.4	120.2	115.3	114.3	120.4	118.8	120.5	119.6	115.5	113.6
M-N4-N5	-	-	-	-	-	-	123.1	121.6	121.9	120.6	116.5	114.4
M-N7-N8	-	-	-	-	-	-	122.7	119.9	121.7	119.5	116.9	115.0
N1-M-N1’	120.0	120.0	120.0	120.0	120.0	120.0	-	-	-	-	-	-
N1-M-N4	-	-	-	-	-	-	117.2	117.6	116.7	117.7	113.4	116.4
N1-M-N7	-	-	-	-	-	-	112.4	114.8	112.2	115.3	114.1	115.5
N4-M-N7	-	-	-	-	-	-	130.4	127.7	131.1	127.0	132.6	128.1
N1-N2-N3	173.1	172.6	173.3	172.5	173.0	171.8	172.6	171.9	171.9	172.0	172.8	171.6
N4-N5-N6	-	-	-	-	-	-	173.0	172.2	173.4	172.4	172.5	171.1
N7-N8-N9	-	-	-	-	-	-	172.4	171.6	172.8	171.8	173.2	171.6
N1-M-N1’-N2’	180.0	180.0	180.0	180.0	180.0	180.0	-	-	-	-	-	-
N1-M-N4-N5	-	-	-	-	-	-	180.0	180.0	180.0	180.0	180.0	180.0
N1-M-N7-N8	-	-	-	-	-	-	180.0	180.0	180.0	180.0	180.0	180.0
N4-M-N7-N8	-	-	-	-	-	-	0.0	0.0	0.0	0.0	0.0	0.0

[a] Calculated at the B3LYP/SBKJ+(d) and MP2/ SBKJ+(d) levels of theory. Bond lengths are in [Å] and angles in [°].

Table S2. Calculated structures[a] for $Ga(N_3)_3{\cdot}CH_3CN$, $In(N_3)_3{\cdot}CH_3CN$ and $Tl(N_3)_3{\cdot}CH_3CN$

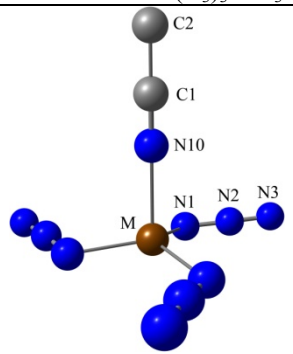

$Ga(N_3)_3{\cdot}CH_3CN$ C_3

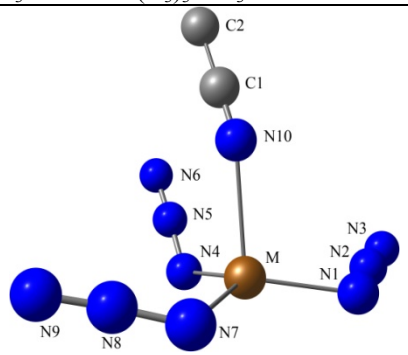

$In(N_3)_3{\cdot}CH_3CN$ C_3 $Tl(N_3)_3{\cdot}CH_3CN$ C_s

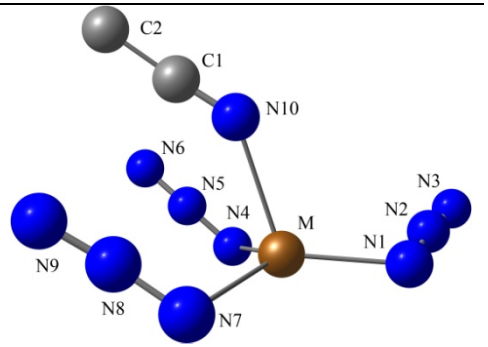

$Tl(N_3)_3{\cdot}CH_3CN$ C_1

	B3LYP	MP2	B3LYP	MP2	B3LYP	MP2
M-N1	1.881	1.868	2.097	2.080	2.207	2.144
M-N4	-	-	-	-	2.266	2.211
M-N7	-	-	-	-	2.207	2.187
M-N10	2.127	2.073	2.360	2.301	2.543	2.438
N1-N2	1.247	1.259	1.248	1.259	1.252	1.271
N2-N3	1.164	1.202	1.167	1.206	1.168	1.202
N4-N5	-	-	-	-	1.241	1.259
N5-N6	-	-	-	-	1.173	1.209
N7-N8	-	-	-	-	1.252	1.263
N8-N9	-	-	-	-	1.168	1.207
N10-C1	1.162	1.181	1.163	1.183	1.167	1.193
C1-C2	1.475	1.476	1.476	1.477	1.477	1.479
M-N1-N2	120.4	117.2	120.7	119.2	114.1	112.3
M-N4-N5	-	-	-	-	114.2	110.3
M-N7-N8	-	-	-	-	114.1	108.0
M-N10-C1	180.0	180.0	180.0	180.0	158.1	139.9
N1-M-N1’	116.9	116.9	118.0	118.0	-	-
N1-M-N4	-	-	-	-	118.8	121.4
N1-M-N7	-	-	-	-	117.2	111.6
N4-M-N7	-	-	-	-	118.8	121.9
N1-M-N10	100.3	100.3	98.1	98.3	101.5	111.3
N4-M-N10	-	-	-	-	89.7	89.6
N7-M-N10	-	-	-	-	101.5	90.4
N1-N2-N3	174.0	173.3	174.0	173.6	173.6	171.8
N4-N5-N6	-	-	-	-	176.2	174.9
N7-N8-N9	-	-	-	-	173.6	174.2
N10-C1-C2	180.0	180.0	180.0	180.0	179.6	177.3
N1-M-N4-N5	23.9	27.3	20.2	23.9	103.0	139.9
N1-M-N7-N8	-	-	-	-	146.0	151.1
N4-M-N7-N8	-	-	-	-	29.6	54.1
N1-M-N10-C1	-	-	-	-	119.4	174.9

[a] Calculated at the B3LYP/ SBKJ+(d) and MP2/ SBKJ+(d) levels of theory. Bond lengths are in [Å] and angles in [°].

Table S3. Calculated structures[a] for $[M(N_3)_4]^-$ (M = Ga, In, Tl)

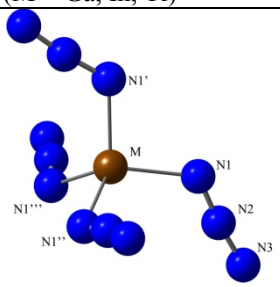

	$[Ga(N_3)_4]^-$ D_{2d}		$[In(N_3)_4]^-$ D_{2d}		$[Tl(N_3)_4]^-$ D_{2d}	$[Tl(N_3)_4]^-$ C_2
	B3LYP	MP2	B3LYP	MP2	B3LYP	MP2
M-N1	1.927	1.905	2.142	2.117	2.269	2.217
M-N1’	1.927	1.905	2.142	2.117	2.269	2.217
M-N1’’	1.927	1.905	2.142	2.117	2.269	2.217
N1-N2	1.237	1.251	1.237	1.251	1.240	1.259
N2-N3	1.171	1.208	1.174	1.212	1.176	1.211
M-N1-N2	121.7	120.6	123.0	123.1	116.9	113.4
N1-M-N1’	101.8	102.2	101.0	101.4	102.8	107.0
N1-M-N1’’	113.4	113.2	113.9	113.7	112.9	105.7
N1-M-N1’’’	113.4	113.2	113.9	113.7	112.9	116.0
N1’-M-N1’’	113.4	113.2	113.9	113.7	112.9	116.0
N1’-M-N1’’’	113.4	113.2	113.9	113.7	112.9	105.7
N1’’-M-N1’’’	101.8	102.2	101.0	101.4	102.8	107.0
N1-N2-N3	174.7	173.7	174.9	173.8	175.0	173.8
N2-N1-M-N1’	180.0	180.0	180.0	180.0	180.0	158.4
N2-N1-M-N1’’	57.8	57.9	57.5	57.6	58.0	34.2
N2-N1-M-N1’’’	57.8	57.9	57.5	57.6	58.0	84.1

[a] Calculated at the B3LYP/SBKJ+(d) and MP2/ SBKJ+(d) levels of theory. Bond lengths are in [Å] and angles in [°].

Table S4. Calculated structures[a] for $[M(N_3)_5]^{2-}$ (M = Ga, In, Tl)

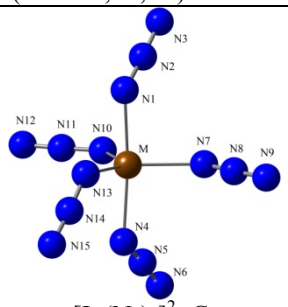

	$[Ga(N_3)_5]^{2-}$ C_s		$[In(N_3)_5]^{2-}$ C_s		$[Tl(N_3)_5]^{2-}$ C_s	
	B3LYP	MP2	B3LYP	MP2	B3LYP	MP2
M-N1	2.077	2.049	2.247	2.211	2.359	2.294
M-N4	2.087	2.055	2.252	2.214	2.365	2.299
M-N7	1.999	1.967	2.215	2.172	2.348	2.270
M-N10	1.999	1.967	2.215	2.172	2.348	2.270
M-N13	1.984	1.960	2.119	2.171	2.333	2.266
N1-N2	1.223	1.234	1.223	1.242	1.225	1.248
N2-N3	1.185	1.214	1.185	1.222	1.186	1.221
N4-N5	1.220	1.233	1.222	1.244	1.225	1.248
N5-N6	1.185	1.212	1.184	1.221	1.185	1.221
N7-N8	1.223	1.234	1.223	1.242	1.226	1.248
N8-N9	1.183	1.209	1.184	1.221	1.186	1.221
N10-N11	1.223	1.234	1.223	1.242	1.226	1.248
N11-N12	1.183	1.208	1.184	1.221	1.186	1.221
N13-N14	1.226	1.235	2.119	1.242	1.227	1.247
N14-N15	1.179	1.208	1.181	1.220	1.184	1.220
M-N1-N2	124.1	125.0	125.0	126.5	120.2	119.3
M-N4-N5	123.7	123.0	124.9	123.0	119.5	116.8
M-N7-N8	124.2	128.7	125.4	128.7	120.4	120.2
M-N10-N11	124.2	128.7	128.7	128.7	120.4	120.2
M-N13-N14	126.9	129.2	127.1	129.2	123.4	123.3
N1-M-N4	173.6	170.5	172.2	170.5	171.7	170.0
N1-M-N7	92.0	92.8	92.2	92.8	92.3	92.9
N1-M-N10	92.0	92.8	92.2	92.8	92.3	92.9
N1-M-N13	84.6	82.9	84.4	82.9	83.0	82.2
N4-M-N7	91.7	93.0	92.0	93.0	92.6	93.1
N4-M-N10	91.7	93.0	92.0	93.0	92.6	93.1
N4-M-N13	88.9	88.9	88.3	87.6	88.7	87.8
N7-M-N10	108.4	104.7	108.9	104.7	108.9	105.7
N7-M-N13	125.8	127.6	125.5	127.6	125.5	127.1
N10-M-N13	125.8	127.6	125.5	127.6	125.5	127.1
N1-N2-N3	175.7	175.4	175.7	175.4	175.4	174.6
N4-N5-N6	176.5	175.8	176.2	175.8	175.9	175.3
N7-N8-N9	175.5	174.8	175.9	174.8	175.7	174.2
N10-N11-N12	175.5	174.8	175.9	174.8	175.7	174.2
N13-N14-N15	173.9	174.5	174.7	174.5	174.4	173.9

[a] Calculated at the B3LYP/SBKJ+(d) and MP2/ SBKJ+(d) levels of theory. Bond lengths are in [Å] and angles in [°].

Table S5. Calculated structures[a] for $[M(N_3)_6]^{3-}$ (M = Ga, In, Tl)

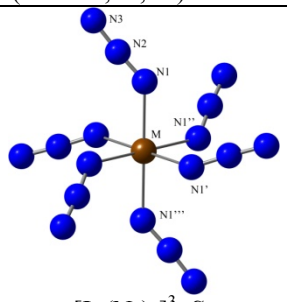

	$[Ga(N_3)_6]^{3-}$ S_6		$[In(N_3)_6]^{3-}$ S_6		$[Tl(N_3)_6]^{3-}$ S_6	
	B3LYP	MP2	B3LYP	MP2	B3LYP	MP2
M-N1	2.103	2.056	2.288	2.242	2.426	2.334
N1-N2	1.212	1.233	1.213	1.236	1.216	1.240
N2-N3	1.193	1.225	1.193	1.228	1.194	1.227
M-N1-N2	129.3	130.1	131.5	133.5	125.9	125.7
N1-M-N1’	90.6	89.8	89.1	89.7	90.3	90.3
N1-M-N1’’	89.4	90.2	90.9	90.3	89.7	89.7
N1-M-N1’’’	180.0	180.0	180.0	180.0	180.0	180.0
N1’-M-N1’’	89.4	90.2	89.1	90.3	90.3	90.3
N1’-M-N1’’’	89.4	90.2	90.9	90.3	89.7	89.7
N1’’-M-N1’’’	90.6	89.8	89.1	89.7	90.3	90.3
N1-N2-N3	175.5	175.1	175.7	175.2	175.5	175.1
N2-N1-M-N1’	142.3	149.6	144.2	151.7	143.7	151.9
N2-N1-M-N1’’	128.4	120.2	126.7	118.0	126.0	117.8

[a] Calculated at the B3LYP/SBKJ+(d) and MP2/ SBKJ+(d) levels of theory. Bond lengths are in [Å] and angles in [°].

Table S6. Comparison of observed and unscaled calculated[a] vibrational frequencies [cm^{-1}] and intensities of $M(N_3)_3$ (M = Ga, In, Tl) in point group C_{3h}

		approx. mode	$Ga(N_3)_3$				$In(N_3)_3$			$Tl(N_3)_3$		
		description in C_{3h}[b]	observed[c] IR	observed[c] Raman	calculated (IR)[Raman] B3LYP	calculated (IR)[Raman] MP2	observed Raman[d]	calculated (IR)[Raman] B3LYP	calculated (IR)[Raman] MP2	observed Raman[e]	calculated (IR)[Raman] B3LYP	calculated (IR)[Raman] MP2
A'	ν_1	ν_{as} N_3 i ph		2177 [10.0]	2227 (0) [336]	2132 (0)[28]	2160 [1.5]	2190 (0) [538]	2122 (0) [33]	2126 [0.8] 2097 [6.0]	2129 (0) [1308]	2130 (0) [113]
	ν_2	ν_s N_3 i ph		1410 [4.4]	1309 (0) [12]	1270 (0)[57]	1348 [3.5]	1293 (0) [2.7]	1249 (0) [47]	1306 [0.5]	1251 (0) [71]	1215 (0) [16]
	ν_3	δ N_3 i pl, i ph		647 [0.6]	629 (0) [24]	652 (0)[23]	613 [1.0]	604 (0) [28]	607 (0) [34]	652 [1.3]	605 (0) [19]	602 (0) [35]
	ν_4	ν_s MN_3		329 [1.6]	437 (0) [59]	461 (0)[36]	294 [10.0][f]	382 (0) [160]	416 (0) [86]	327 [10.0]	311 (0) [384]	377 (0) [234]
	ν_5	δ M-N-N i ph		158 [1.5]	136 (0) [3.3]	127 (0)[4.5]	110 [5.0]	130 (0) [6.1]	118 (0) [4.6]	115 [4.0 sh]	127 (0) [30]	117 (0) [11]
E'	ν_6	ν_{as} N_3 o ph	2146 vs 2117 vs 2090 s 2037 w	2138 [0.3] 2119 [1.5]	2213 (2274) [185]	2120 (1949) [39]	2101 [3.4] 2059 [2.5]	2178 (2436) [299]	2107 (2172) [62]	2055 [2.0] 2037 [2.0] 2079 [0.5] 2009 [1.0]	2125 (2278) [630]	2107 (2664) [112]
	ν_7	ν_s N_3 o ph	1360 w 1296 w 1270 m 1257 m	1304 [2.0] 1280 [0.4]	1300 (716) [3.3]	1267 (351)[28]	1278 [2.6]	1286 (623) [3.8]	1255 (251) [28]	1306 [0.5]	1250 (527) [34]	1219 (240) [21]
	ν_8	δ N_3 i pl, o ph	640 vw 604 vw 577 m	647 [0.6]	662 (84) [4.0]	679 (104)[3.1]	662 [0.8]	614 (23) [13]	670 (20) [3.1]	652 [1.5]	610 (20) [14]	622 (6.3) [7.4]
	ν_9	ν_{as} MN_2	457 m	349 [1.0]	496 (133) [7.3]	504 (117)[6.6]	463 [0.5]	429 (123) [15]	456 (132) [11]	357 [4.5]	362 (85) [41]	400 (112) [24]
	ν_{10}	δ MNN MN_2 i ph		244 [1.4] 205 [1.0]	221 (42) [12]	215 (51)[12]	142 [5.8]	178 (42) [18]	171 (52) [15]	169 [4.0] 139 [4.0]	155 (28) [36]	147 (37) [26]
	ν_{11}	δ MN_3			51 (4.4) [18]	47 (4.4)[19]		38 (7.8) [18]	36 (7.9) [19]		29 (8.3) [20]	27 (10) [18]
A''	ν_{12}	δ N_3 o pl, i ph		549 [0.3]	542 (14) [0]	659 (3.7)[0]	533 [0.5]	546 (11) [0]	587 (2.1) [0]		539 (9.0) [0]	539 (0.7) [0]
	ν_{13}	$\delta_{umbrella}$ MN_3			174 (25) [0]	196 (25)[0]		115 (20) [0]	144 (21) [0]		87 (11) [0]	106 (12) [0]
	ν_{14}	τ MN, i ph			57 (1.0) [0]	75 (2.3)[0]		45 (1.6) [0]	57 (4.7) [0]		35 (0.9) [0]	45 (2.3) [0]
E''	ν_{15}	δ N_3 o pl, o ph		576 [0.2]	546 (0) [4.1]	645 (0)[0.5]	579 [0.7]	547 (0) [7.5]	573 (0) [2.3]	541 [0.2]	540 (0) [7.0]	524 (0) [2.9]
	ν_{16}	τ MN_2		117 [4.7]	98 (0) [12]	118 (0)[15]		78 (0) [10]	89 (0) [14]		62 (0) [6.8]	69 (0) [11]

[a] Calculated at the B3LYP/SBKJ+(d) and MP2/SBKJ+(d) levels of theory; calculated IR intensities are given in parentheses (km mol^{-1}), and Raman intensities in brackets [$Å^4$ amu^{-1}]. [b] The mode assignments were made assuming an ideal arrangement of C_{3h} symmetry; i ph = in phase; o ph = out of phase; i pl = in plane; o pl = out of plane. [c] In addition to the bands listed in this table, Raman bands at 193 [0.4], 139 [0.5] cm^{-1} and IR bands at 2532 vw, 1644br m, 1183 w, 705 w cm^{-1} were observed. [d] In addition to the bands listed in this table, the following Raman bands were observed: 1506 [0.2], 963 [0.8] cm^{-1}. [e] In addition to the bands listed in this table, the following Raman bands were observed: 1043 [0.5], 275 [1.0], 242 [1.1] cm^{-1}. [f] Band falls together with a band from the FEP sample container.

Table S7. Comparison of observed and unscaled calculated[a] vibrational frequencies [cm^{-1}] and intensities of $M(N_3)_3$ (M = Ga, In, Tl) in point group C_s

		approx. mode	$Ga(N_3)_3$				$In(N_3)_3$				$Tl(N_3)_3$	
		description in C_s[b]	observed[c] IR	observed[c] Raman	calculated (IR)[Raman] B3LYP	calculated (IR)[Raman] MP2	observed Raman	calculated (IR)[Raman] B3LYP	calculated (IR)[Raman] MP2	observed Raman	calculated (IR)[Raman] B3LYP	calculated (IR)[Raman] MP2
A'	ν_1	ν_{as} N_3 i ph		2177 [10.0]	2231 (355) [288]	2145 (516) [25]	2160 [1.5]	2193 (291) [511]	2130 (388) [44]	2126 [0.8] 2097 [6.0]	2133 (158) [1317]	2137 (295) [118]
	ν_2	ν_{as} N_3 o ph	2146 vs	2138 [0.3]	2213 (1430) [56]	2132 (895) [16]	2101 [3.4]	2180 (1594) [58]	2117 (1160) [23]	2079 [0.5] 2055 [2.0]	2130 (1526) [60]	2121 (1461) [53]
	ν_3	ν_{as} N_3 o ph	2117 vs 2090 s	2119 [1.5]	2193 (321) [52]	2108 (219) [6.8]	2059 [2.5]	2161 (360) [103]	2093 (286) [7.2]	2037 [2.0] 2009 [1.0]	2108 (344) [249]	2092 (427) [9.5]
	ν_4	ν_s N_3 i ph	1360 w	1410 [4.4]	1320 (50) [11]	1273 (4.7) [60]	1348 [3.5]	1299 (16) [1.9]	1250 (40) [39]	1306 [0.5]	1256 (125) [22]	1216 (29) [15]
	ν_5	ν_s N_3 o ph	1296 w	1304 [2.0]	1309 (129) [0.9]	1270 (71) [11]	1278 [2.6]	1292 (386) [4.8]	1244 (44) [3.2]	1306 [0.5]	1255 (56) [82]	1212 (82) [5.9]
	ν_6	ν_s N_3 o ph	1270 m 1257 m	1280 [0.4]	1306 (458) [2.1]	1266 (221) [5.5]	1278 [2.6]	1290 (153) [1.4]	1243 (133) [25]	1306 [0.5]	1251 (284) [18]	1211 (93) [16]
	ν_7	δ N_3 i pl, $M(N_3)$	640 vw 604 vw	647 [0.6]	660 (32) [5.0]	678 (42) [2.0]	662 [0.8]	611 (8.9) [15]	613 (7.8) [3.1]	652 [1.3]	610 (5.3) [21]	613 (0.7) [1.9]
	ν_8	δ N_3 i pl, i ph, $M(N_3)_2$	577 m		643 (43) [2.1]	663 (57) [1.1]	613 [1.0]	602 (4.4) [12]	605 (15) [8.5]	652 [1.3]	605 (13) [16]	605 (2.8) [33]
	ν_9	δ N_3 i pl, o ph, $M(N_3)_2$		576 [0.2]	623 (4.2) [19]	643 (1.6) [25]	579 [0.7]	598 (6.3) [18]	600 (2.8) [30]	652 [1.3]	599 (1.2) [8.7]	599 (1.9) [15]
	ν_{10}	ν_{as} MN_2			496 (77) [1.0]	502 (68) [1.0]	463 [0.5]	432 (61) [4.6]	448 (63) [1.4]		370 (35) [23]	406 (50) [13]
	ν_{11}	ν_{as} MN_2	457 m		485 (51) [1.0]	491 (44) [0.9]	463 [0.5]	420 (60) [6.1]	439 (59) [1.9]	357 [4.5]	349 (44) [31]	388 (55) [20]
	ν_{12}	ν_s MN_3		329 [1.6]	431 (0.8) [52]	453 (0.3) [31]	294 [10.0][f]	378 (0.5) [148]	411 (0.1) [75]	327 [10.0]	309 (0.05) [360]	370 (0.8) [198]
	ν_{13}	δ M-N-N i pl, o ph		244 [1.4]	231 (42) [2.1]	223 (49) [1.5]		181 (39) [3.0]	172 (44) [1.8]	162 [4.0]	154 (26) [9.6]	149 (34) [3.3]
	ν_{14}	δ M-N-N i pl, i ph		205 [1.0]	196 (5.5) [5.9]	188 (7.5) [6.5]	142 [5.8]	162 (5.0) [10]	151 (7.4) [9.2]	139 [4.0]	146 (4.0) [38]	138 (5.4) [17]
	ν_{15}	δ M-N-N i pl, o ph		158 [1.5]	138 (0.7) [8.0]	125 (0.7) [8.7]	110 [5.0]	130 (1.3) [8.4]	115 (1.2) [8.9]	115 [4.0 sh]	127 (1.4) [13]	113 (0.9) [8.8]
	ν_{16}	δ MN_2			59 (2.3) [2.5]	56 (1.7) [3.1]		45 (3.7) [5.7]	41 (3.7) [2.7]		40 (4.3) [9.8]	42 (4.6) [5.3]
	ν_{17}	δ MN_2			54 (2.0) [8.8]	50 (2.3) [8.8]		40 (4.0) [6.1]	37 (3.9) [8.0]		32 (4.1) [4.3]	30 (4.9) [5.1]
A''	ν_{18}	δ N_3 o pl, o ph, $M(N_3)_2$		549 [0.3]	544 (0.3) [1.8]	517 (1.1) [0.3]	533 [0.7]	546 (4.5) [2.6]	509 (0.7) [0.8]	541 [0.2]	540 (5.3) [0.8]	493 (0.4) [0.7]
	ν_{19}	δ N_3 o pl, i ph, $M(N_3)_3$		549 [0.3]	543 (12) [0.1]	513 (1.9) [0.2]	533 [0.5]	546 (5.4) [0.7]	505 (0.8) [1.1]	541 [0.2]	538 (3.4) [3.4]	491 (0.3) [1.6]
	ν_{20}	δ N_3 o pl, o ph, $M(N_3)_2$		549 [0.3]	536 (0.01) [1.8]	504 (0.00) [0.4]	533 [0.5]	542 (0.04) [3.7]	501 (0.03) [0.8]	541 [0.2]	536 (0.00) [2.4]	489 (0.1) [0.9]
	ν_{21}	$\delta_{umbrella}$ MN_3			165 (25) [0.8]	184 (27) [0.9]	110 [5.0]	108 (20) [0.8]	125 (24) [1.0]		83 (8.4) [1.1]	96 (14) [1.0]
	ν_{22}	τ MN_2 o ph		117 [4.7]	122 (0.03) [7.9]	122 (0.05) [9.7]		97 (0.5) [7.1]	92 (0.00) [9.2]		76 (2.8) [4.6]	74 (0.3) [7.0]
	ν_{23}	τ MN			73 (0.5) [1.6]	84 (0.9) [1.6]		58 (0.5) [1.2]	65 (1.0) [1.3]		44 (0.3) [0.5]	49 (0.3) [0.9]
	ν_{24}	τ MN_2 i ph			45 (0.2) [0.2]	47 (0.4) [0.3]		38 (0.5) [0.2]	37 (0.9) [0.3]		28 (0.2) [0.03]	26 (0.2) [0.1]

[a] Calculated at the B3LYP/SBKJ+(d) and MP2/SBKJ+(d) levels of theory; calculated IR intensities are given in parentheses (km mol^{-1}), and Raman intensities in brackets [$Å^4$ amu^{-1}]. [b] The mode assignments were made assuming an ideal arrangement of C_s symmetry; i ph = in phase; o ph = out of phase; i pl = in plane; o pl = out of plane. [c] In addition to the bands listed in this table, Raman bands at 349 [1.0], 193 [0.4], 139 [0.5] cm^{-1} and IR bands at 2532 vw, 2037 w, 1644br m, 1296 w, 1183 w, 705 w cm^{-1} were observed. [d] In addition to the bands listed in this table, the following Raman bands were observed: 1506 [0.2], 963 [0.8] cm^{-1}. [e] In addition to the bands listed in this table, the following Raman bands were observed: 1043 [0.5], 275 [1.0], 242 [1.1] cm^{-1}. [f] Band falls together with a band from the FEP sample container.

Table S8. Comparison of observed and unscaled calculated[a] vibrational frequencies [cm^{-1}] and intensities of $M(N_3)_3{\cdot}NCCH_3$ (M = Ga, In)

		approx. mode	$Ga(N_3)_3{\cdot}NCCH_3$				$In(N_3)_3{\cdot}NCCH_3$			
		description in	observed[c]		calculated (IR)[Raman]		observed[d]		calculated (IR)[Raman]	
		C_3[b]	IR	Raman	B3LYP	MP2	IR	Raman	B3LYP	MP2
A	ν_1	ν_s CH_3	2930 w	2933[6.3]	3004 (0.5)[258]	3056 (0.3)[217]	2935 vw	2930[3.0]	3004 (0.4)[247]	3057 (0.2)[213]
	ν_2	ν CN	2315 w 2292 w	2315[2.5] 2288[2.3]	2394 (86)[297]	2257 (31)[137]	2287 w 2115 m	2311[1.5] 2284[1.8]	2383 (95)[225]	2243 (31)[118]
	ν_3	ν_{as} N_3 i ph	2254 w 2216sh vw	2166[10.0]	2210 (32)[173]	2173 (7.6)[5.2]	2036 w	2154[10.0]	2183 (18)[309]	2151 (5.2)[5.2]
	ν_4	δ_s CH_3	1357 m	1366[1.0]	1375 (0.2)[20]	1410 (0.2)[10]		1330[0.5]	1375 (0.2)[16]	1411 (0.2)[8.9]
	ν_5	ν_s N_3 i ph		1312[3.8]	1329 (7.7)[27]	1267 (2.6)[67]		1302[2.2]	1315(3.8)[6.2]	1250 (1.2)[63]
	ν_6	ν CC	1039 w, br	941[0.5]	936 (16)[10]	960 (19)[4.3]	940 vw	941[0.3]	932 (18)[6.3]	954 (19)[3.7]
	ν_7	δ N_3 i pl, i ph		671[0.4]	633 (2.4)[18]	655 (4.2)[17]		658[0.9]	609 (0.3)[27]	614 (0.4)[25]
	ν_8	δ N_3 o pl, i ph	592 mw		554 (15)[0.4]	528 (3.3)[0.1]			556 (12)[0.3]	566 (2.3)[0.8]
	ν_9	ν_s MN_3	421sh, w	426[0.9]	433 (7.4)[41]	456 (7.6)[24]		388 [0.8] 383[0.7]	383 (4.0)[116]	414 (4.8)[55]
	ν_{10}	ν MN_{CH3CN}		247[1.2]	214 (56)[1.7]	243 (40)[0.7]		203[2.7]	183 (29)[3.3]	211 (23)[1.6]
	ν_{11}	δ_{umbr} $M(N_3)_3$		197[1.1]	180 (32)[0.9]	197 (45)[1.4]		111[1.1]	124 (14)[5.5]	137 (41)[2.8]
	ν_{12}	δ_s $M(N_3)_3$ i pl		133[0.8]	129 (0.2)[2.8]	116 (0.4)[3.0]			121 (22)[0.5]	105 (1.2)[2.4]
	ν_{13}	δ_s $M(N_3)_3$ o pl			31 (1.9)[0.5]	34 (2.8)[0.2]			24 (1.9)[0.3]	29 (3.6)[0.2]
	ν_{14}	τ C-CH_3			8.1i (n/a) (n/a)[e]	16i (n/a)[n/a][e]			6.9 (0.04)[0.2]	15.3i (n/a)[n/a][e]
E	ν_{15}	ν_{as} CH_3	2997 vw	2992[0.9]	3111 (2.1)[153]	3187 (2.7)[123]		2992[0.4]	3111 (1.6)[150]	3188 (2.3)[123]
	ν_{16}	ν_{as} N_3 o ph	2138 s 2105 vs 2072sh m 2036sh w	2118[2.9] 2099[2.4]	2198 (2475)[139]	2165 (1703)[25]	2097 m 2068 m	2112[3.2] 2080[2.5]	2171 (2655)[221]	2139 (1930)[38]
	ν_{17}	δ_{as} CH_3		1354[0.5]	1434 (31)[21]	1464 (29)[19]	1380 vw	1384[0.8] 1363[1.0]	1434 (31)[21]	1465 (30)[16]
	ν_{18}	ν_s N_3 o ph	1299 ms	1298[2.4]	1322 (568)[7.4]	1266 (240)[27]	1277 m, br	1292[1.0] 1283[0.9]	1309 (521)[3.5]	1249 (178)[28]
	ν_{19}	δ_{rock} + δ_{wag} CH_3	1039 w, br		1045 (5.1)[0.3]	1076 (2.5)[0.1]	1016 mw		1045 (4.9)[0.2]	1073 (2.6)[0.1]
	ν_{20}	δ N_3 i pl, o ph	671 m		655 (73)[3.7]	677 (86)[2.7]		658[0.2]	618 (24)[12]	625 (20)[3.4]
	ν_{21}	δ N_3 o pl, o ph			554 (0.2)[2.9]	524 (0.7)[0.5]	540 s		556 (0.2)[5.8]	577 (3.1)[1.4]
	ν_{22}	ν_{as} MN_3	496 m, br		482 (151)[6.4]	494 (127)[5.2]		493 [0.7]	426 (19)[4.6]	441 (127)[7.3]
	ν_{23}	δ N-C-C	421sh, w	406[0.7]	440 (6.2)[4.0]	448 (9.1)[4.1]	419 vw, sh	405[1.7] 395[1.2]	420 (115)[11]	423 (6.9)[4.3]
	ν_{24}	δ_{as} MN_4		208[1.5]	226 (67)[5.9]	231 (69)[4.0]		162[2.0]	177 (62)[9.4]	172 (74)[5.6]
	ν_{25}	δ_{as} MN_4		173[1.2] 147 [1.2]	173 (1.6)[6.1]	187 (3.4)[7.6]		124[1.3]	132 (5.7)[5.2]	144 (0.6)[8.2]
	ν_{26}	δ_{as} MN_4		110[0.9]	77 (3.8)[6.2]	93 (1.5)[7.2]			63 (4.3)[4.5]	74 (2.0)[7.6]
	ν_{27}	δ_{as} $M(N_3)_3$ i pl			49 (1.5)[15]	49 (1.5)[18]			38 (3.9)[16]	35 (5.1)[17]
	ν_{28}	δ_{as} $M(N_3)_3$ o pl			21 (4.5)[20]	19 (4.0)[19]			15 (3.9)[21]	12.3 (4.1)[19]

[a] Calculated at the B3LYP/SBKJ+(d) and MP2/SBKJ+(d) levels of theory; calculated IR intensities are given in parentheses (km mol^{-1}), and Raman intensities in brackets [$Å^4$ amu^{-1}]. [b] The mode assignments were made assuming an ideal arrangement of C_3 symmetry; i ph = in phase; o ph = out of phase; i pl = in plane; o pl = out of plane. [c] In addition to the bands listed in this table, Raman bands at 332 [1.0], 317 [0.7] cm^{-1} and IR bands at 1680 w, 1638 w, 1506 mw, 1180 w, 703 vw cm^{-1} were observed. [d] In addition to the bands listed in this table, the following Raman bands were observed: 323 [1.1], 294 [1.5] cm^{-1}. [e] Approximately zero-frequency mode corresponding to free internal rotation of the methyl group about the C_3 symmetry axis.

Table S9. Comparison of observed and unscaled calculated vibrational frequencies [cm^{-1}] and intensities of $Tl(N_3)_3{\cdot}NCCH_3$

		$Tl(N_3)_3{\cdot}NCCH_3$ C_1 symmetry			$Tl(N_3)_3{\cdot}NCCH_3$ C_s symmetry	
observed[a] IR	observed[a] Raman	approx. mode description[b]	calculated (MP2) (IR)[Raman][c]		approx. mode description[b]	calculated (B3LYP) (IR)[Raman][c]
	2973 [1.5]	ν_{as} CH_3	3192 (2.1) [35]	A‘	ν_{as} CH_3	3114 (1.5) [48]
	2973 [1.5]	ν_{as} CH_3	3184 (1.1) [75]	A‘‘	ν_{as} CH_3	3111 (0.1) [78]
2926 vw	2942 [7.8]	ν_s CH_3	3056 (1.1) [202]	A‘	ν_s CH_3	3005 (0.4) [216]
2296 w	2255 [2.3]	ν CN	2179 (46) [44]	A‘	ν CN	2356 (78) [106]
2262 mw	2122 [10.0]	ν_{as} N_3 i ph	2162 (260) [43]	A‘	ν_{as} N_3 i ph	2150 (84) [1009]
2074 vs	2100 [5.6]	ν_{as} N_3 o ph	2141 (1199) [48]	A‘‘	ν_{as} N_3 o ph	2123 (1463) [8.3]
2046 vs	2072 [2.9] 2057 [2.9]	ν_{as} N_3 o ph	2129 (213) [8.0]	A‘	ν_{as} N_3 o ph	2107 (641) [224]
1373(br) w		δ_{twist} CH_2	1464 (12) [7.9]	A‘‘	δ_{twist} CH_2	1440 (13) [8.3]
	1385 [1.7]	δ_{twist} CH_2	1458 (14) [11]	A‘‘	δ_{twist} CH_2	1434 (15) [13]
1325 mw		$\delta_{umbrella}$ CH_3	1406 (8.9) [4.9]	A‘	$\delta_{umbrella}$ CH_3	1373 (4.0) [8.7]
1264 mw	1278 [1.3]	ν_s N_3 TlN_3	1218 (17) [19]	A‘	ν_s N_3 TlN_3	1300 (82) [8.7]
		ν_s N_3 i ph $Tl(N_3)_2$	1215 (36) [14]	A‘	ν_s N_3 i ph $Tl(N_3)_2$	1290 (0.4) [43]
1250 m		ν_s N_3 o ph $Tl(N_3)_2$	1215 (63) [11]	A‘‘	ν_s N_3 o ph $Tl(N_3)_2$	1266 (289) [9.9]
1045 w		δ_{wag} CH_3	1071 (1.9) [0.7]	A‘‘	δ_{wag} CH_3	1049 (1.1) [0.1]
1005 vw		δ_{rock} CH_3	1066 (4.9) [0.9]	A‘	δ_{rock} CH_3	1043 (3.8) [1.1]
926 vw	921 [1.0]	ν CC	933 (12) [3.2]	A‘	ν CC	923 (14) [5.3]
686 w 659 mw	669 [0.8]	δ N_3 i pl, i ph $Tl(N_3)_2$	619 (0.2) [3.1]	A‘	δ N_3 i pl, i ph $Tl(N_3)_3$	621 (4.2) [18]
649(sh) vw		δ N_3 i pl, o ph $Tl(N_3)_2$	611 (1.9) [39]	A‘	δ N_3 i pl, o ph $Tl(N_3)_3$	618 (3.5) [29]
640 w		δ N_3 i pl TlN_3	602 (0.9) [11]	A‘‘	δ N_3 i pl, o ph $Tl(N_3)_2$	615 (6.3) [4.5]
591 vw	579 [0.8]	δ N_3 o pl TlN_3	563 (0.1) [0.3]	A‘‘	δ N_3 o pl TlN_3	566 (1.9) [0.9]
582 w		δ N_3 o pl TlN_3	548 (0.1) [0.5]	A‘	δ N_3 o pl, i ph $Tl(N_3)_2$	549 (6.4) [0.1]
574 vw		δ N_3 o pl TlN_3	534 (0.3) [0.9]	A‘‘	δ N_3 o pl, o ph $Tl(N_3)_2$	548 (0.1) [3.6]
422 w		ν TlN o ph $Tl(N_3)_2$	411 (52) [9.3]	A‘‘	δ NCC o pl	415 (1.7) [1.5]
		δ NCC o pl	398 (4.2) [0.6]	A‘	δ NCC i pl	390 (4.6) [1.5]
	361 [1.5]	ν TlN i ph $Tl(N_3)_2$	383 (28) [107]	A‘‘	ν TlN o ph $Tl(N_3)_2$	371 (43) [16]
		δ NCC i pl	376 (13) [3.3]	A‘	ν TlN o ph $Tl(N_3)_3$	343 (42) [67]
	298 [6.5]	ν TlN $Tl(N_3)$	374 (19) [77]	A‘	ν TlN i ph $Tl(N_3)_3$	316 (1.3) [290]
	235 [1.8]	ν TlN $Tl(NCCH_3)$	207 (13) [1.6]	A‘	δ TlN_2 $Tl(N_3)_2$	173 (4.3) [35]
		δ TlN_4	159 (26) [3.6]	A‘	ν TlN $Tl(NCCH_3)$	160 (16) [1.5]
		δ TlN_4	149 (16) [3.3]	A‘	δ TlNN i pl $Tl(N_3)$	152 (11) [15]
		δ TlN_4	140 (9.9) [4.4]	A‘‘	δ TlNN i pl o ph $Tl(N_3)_2$	149 (29) [3.3]
	150 [0.4 sh]	δ TlN_4	137 (0.5) [11]	A‘	δ TlN2 $Tl(N_3)(NCCH_3)$	119 (2.6) [2.2]
		δ TlN_4	122 (0.6) [2.1]	A‘‘	δ TlNC o pl	95 (2.4) [1.1]
		δ TlN_4	115 (29) [0.9]	A‘	δ TlNN i pl o ph $Tl(N_3)_2$	87 (18) [1.6]
		τ	96 (5.5) [3.1]	A‘‘	$\delta_{umbrella}$ TlN_3 $Tl(N_3)_3$	66 (7.4) [0.7]
		τ	82 (5.6) [0.6]	A‘‘	δ_{wag} TlN_3 $Tl(N_3)_3$	58 (0.3) [2.0]
		τ	70 (2.8) [2.2]	A‘	δ TlNC i pl	48 (4.6) [3.4]
		τ	64 (1.3) [0.6]	A‘‘	τ	43 (0.1) [0.9]
		τ	48 (1.7) [1.8]	A‘	τ	37 (5.5) [1.1]
		τ	36 (2.8) [5.4]	A‘‘	τ	26 (0.8) [11]
		τ	24 (2.5) [4.2]	A‘‘	τ	16 (1.7) [12]
		τ	16 (0.5) [6.4]	A‘	τ	14 (1.0) [0.9]

[a] In addition to the bands listed in this table Raman bands at 273 [2.5 sh] cm^{-1} and IR bands at 3300(br) vw, 3278 vw, 3260 vw, 2556(br) vw, 2493(br) vw, 2459 vw, 1628(br) vw, 1491 w, 981 vw cm^{-1} were observed. [b] The mode assignments were made assuming an ideal arrangement of C_1 symmetry; i ph = in phase; o ph = out of phase; i pl = in plane; o pl = out of plane. [c] Calculated at the B3LYP/SBKJ+(d) and MP2/SBKJ+(d) levels of theory; calculated IR intensities are given in parentheses (km mol^{-1}), and Raman intensities in brackets [$Å^4$ amu^{-1}].

Table S10. Unscaled calculated[a] vibrational frequencies [cm^{-1}] and intensities of $[M(N_3)_4]^-$ (M = Ga, In).

			$[Ga(N_3)_4]^-$		$[In(N_3)_4]^-$	
		approx. mode description in point group D_{2d}[b]	calculated (IR)[Raman] B3LYP	MP2	calculated (IR)[Raman] B3LYP	MP2
A_1	ν_1	ν_{as} N_3 i ph	2199 (0) [255]	2200 (0) [14]	2177 (0) [313]	2181 (0) [17]
	ν_2	ν_s N_3 i ph	1354 (0) [66]	1278 (0) [119]	1344 (0) [8.2]	1258 (0) [116]
	ν_3	δ N_3 i pl, o ph	633 (0) [0.05]	629 (0) [12]	607 (0) [71]	591 (0) [22]
	ν_4	ν_s MN_4	410 (0) [60]	432 (0) [29]	361 (0) [170]	390 (0) [59]
	ν_5	δ_{sciss} MN_4 i ph	173 (0) [4.8]	164 (0) [5.0]	142 (0) [4.7]	131 (0) [4.1]
	ν_6	δ MNN o ph	48 (0) [1.3]	41 (0) [2.7]	38 (0) [0.7]	34 (0) [1.0]
A_2	ν_7	δ N_3 o pl, i ph	558 (0) [0]	521 (0) [0]	565 (0) [0]	534 (0) [0]
	ν_8	δ MNN i ph	90 (0) [0]	84 (0) [0]	83 (0) [0]	87 (0) [0]
B_1	ν_9	δ N_3 o pl, o ph	561 (0) [1.3]	521 (0) [0.2]	567 (0) [4.6]	529 (0) [1.4]
	ν_{10}	δ_{wag} MN_4	174 (0) [13]	181 (0) [16]	134 (0) [11]	138 (0) [17]
	ν_{11}	τ MN i ph	30 (0) [18]	23 (0) [19]	24 (0) [18]	19 (0) [18]
B_2	ν_{12}	ν_{as} N_3 o ph	2158 (36) [132]	2168 (20) [13]	2140 (5.7) [178]	2151 (0.03) [6.3]
	ν_{13}	ν_s N_3 o ph	1348 (0) [28]	1279 (1.7) [53]	1340 (0.6) [21]	1258 (3.7) [61]
	ν_{14}	δ N_3 i pl, i ph	641 (41) [2.3]	632 (34) [1.1]	621 (19) [6.4]	593 (13) [2.6]
	ν_{15}	ν_{as} MN_4	431 (42) [3.4]	444 (38) [3.4]	376 (52) [8.6]	396 (53) [5.4]
	ν_{16}	δ_{sciss} MN_4 o ph	190 (2.4) [3.6]	182 (4.7) [3.7]	154 (1.8) [4.6]	142 (4.4) [4.2]
	ν_{17}	δ MNN o ph	65 (7.1) [3.1]	50 (6.5) [4.7]	48 (11) [0.9]	44 (11) [1.8]
E	ν_{18}	ν_{as} N_3 o ph	2167 (4124) [12]	2187 (2429) [3]	2148 (4408) [5.7]	2168 (2650) [6.7]
	ν_{19}	ν_s N_3 o ph	1343 (552) [1.7]	1274 (211) [3.7]	1337 (511) [3.7]	1257 (142) [2.6]
	ν_{20}	δ N_3 i pl, o ph	639 (8.5) [2.7]	634 (34.8) [0.1]	613 (0.3) [14.4]	599 (5.6) [1.0]
	ν_{21}	δ N_3 o pl, o ph	567 (17) [2.5]	529 (2.5) [0.01]	575 (15) [1.6]	556 (1.7) [0]
	ν_{22}	ν_{as} MN_4	438 (239) [3.5]	453 (220) [4.1]	380 (166) [0.3]	400 (169) [2.0]
	ν_{23}	$\delta_{umbrella}$ MN_3	220 (147) [0.8]	215 (160) [0.1]	160 (129) [1.3]	153 (144) [0.4]
	ν_{24}	δ MNN o ph	99 (0.8) [19]	86 (0.01) [18]	84 (4.7) [22]	75 (1.3) [21]
	ν_{25}	τ MN o ph	30 (1.2) [0.03]	31 (1.7) [0.01]	28 (2.4) [0.3]	28 (3.0) [0.3]

[a] Calculated at the B3LYP/SBKJ+(d) and MP2/SBKJ+(d) levels of theory; calculated IR intensities are given in parentheses (km mol^{-1}), and Raman intensities in brackets [$Å^4$ amu^{-1}]. [b] The mode assignments were made assuming an ideal arrangement of D_{2d} symmetry; i ph = in phase; o ph = out of phase; i pl = in plane; o pl = out of plane.

Table S11. Unscaled calculated vibrational frequencies [cm^{-1}] and intensities of $[Tl(N_3)_4]^-$.

$[Tl(N_3)_4]^-$ D_{2d} symmetry			$[Tl(N_3)_4]^-$ C_2 symmetry		
	approx. mode description[a]	calculated (B3LYP) (IR)[Raman][b]		approx. mode description[a]	calculated (MP2) (IR)[Raman][b]
A_1	ν_{as} N_3 i ph	2125 (0) [1202]	A	ν_{as} N_3 i ph	2166 (0.0) [82]
	ν_s N_3 i ph	1309 (0) [81]		ν_{as} N_3 o ph	2134 (751) [38]
	δ N_3 i pl, o ph	610 (0) [27]		ν_s N_3 o ph	1235 (32) [10]
	ν_s MN_4	302 (0) [466]		ν_s N_3 i ph	1226 (0.00) [75]
	δ_{sciss} MN_4 i ph	129 (0) [22]		δ N_3 i pl, o ph	617 (0.9) [1.2]
	δ MNN o ph	33 (0) [0.9]		δ N_3 i pl, i ph	602 (0.0) [50]
A_2	δ N_3 o pl, i ph	571 (0) [0]		δ N_3 o pl, o ph	536 (0.0) [1.2]
	δ MNN i ph	70 (0) [0]		δ N_3 o pl, i ph	529 (0.5) [0.3]
B_1	δ N_3 o pl, o ph	570 (0) [6.5]		ν_s MN_4	364 (0.0) [200]
	δ_{wag} MN_4	107 (0) [7.6]		ν_{as} MN_4	356 (76) [0.1]
	τ MN i ph	17 (0) [24]		δ MN_4	125 (0.0) [11]
B_2	ν_{as} N_3 o ph	2096 (28) [406]		δ MN_4	110 (35) [0.6]
	ν_s N_3 o ph	1306 (0.5) [1.6]		δ MN_4	88 (5.2) [5.5]
	δ N_3 i pl, i ph	616 (6.2) [23]		δ MNN	85 (0.0) [5.3]
	ν_{as} MN_4	316 (39) [36]		δ MNN	35 (0.0) [4.3]
	δ_{sciss} MN_4 o ph	139 (0.4) [15]		τ MN	30 (0.0) [7.2]
	δ MNN o ph	42 (11) [0.6]		τ MN	11 (3) [0.1]
E	ν_{as} N_3 o ph	2104 (4277) [72]	B	ν_{as} N_3 o ph	2153 (1946) [18]
	ν_s N_3 o ph	1308 (466) [12]		ν_{as} N_3 o ph	2122 (5.7) [1.0]
	δ N_3 i pl, o ph	612 (7.1) [44]		ν_s N_3 o ph	1238 (91) [1.5]
	δ N_3 o pl, o ph	586 (11) [0.1]		ν_s N_3 o ph	1225 (0.1) [18]
	ν_{as} MN_4	331 (121) [9.3]		δ N_3 i pl, o ph	615 (0.4) [2.9]
	$\delta_{umbrella}$ MN_3	134 (95) [2.2]		δ N_3 i pl, o ph	603 (2.2) [9.4]
	δ MNN o ph	71 (11) [22]		δ N_3 o pl, o ph	538 (0.01) [0.2]
	τ MN o ph	19 (2.6) [0.04]		δ N_3 o pl, o ph	533 (0.02) [0.8]
	-	-		ν_{as} MN_4	381 (68) [3.9]
	-	-		ν_{as} MN_4	349 (39) [8.6]
	-	-		δ MN_4	146 (77.9) [0.8]
	-	-		δ MN_4	127 (3.4) [6.6]
	-	-		δ MNN	63 (0.8) [7.1]
	-	-		δ MNN	47 (9.5) [6.2]
	-	-		δ MNN	36 (0.6) [0.1]
	-	-		τ MN	16 (2.0) [4.7]

[a] The mode assignments were made assuming an ideal arrangement of C_1 symmetry; i ph = in phase; o ph = out of phase; i pl = in plane; o pl = out of plane. [b] Calculated at the B3LYP/SBKJ+(d) and MP2/SBKJ+(d) levels of theory; calculated IR intensities are given in parentheses (km mol^{-1}), and Raman intensities in brackets [$Å^4$ amu^{-1}].

Table S12. Comparison of observed and unscaled calculated[a] vibrational frequencies [cm^{-1}] and intensities of $[M(N_3)_5]^{2-}$ (M = Ga, In, Tl) in point group C_s.

	approx. mode			$[Ga(N_3)_5]^{2-}$		$[In(N_3)_5]^{2-}$		$[Tl(N_3)_5]^{2-}$	
	description in C_s[b]	observed[c] IR	observed[c] Raman	calculated (IR)[Raman] B3LYP	calculated (IR)[Raman] MP2	calculated (IR)[Raman] B3LYP	calculated (IR)[Raman] MP2	calculated (IR)[Raman] B3LYP	calculated (IR)[Raman] MP2
A'	ν_1 ν_{as} N_3 i ph		2113 [4.6]	2168 (93) [158]	2182 (9.4) [8.5]	2152 (43) [154]	2193 (3.6) [6.7]	2105 (46) [1317]	2168 (8.6) [31]
	ν_2 ν_{as} N_3 o ph 3 *eq*, 1 *ax*	2109 s	2097 [0.4]	2139 (981) [67]	2165 (1180) [1.3]	2123 (1011) [83]	2179 (1227) [0.6]	2083 (967) [234]	2150 (1349) [15]
	ν_3 ν_{as} N_3 o ph 2 *eq*, 2 *ax*	2080 vs	2078 [1.6]	2114 (1316) [54]	2159 (353) [6.8]	2110 (1620) [60]	2175 (270) [7.4]	2074 (1583) [165]	2145 (426) [14]
	ν_4 ν_{as} N_3 o ph 3 *eq*, 1 *ax*	2064 vs	2057 [0.4]	2109 (1473) [47]	2155 (287) [3.2]	2104 (1249) [53]	2170 (351) [4.8]	2069 (1333) [151]	2136 (461) [31]
	ν_5 ν_s N_3 i ph	1349 m	1355 [4.4]	1371 (12) [47]	1296 (16) [50]	1362 (5.7) [116]	1262 (1.9) [81]	1339 (12) [5.3]	1243 (17) [49]
	ν_6 ν_s N_3 o ph, 3 *eq*		1337 [3.7 sh]	1367 (30) [44]	1294 (6.5) [105]	1359 (23) [51]	1258 (15) [90]	1338 (13) [12]	1236 (0.2) [63]
	ν_7 ν_s N_3 o ph, 2 *ax*			1360 (72) [22]	1273 (22) [52]	1355 (75) [24]	1246 (23) [46]	1336 (61) [7.1]	1228 (14) [54]
	ν_8 ν_s N_3 o ph, 2 *eq*, 1 *ax*	1298 m	1303 [3.6]	1357 (111) [15]	1270 (13) [61]	1352 (109) [16]	1244 (12) [76]	1333 (107) [3.7]	1224 (9.5) [49]
	ν_9 δ N_3 i pl, 1 *eq*	641 w		644 (26) [13]	636 (13) [2.9]	629 (4.1) [12]	631 (0.3) [1.7]	619 (11) [21]	597 (2.1) [5.4]
	ν_{10} δ N_3 i pl, 1 *ax*			640 (2.0) [0.9]	627 (6.8) [3.7]	624 (16) [25]	617 (2.6) [1.3]	618 (1.2) [15]	593 (1.5) [21]
	ν_{11} δ N_3 i pl, 1 *ax*			636 (9.5) [1.2]	626 (2.3) [2.4]	623 (5.4) [20]	600 (0.9) [1.2]	615 (9.4) [15]	592 (1.0) [4.0]
	ν_{12} δ N_3 i pl, o ph, 3 *eq*			634 (11) [2.9]	623 (10) [0.7]	619 (4.7) [5.2]	594 (4.9) [30]	614 (1.3) [5.0]	585 (1.9) [14]
	ν_{13} δ N_3 o pl, i ph, 2 *eq*			575 (9.0) [0.1]	529 (1.5) [0.1]	601 (7.7) [0.3]	584 (8.3) [7.8]	580 (5.9) [0.1]	527 (0.6) [0.05]
	ν_{14} ν_{as} MN_3 *eq*		418 [2.0]	388 (72) [4.9]	412 (68) [5.4]	338 (64) [5.3]	361 (71) [11]	289 (48) [11]	331 (2.1) [186]
	ν_{15} ν_s MN_5		401 [10.0]	363 (0.6) [57]	392 (4.1) [30]	324 (1.3) [79]	355 (6.5) [57]	278 (61) [14]	327 (66) [8.3]
	ν_{16} ν_{as} MN_2 *ax*			329 (98) [2.5]	353 (108) [1.4]	317 (97) [4.7]	346 (103) [6.4]	268 (0.2) [474]	318 (77) [16]
	ν_{17} ν_s MN_2 *ax*		286 [1.8 sh]	274 (4.3) [12]	281 (2.0) [11]	263 (0.6) [11]	281 (0.3) [13]	241 (0.3) [8.6]	255 (2.7) [13]
	ν_{18} $\delta_{umbrella}$ MN_3		229 [2.0]	228 (157) [2.9]	232 (143) [3.4]	175 (16) [3.4]	177 (42) [1.9]	150 (10) [16]	153 (9.5) [4.3]
	ν_{19} δ_{sciss} MN_2, 1 *ax*, 1 *eq*			217 (14) [2.4]	219 (30) [1.4]	174 (90) [1.1]	171 (61) [1.4]	136 (59) [5.7]	142 (65) [1.1]
	ν_{20} δ_{sciss} MN_2, 2 *ax*			185 (41) [0.7]	192 (51) [0.7]	153 (32) [1.5]	151 (41) [2.0]	126 (44) [9.7]	129 (52) [1.7]
	ν_{21} δ MNN i ph, 2 *eq*		142 [0.8 sh]	135 (2.1) [8.3]	128 (1.8) [6.1]	116 (1.5) [13]	106 (2.1) [5.6]	109 (0.6) [30]	99 (0.7) [9.7]
	ν_{22} δ MNN o ph, 1 *ax*, 1 *eq*			120 (9.9) [2.9]	107 (11) [3.5]	103 (5.1) [2.5]	89 (6.0) [3.0]	97 (4.9) [2.4]	88 (7.7) [1.6]
	ν_{23} δ MNN i ph, 1 *ax*, 1 *eq*			76 (8.8) [3.0]	70 (7.7) [5.2]	61 (8.8) [2.0]	52 (7.0) [7.1]	57 (11) [3.9]	52 (8.6) [5.7]
	ν_{24} δ MNN i ph, 2 *ax*			61 (1.3) [14]	56 (1.5) [13]	52 (3.5) [13]	44 (5.5) [12]	47 (4.6) [14]	42 (6.3) [10]
	ν_{25} δ MN_4 o ph, 2 *ax*, 2 *eq*			38 (0.1) [2.3]	35 (0.3) [3.0]	31 (0.3) [2.3]	30 (1.2) [1.1]	25 (0.9) [1.1]	25 (1.4) [1.4]
	ν_{26} τ MNN i ph 2 *eq*			24 (0.9) [0.5]	16 (1.0) [0.6]	12 (1.6) [0.4]	19 (1.4) [0.03]	19 (2.2) [0.3]	15 (2.3) [0.4]
A''	ν_{27} ν_{as} N_3 o ph 2 *eq*	2109 s	2113 [4.6]	2137 (2495) [9.1]	2183 (1239) [3.5]	2121 (2607) [12]	2195 (1331) [4.7]	2083 (2647) [20]	2162 (1538) [16]
	ν_{28} ν_s N_3 o ph 2 *eq*	1316 m	1342 [4.2]	1366 (123) [2.8]	1294 (47) [4.4]	1359 (124) [1.2]	1262 (33) [0.2]	1337 (114) [6.0]	1236 (26) [6.1]
	ν_{29} δ N_3 i pl, i ph, 2 *eq*			630 (0.5) [0.4]	624 (7.3) [0.1]	620 (5.5) [0.5]	661 (1.4) [0.4]	616 (5.4) [2.4]	585 (0.1) [0.5]
	ν_{30} δ N_3 o pl, i ph, 1 *ax*, 1 *eq*			591 (12) [0.02]	552 (1.8) [0.02]	614 (0.0) [8.4]	615 (0.00) [0.1]	583 (0.0) [3.1]	532 (0.7) [0.2]
	ν_{31} δ N_3 o pl, i ph, 1 *ax*, 1 *eq*			589 (0.3) [0.9]	546 (0.4) [0.2]	598 (0.1) [0.1]	597 (0.1) [1.2]	575 (7.7) [0.6]	528 (0.05) [0.3]
	ν_{32} δ N_3 o pl, 1 *ax*			585 (4.0) [0.4]	544 (0.6) [0.2]	586 (7.6) [0.0]	595 (2.0) [1.1]	574 (0.8) [1.8]	528 (0.1) [2.1]
	ν_{33} δ N_3 o pl, o ph, 2 *eq*			577 (0.00) [0.00]	530 (0.00) [0.1]	583 (0.3) [1.1]	559 (0.04) [0.4]	573 (0.9) [2.8]	525 (0.4) [1.1]
	ν_{34} ν_{as} MN_2 *eq*			375 (143) [2.9]	402 (137) [3.2]	326 (104) [2.4]	350 (104) [3.4]	282 (72) [0.2]	322 (90) [1.3]
	ν_{35} δ_{sciss} MN_4 2 *ax*, 2 *eq*		248 [0.2 sh]	231 (2.9) [12]	241 (0.3) [13]	173 (3.1) [8.3]	187 (0.0) [14]	141 (1.7) [5.2]	150 (0.7) [11]
	ν_{36} δ_{sciss} MN_4 2 *ax*, 2 *eq*			224 (85) [0.9]	228 (90) [0.9]	164 (76) [0.6]	166 (73) [1.2]	125 (69) [0.5]	125 (69) [2.4]
	ν_{37} δ MNN o ph, 2 *eq*			116 (1.4) [17]	105 (1.0) [25]	127 (0.0) [9.5]	132 (0.5) [9.6]	110 (0.3) [7.7]	107 (2.8) [9.3]
	ν_{38} δ MN_3 o ph, 3 *eq*			87 (0.7) [3.9]	91 (2.9) [1.9]	95 (1.6) [7.9]	92 (10) [7.3]	87 (0.6) [8.2]	74 (5.5) [13]

ν_{39}	τ MNN o ph, 2 *ax*, 2 *eq*	67 (0.2) [1.5]	69 (0.1) [2.3]	51 (0.1) [2.4]	77 (2.0) [2.6]	57 (0.00) [0.7]	59 (0.3) [0.7]
ν_{40}	τ MNN i ph 1 *ax*, 1 *eq*	48 (2.3) [0.2]	51 (2.4) [0.05]	41 (3.3) [0.4]	51 (2.5) [4.3]	42 (4.9) [0.4]	43 (4.6) [0.9]
ν_{41}	τ MNN o ph, 2 *eq*	34 (0.03) [21]	23 (0.5) [10]	23 (0.4) [9.3]	35 (0.0) [18]	24 (0.03) [27]	20 (0.04) [24]
ν_{42}	τ MNN i ph, 2 *eq*	28 (0.5) [12]	21 (0.00) [19]	11 (0.0) [19]	16 (0.4) [8.5]	19 (0.2) [15]	10 (0.2) [11]

[a] Calculated at the B3LYP/SBKJ+(d) and MP2/SBKJ+(d) levels of theory; calculated IR intensities are given in parentheses (km mol^{-1}), and Raman intensities in brackets [$Å^4$ amu^{-1}]. [b] The mode assignments were made assuming an ideal arrangement of C_s symmetry; i ph = in phase; o ph = out of phase; i pl = in plane; o pl = out of plane; *ax* = axial; *eq* = equatorial. [c] As $[PPh]^+$ salt. In addition to the bands listed in this table and the ones of the PPh_4^+ cation, Raman bands at 1241 [0.6], 993 [1.0], 826 [0.5], 727 [4.8] cm^{-1} and IR bands at 2000 s, 1984 s cm^{-1} were observed.

Table S13. Comparison of observed and unscaled calculated[a] vibrational frequencies [cm^{-1}] and intensities of $[M(N_3)_6]^{3-}$ (M = Ga, In, Tl) in point group S_6

	approx. mode		$[Ga(N_3)_6]^{3-}$				$[In(N_3)_6]^{3-}$				$[Tl(N_3)_6]^{3-}$	
		description in S_6[b]	calculated (IR)[Raman]		observed[c]		calculated (IR)[Raman]		observed[d]		calculated (IR)[Raman]	
			B3LYP	MP2	Raman	IR	B3LYP	MP2	Raman	IR	B3LYP	MP2
A_g	ν_1	ν_{as} N_3 i ph	2146 (0) [18.6]	2186 (0) [5.7]	2090 [3.5]	2092 m	2141 (0) [72]	2186 (0) [4.8]	2060 [5.5]	2057 m	2093 (0) [1401]	2160 (0)[19]
	ν_2	ν_s N_3 i ph	1377 (0) [546]	1282 (0) [251]	1346 [10.0]		1374 (0) [374]	1252 (0) [227]	1327 [2.1]		1351 (0) [463]	1233 (0)[237]
	ν_3	δ N_3 i pl i ph	637 (0) [35]	622 (0) [7.1]			627 (0) [58]	595 (0) [13]	649 [1.1]		631 (0) [0.4]	613 (0)[34]
	ν_4	δ N_3 o pl i ph	592 (0) [13]	612 (0) [2.2]	527 [0.3]		592 (0) [3.5]	558 (0) [0.01]		533 [0.3]	601 (0) [2.1]	592 (0)[0.6]
	ν_5	ν MN MN_6 i ph	316 (0) [111]	351 (0) [19]	351 [6.0]		285 (0) [138]	317 (0) [42]	320 [10.0]		229 (0) [621]	302 (0)[199]
	ν_6	δ MN_6	208 (0) [13]	220 (0) [2.2]	183 [1.0] 174 [0.3sh]		152 (0) [9.8]	158 (0) [7.8]	122 [sh]		119 (0) [3.9]	134 (0)[1.0]
	ν_7	δ MNN i ph	113 (0) [1.2]	90 (0) [0.9]			101 (0) [2.6]	75 (0) [0.7]			102 (0) [61]	82 (0)[4.0]
	ν_8	τ MN_6 i ph	23 (0) [25]	5 (0) [8.0]			14 (0) [28]	25 (0) [17]			26 (0) [29]	26 (0)[10]
E_g	ν_9	ν_{as} N_3 o ph	2097 (0) [141]	2191 (0) [31]	2055 [2.6]		2095 (0) [143]	2195 (0) [18]	2027 [1.0]		2056 (0) [373]	2157 (0)[86]
	ν_{10}	ν_s N_3 o ph	1370 (0) [132]	1284 (0) [177]	1291 [2.0]		1369 (0) [124]	1255 (0) [146]	1327 [2.1]		1353 (0) [82]	1238 (0)[169]
	ν_{11}	δ N_3 i pl o ph	637 (0) [4.1]	630 (0) [3.0]			626 (0) [13]	594 (0) [2.5]	649 [1.1]		634 (0) [60.3]	609 (0)[18]
	ν_{12}	δ N_3 o pl o ph	588 (0) [1.9]	596 (0) [2.0]			589 (0) [2.6]	566 (0) [1.9]		533 [0.3]	599 (0) [14]	589 (0)[1]
	ν_{13}	ν MN MN_4 o ph	251 (0) [47]	267 (0) [58]	285 [4.0]		233 (0) [43]	252 (0) [37]	231 [1.6]		216 (0) [27]	238 (0)[61]
	ν_{14}	δ MN_6	167 (0) [5.1]	183 (0) [6.2]	183 [1.0] 174 [0.3sh]		141 (0) [10]	152 (0) [16]	122 [sh]		115 (0) [16]	127 (0)[8]
	ν_{15}	δ MNN o ph	64 (0) [16]	62 (0) [29]			54 (0) [14]	58 (0) [37]			52 (0) [17.2]	53 (0)[25]
	ν_{16}	τ MN_6 o ph	31 (0) [44]	40 (0) [45]			18 (0) [43]	31 (0) [46]			34 (0) [61]	31 (0)[47]
A_u	ν_{17}	ν_{as} N_3 o ph	2103 (2131) [0]	2180 (480) [0]	2041 [1.0]	2054 vs	2101 (2392) [0]	2187 (469) [0]	2012 [1.1]	2033 s	2060 (1292) [0]	2152 (469)[0]
	ν_{18}	ν_s N_3 o ph	1372 (44) [0]	1284 (13) [0]		1339 m	1371 (45.6) [0]	1255 (10) [0]		1275 mw	1350 (23) [0]	1238 (5.1)[0]
	ν_{19}	δ N_3 i pl o ph	637 (0.6) [0]	622 (4.4) [0]			625 (0.2) [0]	588 (2.7) [0]			625 (0.6) [0]	603 (0.1)[0]
	ν_{20}	δ N_3 o pl o ph	590 (23) [0]	596 (8.9) [0]		612sh vw	591 (21) [0]	552 (4.3) [0]			592 (15) [0]	583 (2.7)[0]
	ν_{21}	ν MN MN_6 o ph	295 (122) [0]	320 (141) [0]			275 (109) [0]	298 (121) [0]			232 (69) [0]	273 (96)[0]
	ν_{22}	δ MN_6	221 (141) [0]	213 (62) [0]			162 (97) [0]	157 (38) [0]			125 (9.1) [0]	127 (20)[0]
	ν_{23}	δ MNN o ph	154 (46) [0]	143 (22) [0]			127 (31) [0]	115 (23) [0]			114 (67) [0]	105 (35)[0]
	ν_{24}	δ MNN o ph	48 (2.3) [0]	53 (19.0) [0]			38 (0.9) [0]	37 (11) [0]			35 (0.0) [0]	42 (20)[0]
	ν_{25}	τ MN_6 o ph	29 (6.1) [0]	45 (0.03) [0]			16 (6.5) [0]	28 (6.5) [0]			28 (15) [0]	31 (1.1)[0]
E_u	ν_{26}	ν_{as} N_3 o ph	2109 (6079) [0]	2192 (3255) [0]		2035 vs	2106 (6079) [0]	2195 (2989) [0]		2025 vs 2016 sh	2068 (7044) [0]	2162 (3457)[0]
	ν_{27}	ν_s N_3 o ph	1374 (105) [0]	1284 (60) [0]		1339 m	1372 (103) [0]	1255 (37) [0]		1275 mw	1355 (108) [0]	1237 (30)[0]
	ν_{28}	δ N_3 i pl o ph	639 (55) [0]	629 (19) [0]		650 vw	628 (43) [0]	596 (8.6) [0]			635 (38) [0]	608 (7.7)[0]
	ν_{29}	δ N_3 o pl o ph	589 (7.9) [0]	607 (5.6) [0]		612sh vw	590 (8.1) [0]	562 (3.5) [0]			603 (10) [0]	589 (2.4)[0]
	ν_{30}	ν MN MN_4 o ph	298 (233) [0]	333 (293) [0]			276 (209) [0]	307 (235) [0]			239 (103) [0]	284 (165)[0]
	ν_{31}	δ MN_6	219 (301) [0]	221 (310) [0]			167 (202) [0]	162 (241) [0]			133 (225) [0]	133 (222)[0]
	ν_{32}	$\delta_{wag/rock}$ MN_6	138 (22) [0]	158 (50) [0]			99 (15) [0]	112 (20) [0]			80 (12) [0]	91 (23)[0]
	ν_{33}	δ MNN o ph	58 (20) [0]	43 (12) [0]			47 (19) [0]	41 (12) [0]			45 (16) [0]	40 (13)[0]
	ν_{34}	τ MN_6 o ph	20 (0.9) [0]	26 (1.5) [0]			14 (1.7) [0]	15 (2.5) [0]			18 (1.7) [0]	20 (3.1)[0]

[a] Calculated at the B3LYP/SBKJ+(d) and MP2/SBKJ+(d) levels of theory; calculated IR intensities are given in parentheses (km mol^{-1}), and Raman intensities in brackets [$Å^4$ amu^{-1}]. [b] The mode assignments were made assuming an ideal arrangement of S_6 symmetry; i ph = in phase; o ph = out of phase; i pl = in plane; o pl = out of plane. [c]

As $[PPh]^+$ salt. In addition to the bands listed in this table and the ones of the PPh_4^+ cation, a Raman band at 442 [0.1] cm^{-1} was observed. [d] As $[PPh]^+$ salt. In addition to the bands listed in this table and the ones of the PPh_4^+ cation, a Raman band at 393 [0.2] cm^{-1} and an IR band at 847sh vw cm^{-1} were observed.

Table S14. Crystal data and structure refinement for C48H40GaN15P2.

Identification code	tppgan3m	
Empirical formula	C48 H40 Ga N15 P2	
Formula weight	958.61	
Temperature	140(2) K	
Wavelength	0.71073 Å	
Crystal system	Monoclinic	
Space group	C2/c	
Unit cell dimensions	a = 11.771(4) Å	α= 90°.
	b = 18.031(6) Å	β= 91.974(5)°.
	c = 21.793(7) Å	γ = 90°.
Volume	4622(2) $Å^3$	
Z	4	
Density (calculated)	1.377 Mg/m^3	
Absorption coefficient	0.717 mm^{-1}	
F(000)	1976	
Crystal size	0.23 x 0.15 x 0.09 mm^3	
Theta range for data collection	1.87 to 27.53°.	
Index ranges	-15<=h<=15, -23<=k<=22, -28<=l<=28	
Reflections collected	19912	
Independent reflections	5242 [R(int) = 0.0369]	
Completeness to theta = 27.53°	98.5 %	
Absorption correction	Multi-scan	
Transmission factors	min/max: 0.828	
Refinement method	Full-matrix least-squares on F^2	
Data / restraints / parameters	5242 / 0 / 312	
Goodness-of-fit on F^2	1.029	
Final R indices [I>2sigma(I)]	R1 = 0.0383, wR2 = 0.0889	
R indices (all data)	R1 = 0.0530, wR2 = 0.0971	
Largest diff. peak and hole	0.491 and -0.359 $e.Å^{-3}$	

Table S15. Atomic coordinates (x 10^4) and equivalent isotropic displacement parameters ($Å^2$x 10^3) for C48H40GaN15P2. U(eq) is defined as one third of the trace of the orthogonalized U^{ij} tensor.

	x	y	z	U(eq)
C(1)	3796(2)	6990(1)	8527(1)	33(1)
C(2)	3184(2)	6777(1)	7994(1)	38(1)
C(3)	2890(2)	7301(1)	7556(1)	45(1)
C(4)	3202(2)	8035(1)	7646(1)	48(1)
C(5)	3808(2)	8246(1)	8167(1)	48(1)
C(6)	4111(2)	7724(1)	8611(1)	41(1)
C(7)	5180(2)	6608(1)	9646(1)	34(1)
C(8)	4899(2)	7167(1)	10058(1)	42(1)
C(9)	5683(2)	7392(1)	10505(1)	49(1)
C(10)	6741(2)	7057(1)	10546(1)	49(1)
C(11)	7025(2)	6505(1)	10148(1)	44(1)
C(12)	6247(2)	6275(1)	9694(1)	37(1)
C(13)	2901(2)	6044(1)	9515(1)	31(1)
C(14)	3072(2)	5775(1)	10111(1)	39(1)
C(15)	2151(2)	5587(1)	10457(1)	42(1)
C(16)	1068(2)	5661(1)	10214(1)	38(1)
C(17)	892(2)	5914(1)	9622(1)	41(1)
C(18)	1803(2)	6112(1)	9268(1)	37(1)
C(19)	4669(2)	5496(1)	8699(1)	30(1)
C(20)	4236(2)	4791(1)	8791(1)	35(1)
C(21)	4737(2)	4189(1)	8513(1)	41(1)
C(22)	5679(2)	4288(1)	8158(1)	41(1)
C(23)	6103(2)	4987(1)	8058(1)	38(1)
C(24)	5595(2)	5596(1)	8319(1)	35(1)
Ga(1)	0	5363(1)	7500	35(1)
N(1)	766(2)	5298(1)	6672(1)	50(1)
N(2)	1338(1)	5799(1)	6506(1)	36(1)
N(3)	1901(2)	6266(1)	6321(1)	53(1)
N(4)	-1331(2)	4875(1)	7143(1)	50(1)
N(5)	-1291(2)	4543(1)	6665(1)	43(1)
N(6)	-1312(2)	4208(1)	6219(1)	57(1)
N(7)	-152(5)	6417(2)	7317(2)	54(1)
N(8)	20(5)	6903(2)	7687(2)	48(1)
N(9)	148(4)	7388(3)	8011(3)	80(2)
P(1)	4132(1)	6289(1)	9090(1)	30(1)

Table S16. Bond lengths [Å] and angles [°] for C48H40GaN15P2.

C(1)-C(6)	1.385(3)
C(1)-C(2)	1.398(3)
C(1)-P(1)	1.796(2)
C(2)-C(3)	1.378(3)
C(3)-C(4)	1.387(3)
C(4)-C(5)	1.374(3)
C(5)-C(6)	1.388(3)
C(7)-C(12)	1.392(3)
C(7)-C(8)	1.397(3)
C(7)-P(1)	1.795(2)
C(8)-C(9)	1.379(3)
C(9)-C(10)	1.384(4)
C(10)-C(11)	1.371(3)
C(11)-C(12)	1.388(3)
C(13)-C(18)	1.388(3)
C(13)-C(14)	1.394(3)
C(13)-P(1)	1.8018(19)
C(14)-C(15)	1.383(3)
C(15)-C(16)	1.370(3)
C(16)-C(17)	1.377(3)
C(17)-C(18)	1.388(3)
C(19)-C(20)	1.388(3)
C(19)-C(24)	1.402(3)
C(19)-P(1)	1.791(2)
C(20)-C(21)	1.384(3)
C(21)-C(22)	1.385(3)
C(22)-C(23)	1.377(3)
C(23)-C(24)	1.382(3)
Ga(1)-N(4)	1.9367(19)
Ga(1)-N(4)#1	1.9367(19)
Ga(1)-N(7)#1	1.948(4)
Ga(1)-N(7)	1.948(4)
Ga(1)-N(1)#1	2.0486(18)
Ga(1)-N(1)	2.0486(18)
N(1)-N(2)	1.191(2)
N(2)-N(3)	1.152(2)
N(4)-N(5)	1.204(3)
N(5)-N(6)	1.145(3)

N(7)-N(7)#1	0.864(8)
N(7)-N(8)#1	0.889(5)
N(7)-N(8)	1.203(5)
N(7)-N(9)#1	1.891(6)
N(8)-N(8)#1	0.814(8)
N(8)-N(7)#1	0.889(5)
N(8)-N(9)	1.131(6)
N(8)-N(9)#1	1.759(6)
N(9)-N(8)#1	1.759(6)
N(9)-N(7)#1	1.891(6)

C(6)-C(1)-C(2)	119.94(19)
C(6)-C(1)-P(1)	122.03(16)
C(2)-C(1)-P(1)	118.03(15)
C(3)-C(2)-C(1)	119.8(2)
C(2)-C(3)-C(4)	119.8(2)
C(5)-C(4)-C(3)	120.6(2)
C(4)-C(5)-C(6)	120.1(2)
C(1)-C(6)-C(5)	119.7(2)
C(12)-C(7)-C(8)	119.79(19)
C(12)-C(7)-P(1)	120.61(16)
C(8)-C(7)-P(1)	119.50(16)
C(9)-C(8)-C(7)	119.9(2)
C(8)-C(9)-C(10)	119.8(2)
C(11)-C(10)-C(9)	120.9(2)
C(10)-C(11)-C(12)	120.0(2)
C(11)-C(12)-C(7)	119.7(2)
C(18)-C(13)-C(14)	119.68(18)
C(18)-C(13)-P(1)	122.17(15)
C(14)-C(13)-P(1)	118.15(15)
C(15)-C(14)-C(13)	120.08(19)
C(16)-C(15)-C(14)	120.17(19)
C(15)-C(16)-C(17)	120.10(19)
C(16)-C(17)-C(18)	120.8(2)
C(17)-C(18)-C(13)	119.19(19)
C(20)-C(19)-C(24)	120.04(18)
C(20)-C(19)-P(1)	121.67(15)
C(24)-C(19)-P(1)	118.19(15)
C(21)-C(20)-C(19)	119.39(19)
C(20)-C(21)-C(22)	120.3(2)

C(23)-C(22)-C(21)	120.5(2)
C(22)-C(23)-C(24)	119.94(19)
C(23)-C(24)-C(19)	119.7(2)
N(4)-Ga(1)-N(4)#1	125.88(13)
N(4)-Ga(1)-N(7)#1	126.37(18)
N(4)#1-Ga(1)-N(7)#1	107.11(17)
N(4)-Ga(1)-N(7)	107.11(17)
N(4)#1-Ga(1)-N(7)	126.37(18)
N(7)#1-Ga(1)-N(7)	25.6(2)
N(4)-Ga(1)-N(1)#1	87.31(8)
N(4)#1-Ga(1)-N(1)#1	89.70(8)
N(7)#1-Ga(1)-N(1)#1	85.14(14)
N(7)-Ga(1)-N(1)#1	101.34(14)
N(4)-Ga(1)-N(1)	89.70(8)
N(4)#1-Ga(1)-N(1)	87.31(8)
N(7)#1-Ga(1)-N(1)	101.34(14)
N(7)-Ga(1)-N(1)	85.14(14)
N(1)#1-Ga(1)-N(1)	173.42(11)
N(2)-N(1)-Ga(1)	119.61(15)
N(3)-N(2)-N(1)	176.7(2)
N(5)-N(4)-Ga(1)	121.22(15)
N(6)-N(5)-N(4)	176.0(2)
N(7)#1-N(7)-N(8)#1	86.6(5)
N(7)#1-N(7)-N(8)	47.6(3)
N(8)#1-N(7)-N(8)	42.6(4)
N(7)#1-N(7)-N(9)#1	110.0(3)
N(8)#1-N(7)-N(9)#1	23.4(4)
N(8)-N(7)-N(9)#1	64.9(3)
N(7)#1-N(7)-Ga(1)	77.19(11)
N(8)#1-N(7)-Ga(1)	161.3(6)
N(8)-N(7)-Ga(1)	124.1(3)
N(9)#1-N(7)-Ga(1)	168.2(3)
N(8)#1-N(8)-N(7)#1	89.7(3)
N(8)#1-N(8)-N(9)	128.8(4)
N(7)#1-N(8)-N(9)	138.4(7)
N(8)#1-N(8)-N(7)	47.7(3)
N(7)#1-N(8)-N(7)	45.8(5)
N(9)-N(8)-N(7)	175.8(6)
N(8)#1-N(8)-N(9)#1	30.1(2)
N(7)#1-N(8)-N(9)#1	119.8(4)

N(9)-N(8)-N(9)#1	99.3(6)
N(7)-N(8)-N(9)#1	76.8(3)
N(8)-N(9)-N(8)#1	21.1(2)
N(8)-N(9)-N(7)#1	18.2(3)
N(8)#1-N(9)-N(7)#1	38.26(17)
C(19)-P(1)-C(7)	109.37(10)
C(19)-P(1)-C(1)	108.00(9)
C(7)-P(1)-C(1)	111.52(10)
C(19)-P(1)-C(13)	110.63(9)
C(7)-P(1)-C(13)	106.09(9)
C(1)-P(1)-C(13)	111.24(9)

Symmetry transformations used to generate equivalent atoms:

#1 -x,y,-z+3/2

Table S17. Anisotropic displacement parameters ($Å^2 x\ 10^3$) for C48H40GaN15P2. The anisotropic displacement factor exponent takes the form: $-2\pi^2[\ h^2\ a^{*2}U^{11} + ...\ + 2\ h\ k\ a^*\ b^*\ U^{12}\ ]$

	U^{11}	U^{22}	U^{33}	U^{23}	U^{13}	U^{12}
C(1)	33(1)	31(1)	34(1)	3(1)	4(1)	1(1)
C(2)	44(1)	34(1)	36(1)	1(1)	0(1)	-3(1)
C(3)	49(1)	50(1)	37(1)	9(1)	-1(1)	0(1)
C(4)	50(1)	45(1)	48(1)	17(1)	5(1)	3(1)
C(5)	57(2)	31(1)	57(1)	9(1)	5(1)	-6(1)
C(6)	44(1)	36(1)	43(1)	0(1)	0(1)	-4(1)
C(7)	37(1)	33(1)	33(1)	2(1)	-2(1)	-7(1)
C(8)	46(1)	37(1)	43(1)	-2(1)	-5(1)	-2(1)
C(9)	65(2)	41(1)	40(1)	-3(1)	-6(1)	-13(1)
C(10)	54(2)	56(1)	35(1)	9(1)	-10(1)	-25(1)
C(11)	35(1)	61(2)	37(1)	13(1)	-4(1)	-10(1)
C(12)	34(1)	44(1)	33(1)	6(1)	1(1)	-7(1)
C(13)	30(1)	29(1)	32(1)	-1(1)	2(1)	0(1)
C(14)	33(1)	48(1)	37(1)	5(1)	-1(1)	0(1)
C(15)	43(1)	49(1)	34(1)	6(1)	4(1)	-4(1)
C(16)	36(1)	37(1)	40(1)	-6(1)	8(1)	-5(1)
C(17)	31(1)	47(1)	46(1)	-3(1)	-2(1)	-3(1)
C(18)	36(1)	40(1)	33(1)	-1(1)	-2(1)	-2(1)
C(19)	29(1)	31(1)	30(1)	1(1)	-2(1)	1(1)
C(20)	37(1)	34(1)	33(1)	3(1)	2(1)	-1(1)
C(21)	54(1)	28(1)	41(1)	3(1)	1(1)	2(1)
C(22)	47(1)	41(1)	34(1)	-3(1)	-3(1)	13(1)
C(23)	31(1)	51(1)	32(1)	-3(1)	-1(1)	3(1)
C(24)	32(1)	39(1)	35(1)	-1(1)	1(1)	-4(1)
Ga(1)	36(1)	32(1)	37(1)	0	7(1)	0
N(1)	51(1)	62(1)	37(1)	3(1)	12(1)	-17(1)
N(2)	30(1)	45(1)	33(1)	9(1)	2(1)	6(1)
N(3)	45(1)	50(1)	64(1)	18(1)	17(1)	3(1)
N(4)	37(1)	73(1)	38(1)	0(1)	3(1)	-13(1)
N(5)	33(1)	55(1)	40(1)	10(1)	-3(1)	-10(1)
N(6)	51(1)	70(2)	48(1)	-4(1)	-7(1)	-14(1)
N(7)	86(4)	35(2)	43(3)	0(2)	10(3)	14(2)
N(8)	45(2)	38(2)	63(3)	-13(2)	23(3)	-4(2)
N(9)	81(3)	54(3)	106(4)	-33(3)	35(3)	-24(3)
P(1)	30(1)	29(1)	31(1)	0(1)	1(1)	-2(1)

Table S18. Hydrogen coordinates (x 10^4) and isotropic displacement parameters (Å^{2}x 10^3) for C48H40GaN15P2.

	x	y	z	U(eq)
H(2)	2976	6284	7935	46
H(3)	2483	7162	7201	54
H(4)	2998	8388	7351	57
H(5)	4016	8740	8222	58
H(6)	4524	7866	8963	49
H(8)	4185	7388	10030	51
H(9)	5501	7767	10777	59
H(10)	7267	7209	10849	58
H(11)	7739	6284	10181	53
H(12)	6437	5901	9422	44
H(14)	3806	5721	10276	47
H(15)	2267	5410	10855	50
H(16)	450	5540	10449	45
H(17)	155	5953	9457	49
H(18)	1679	6288	8870	44
H(20)	3615	4723	9038	42
H(21)	4439	3716	8565	49
H(22)	6028	3878	7986	49
H(23)	6730	5050	7816	46
H(24)	5866	6071	8243	42

Table S19. Crystal data and structure refinement for C72H60In N18P3.

Identification code	inazidem	
Empirical formula	C72 H60 In N18 P3	
Formula weight	1385.11	
Temperature	163(2) K	
Wavelength	0.71073 Å	
Crystal system	Monoclinic	
Space group	P2(1)/n	
Unit cell dimensions	a = 13.1599(14) Å	α= 90°.
	b = 22.704(2) Å	β= 96.707(2)°.
	c = 22.032(2) Å	γ = 90°.
Volume	6537.6(12) $Å^3$	
Z	4	
Density (calculated)	1.407 Mg/m^3	
Absorption coefficient	0.494 mm^{-1}	
F(000)	2848	
Crystal size	0.23 x 0.16 x 0.10 mm^3	
Theta range for data collection	1.29 to 27.52°.	
Index ranges	-16<=h<=16, -26<=k<=29, -28<=l<=26	
Reflections collected	40351	
Independent reflections	14707 [R(int) = 0.0649]	
Completeness to theta = 27.52°	97.7 %	
Absorption correction	Multi-scan	
Transmission factors	min/max: 0.852	
Refinement method	Full-matrix least-squares on F^2	
Data / restraints / parameters	14707 / 0 / 847	
Goodness-of-fit on F^2	0.892	
Final R indices [I>2sigma(I)]	R1 = 0.0382, wR2 = 0.0609	
R indices (all data)	R1 = 0.0626, wR2 = 0.0643	
Largest diff. peak and hole	0.855 and -0.682 $e.Å^{-3}$	

Table S20. Atomic coordinates (x 10^4) and equivalent isotropic displacement parameters ($Å^2$x 10^3) for C72H60InN18P3. U(eq) is defined as one third of the trace of the orthogonalized U^{ij} tensor.

	x	y	z	U(eq)
In(1)	6985(1)	3486(1)	7654(1)	24(1)
N(1)	8282(2)	4097(1)	7587(1)	36(1)
N(2)	8995(2)	4183(1)	7955(1)	31(1)
N(3)	9708(2)	4289(1)	8299(1)	50(1)
N(4)	7503(2)	2934(1)	6934(1)	35(1)
N(5)	7988(2)	3101(1)	6544(1)	33(1)
N(6)	8472(2)	3230(1)	6162(1)	68(1)
N(7)	6107(2)	4054(1)	6972(1)	40(1)
N(8)	5467(2)	4382(1)	7066(1)	37(1)
N(9)	4838(2)	4728(1)	7138(1)	75(1)
N(10)	5710(2)	2846(1)	7692(1)	34(1)
N(11)	4848(2)	3011(1)	7667(1)	33(1)
N(12)	3994(2)	3147(1)	7638(1)	60(1)
N(13)	6368(1)	4016(1)	8386(1)	29(1)
N(14)	6149(1)	3764(1)	8833(1)	27(1)
N(15)	5944(2)	3540(1)	9275(1)	41(1)
N(16)	7926(2)	2977(1)	8380(1)	32(1)
N(17)	7771(2)	2469(1)	8468(1)	38(1)
N(18)	7651(2)	1974(1)	8564(1)	66(1)
P(1)	1123(1)	3511(1)	429(1)	26(1)
P(2)	2000(1)	5427(1)	5675(1)	21(1)
P(3)	6927(1)	3304(1)	1665(1)	22(1)
C(1)	843(2)	2746(1)	511(1)	26(1)
C(2)	1064(2)	2331(1)	89(1)	44(1)
C(3)	788(2)	1748(1)	166(1)	50(1)
C(4)	312(2)	1581(1)	654(1)	42(1)
C(5)	77(2)	1993(1)	1069(1)	36(1)
C(6)	335(2)	2570(1)	995(1)	33(1)
C(7)	1793(2)	3800(1)	1123(1)	24(1)
C(8)	2197(2)	3436(1)	1599(1)	30(1)
C(9)	2742(2)	3679(1)	2112(1)	36(1)
C(10)	2895(2)	4275(1)	2152(1)	37(1)
C(11)	2502(2)	4643(1)	1681(1)	36(1)
C(12)	1955(2)	4404(1)	1166(1)	31(1)
C(13)	-68(2)	3889(1)	245(1)	24(1)

C(14)	-446(2)	4283(1)	643(1)	30(1)
C(15)	-1397(2)	4542(1)	489(1)	33(1)
C(16)	-1955(2)	4418(1)	-65(1)	35(1)
C(17)	-1585(2)	4024(1)	-467(1)	35(1)
C(18)	-652(2)	3757(1)	-310(1)	28(1)
C(19)	1925(2)	3609(1)	-168(1)	29(1)
C(20)	1636(2)	3947(1)	-685(1)	29(1)
C(21)	2313(2)	4023(1)	-1116(1)	37(1)
C(22)	3272(2)	3767(1)	-1032(1)	43(1)
C(23)	3553(2)	3428(1)	-520(1)	49(1)
C(24)	2889(2)	3346(1)	-88(1)	45(1)
C(25)	3320(2)	5621(1)	5881(1)	22(1)
C(26)	4083(2)	5276(1)	5674(1)	31(1)
C(27)	5098(2)	5416(1)	5839(1)	38(1)
C(28)	5361(2)	5898(1)	6204(1)	39(1)
C(29)	4612(2)	6234(1)	6416(1)	40(1)
C(30)	3594(2)	6096(1)	6259(1)	34(1)
C(31)	1641(2)	4904(1)	6219(1)	22(1)
C(32)	2381(2)	4646(1)	6635(1)	27(1)
C(33)	2102(2)	4216(1)	7033(1)	32(1)
C(34)	1090(2)	4050(1)	7016(1)	34(1)
C(35)	350(2)	4314(1)	6606(1)	33(1)
C(36)	618(2)	4738(1)	6209(1)	28(1)
C(37)	1196(2)	6068(1)	5666(1)	22(1)
C(38)	946(2)	6295(1)	6221(1)	26(1)
C(39)	360(2)	6800(1)	6221(1)	32(1)
C(40)	18(2)	7078(1)	5682(1)	34(1)
C(41)	259(2)	6852(1)	5136(1)	37(1)
C(42)	847(2)	6351(1)	5126(1)	28(1)
C(43)	1931(2)	5099(1)	4929(1)	21(1)
C(44)	1593(2)	4525(1)	4828(1)	27(1)
C(45)	1625(2)	4265(1)	4261(1)	32(1)
C(46)	1965(2)	4584(1)	3793(1)	33(1)
C(47)	2289(2)	5155(1)	3881(1)	31(1)
C(48)	2284(2)	5415(1)	4450(1)	26(1)
C(49)	6386(2)	2912(1)	2258(1)	22(1)
C(50)	5346(2)	2769(1)	2165(1)	30(1)
C(51)	4926(2)	2424(1)	2587(1)	34(1)
C(52)	5528(2)	2224(1)	3102(1)	34(1)
C(53)	6553(2)	2363(1)	3198(1)	32(1)

C(54)	6987(2)	2707(1)	2772(1)	25(1)
C(55)	8104(2)	3664(1)	1957(1)	21(1)
C(56)	8979(2)	3318(1)	2092(1)	25(1)
C(57)	9909(2)	3579(1)	2289(1)	29(1)
C(58)	9976(2)	4181(1)	2346(1)	31(1)
C(59)	9119(2)	4528(1)	2217(1)	31(1)
C(60)	8180(2)	4271(1)	2023(1)	27(1)
C(61)	6029(2)	3847(1)	1351(1)	24(1)
C(62)	5680(2)	4264(1)	1745(1)	32(1)
C(63)	5057(2)	4716(1)	1517(1)	40(1)
C(64)	4758(2)	4751(1)	899(1)	45(1)
C(65)	5071(2)	4333(1)	504(1)	44(1)
C(66)	5712(2)	3879(1)	729(1)	33(1)
C(67)	7217(2)	2781(1)	1101(1)	22(1)
C(68)	7591(2)	2973(1)	567(1)	30(1)
C(69)	7795(2)	2571(1)	127(1)	32(1)
C(70)	7668(2)	1979(1)	224(1)	36(1)
C(71)	7328(2)	1787(1)	756(1)	43(1)
C(72)	7092(2)	2187(1)	1192(1)	32(1)

Table S21. Bond lengths [Å] and angles [°] for C72H60InN18P3.

In(1)-N(4)	2.193(2)
In(1)-N(7)	2.202(2)
In(1)-N(1)	2.217(2)
In(1)-N(16)	2.228(2)
In(1)-N(10)	2.229(2)
In(1)-N(13)	2.2383(19)
N(1)-N(2)	1.183(3)
N(2)-N(3)	1.160(3)
N(4)-N(5)	1.190(3)
N(5)-N(6)	1.151(3)
N(7)-N(8)	1.161(3)
N(8)-N(9)	1.165(3)
N(10)-N(11)	1.190(3)
N(11)-N(12)	1.160(3)
N(13)-N(14)	1.202(3)
N(14)-N(15)	1.158(3)
N(16)-N(17)	1.191(3)
N(17)-N(18)	1.159(3)
P(1)-C(1)	1.788(3)
P(1)-C(13)	1.792(2)
P(1)-C(19)	1.795(2)
P(1)-C(7)	1.797(2)
P(2)-C(31)	1.791(2)
P(2)-C(25)	1.797(2)
P(2)-C(37)	1.798(2)
P(2)-C(43)	1.798(2)
P(3)-C(61)	1.790(2)
P(3)-C(67)	1.792(2)
P(3)-C(49)	1.796(2)
P(3)-C(55)	1.803(2)
C(1)-C(2)	1.378(3)
C(1)-C(6)	1.382(3)
C(2)-C(3)	1.387(4)
C(3)-C(4)	1.362(4)
C(4)-C(5)	1.368(3)
C(5)-C(6)	1.368(3)
C(7)-C(12)	1.388(3)
C(7)-C(8)	1.392(3)

C(8)-C(9)	1.381(3)
C(9)-C(10)	1.369(3)
C(10)-C(11)	1.384(3)
C(11)-C(12)	1.382(3)
C(13)-C(14)	1.384(3)
C(13)-C(18)	1.398(3)
C(14)-C(15)	1.390(3)
C(15)-C(16)	1.378(3)
C(16)-C(17)	1.385(3)
C(17)-C(18)	1.377(3)
C(19)-C(20)	1.389(3)
C(19)-C(24)	1.395(3)
C(20)-C(21)	1.386(3)
C(21)-C(22)	1.382(3)
C(22)-C(23)	1.379(4)
C(23)-C(24)	1.378(3)
C(25)-C(30)	1.384(3)
C(25)-C(26)	1.392(3)
C(26)-C(27)	1.379(3)
C(27)-C(28)	1.379(3)
C(28)-C(29)	1.371(3)
C(29)-C(30)	1.381(3)
C(31)-C(32)	1.386(3)
C(31)-C(36)	1.395(3)
C(32)-C(33)	1.389(3)
C(33)-C(34)	1.380(3)
C(34)-C(35)	1.385(3)
C(35)-C(36)	1.375(3)
C(37)-C(42)	1.384(3)
C(37)-C(38)	1.400(3)
C(38)-C(39)	1.382(3)
C(39)-C(40)	1.373(3)
C(40)-C(41)	1.377(3)
C(41)-C(42)	1.377(3)
C(43)-C(44)	1.388(3)
C(43)-C(48)	1.399(3)
C(44)-C(45)	1.387(3)
C(45)-C(46)	1.377(3)
C(46)-C(47)	1.372(3)
C(47)-C(48)	1.386(3)

C(49)-C(54)	1.383(3)
C(49)-C(50)	1.398(3)
C(50)-C(51)	1.380(3)
C(51)-C(52)	1.383(3)
C(52)-C(53)	1.377(3)
C(53)-C(54)	1.393(3)
C(55)-C(60)	1.387(3)
C(55)-C(56)	1.398(3)
C(56)-C(57)	1.383(3)
C(57)-C(58)	1.373(3)
C(58)-C(59)	1.378(3)
C(59)-C(60)	1.389(3)
C(61)-C(66)	1.387(3)
C(61)-C(62)	1.397(3)
C(62)-C(63)	1.373(3)
C(63)-C(64)	1.375(4)
C(64)-C(65)	1.381(4)
C(65)-C(66)	1.386(3)
C(67)-C(72)	1.376(3)
C(67)-C(68)	1.399(3)
C(68)-C(69)	1.380(3)
C(69)-C(70)	1.373(3)
C(70)-C(71)	1.374(3)
C(71)-C(72)	1.383(3)

N(4)-In(1)-N(7)	91.28(8)
N(4)-In(1)-N(1)	90.14(8)
N(7)-In(1)-N(1)	86.27(8)
N(4)-In(1)-N(16)	91.71(8)
N(7)-In(1)-N(16)	175.44(8)
N(1)-In(1)-N(16)	90.27(8)
N(4)-In(1)-N(10)	87.31(8)
N(7)-In(1)-N(10)	94.02(8)
N(1)-In(1)-N(10)	177.44(8)
N(16)-In(1)-N(10)	89.56(8)
N(4)-In(1)-N(13)	176.44(7)
N(7)-In(1)-N(13)	88.43(8)
N(1)-In(1)-N(13)	93.38(8)
N(16)-In(1)-N(13)	88.80(7)
N(10)-In(1)-N(13)	89.17(7)

N(2)-N(1)-In(1)	127.81(17)
N(3)-N(2)-N(1)	176.8(3)
N(5)-N(4)-In(1)	125.33(18)
N(6)-N(5)-N(4)	176.1(3)
N(8)-N(7)-In(1)	125.94(19)
N(7)-N(8)-N(9)	176.8(3)
N(11)-N(10)-In(1)	120.65(17)
N(12)-N(11)-N(10)	176.9(3)
N(14)-N(13)-In(1)	118.43(16)
N(15)-N(14)-N(13)	177.5(3)
N(17)-N(16)-In(1)	121.85(17)
N(18)-N(17)-N(16)	177.8(3)
C(1)-P(1)-C(13)	107.64(10)
C(1)-P(1)-C(19)	109.84(11)
C(13)-P(1)-C(19)	110.36(11)
C(1)-P(1)-C(7)	110.86(11)
C(13)-P(1)-C(7)	110.34(11)
C(19)-P(1)-C(7)	107.82(11)
C(31)-P(2)-C(25)	108.44(10)
C(31)-P(2)-C(37)	110.03(10)
C(25)-P(2)-C(37)	110.80(11)
C(31)-P(2)-C(43)	110.39(11)
C(25)-P(2)-C(43)	106.07(10)
C(37)-P(2)-C(43)	111.01(11)
C(61)-P(3)-C(67)	111.90(11)
C(61)-P(3)-C(49)	108.86(11)
C(67)-P(3)-C(49)	108.05(11)
C(61)-P(3)-C(55)	109.10(11)
C(67)-P(3)-C(55)	107.71(10)
C(49)-P(3)-C(55)	111.23(10)
C(2)-C(1)-C(6)	118.7(2)
C(2)-C(1)-P(1)	122.4(2)
C(6)-C(1)-P(1)	118.86(19)
C(1)-C(2)-C(3)	119.5(3)
C(4)-C(3)-C(2)	120.8(3)
C(3)-C(4)-C(5)	119.9(3)
C(6)-C(5)-C(4)	119.7(3)
C(5)-C(6)-C(1)	121.3(2)
C(12)-C(7)-C(8)	119.6(2)
C(12)-C(7)-P(1)	118.37(19)

C(8)-C(7)-P(1)	122.0(2)
C(9)-C(8)-C(7)	119.6(3)
C(10)-C(9)-C(8)	120.5(3)
C(9)-C(10)-C(11)	120.6(3)
C(12)-C(11)-C(10)	119.4(3)
C(11)-C(12)-C(7)	120.4(2)
C(14)-C(13)-C(18)	119.4(2)
C(14)-C(13)-P(1)	122.32(18)
C(18)-C(13)-P(1)	118.18(18)
C(13)-C(14)-C(15)	119.9(2)
C(16)-C(15)-C(14)	120.0(2)
C(15)-C(16)-C(17)	120.5(2)
C(18)-C(17)-C(16)	119.6(2)
C(17)-C(18)-C(13)	120.5(2)
C(20)-C(19)-C(24)	119.9(2)
C(20)-C(19)-P(1)	122.80(18)
C(24)-C(19)-P(1)	117.2(2)
C(21)-C(20)-C(19)	119.6(2)
C(22)-C(21)-C(20)	120.4(3)
C(23)-C(22)-C(21)	119.8(3)
C(24)-C(23)-C(22)	120.6(3)
C(23)-C(24)-C(19)	119.7(3)
C(30)-C(25)-C(26)	119.2(2)
C(30)-C(25)-P(2)	121.24(18)
C(26)-C(25)-P(2)	119.51(19)
C(27)-C(26)-C(25)	119.9(2)
C(26)-C(27)-C(28)	120.4(2)
C(29)-C(28)-C(27)	119.9(2)
C(28)-C(29)-C(30)	120.3(3)
C(29)-C(30)-C(25)	120.3(2)
C(32)-C(31)-C(36)	119.9(2)
C(32)-C(31)-P(2)	120.16(18)
C(36)-C(31)-P(2)	119.84(17)
C(31)-C(32)-C(33)	119.7(2)
C(34)-C(33)-C(32)	120.0(2)
C(33)-C(34)-C(35)	120.1(2)
C(36)-C(35)-C(34)	120.3(2)
C(35)-C(36)-C(31)	119.8(2)
C(42)-C(37)-C(38)	119.5(2)
C(42)-C(37)-P(2)	121.38(18)

C(38)-C(37)-P(2)	119.10(18)
C(39)-C(38)-C(37)	119.6(2)
C(40)-C(39)-C(38)	120.5(2)
C(39)-C(40)-C(41)	119.9(2)
C(42)-C(41)-C(40)	120.6(2)
C(41)-C(42)-C(37)	120.0(2)
C(44)-C(43)-C(48)	119.3(2)
C(44)-C(43)-P(2)	121.10(18)
C(48)-C(43)-P(2)	119.46(18)
C(45)-C(44)-C(43)	120.0(2)
C(46)-C(45)-C(44)	119.9(2)
C(47)-C(46)-C(45)	120.9(2)
C(46)-C(47)-C(48)	119.8(2)
C(47)-C(48)-C(43)	120.1(2)
C(54)-C(49)-C(50)	119.9(2)
C(54)-C(49)-P(3)	121.63(17)
C(50)-C(49)-P(3)	118.20(18)
C(51)-C(50)-C(49)	119.7(2)
C(50)-C(51)-C(52)	120.1(2)
C(53)-C(52)-C(51)	120.5(2)
C(52)-C(53)-C(54)	119.8(2)
C(49)-C(54)-C(53)	119.9(2)
C(60)-C(55)-C(56)	119.3(2)
C(60)-C(55)-P(3)	122.40(18)
C(56)-C(55)-P(3)	118.22(18)
C(57)-C(56)-C(55)	120.1(2)
C(58)-C(57)-C(56)	120.0(2)
C(57)-C(58)-C(59)	120.5(2)
C(58)-C(59)-C(60)	120.0(2)
C(55)-C(60)-C(59)	120.0(2)
C(66)-C(61)-C(62)	119.7(2)
C(66)-C(61)-P(3)	121.85(19)
C(62)-C(61)-P(3)	118.41(18)
C(63)-C(62)-C(61)	120.4(2)
C(62)-C(63)-C(64)	119.6(3)
C(63)-C(64)-C(65)	120.8(3)
C(64)-C(65)-C(66)	119.9(3)
C(65)-C(66)-C(61)	119.5(3)
C(72)-C(67)-C(68)	119.2(2)
C(72)-C(67)-P(3)	120.70(18)

C(68)-C(67)-P(3)	120.10(18)
C(69)-C(68)-C(67)	120.1(2)
C(70)-C(69)-C(68)	120.1(2)
C(69)-C(70)-C(71)	120.0(2)
C(70)-C(71)-C(72)	120.5(3)
C(67)-C(72)-C(71)	120.1(2)

Symmetry transformations used to generate equivalent atoms:

Table S22. Anisotropic displacement parameters ($Å^2 x\ 10^3$) for C72H60InN18P3. The anisotropic displacement factor exponent takes the form: $-2\pi^2[\ h^2\ a^{*2}U^{11} + ...\ + 2\ h\ k\ a^*\ b^*\ U^{12}\ ]$

	U^{11}	U^{22}	U^{33}	U^{23}	U^{13}	U^{12}
In(1)	27(1)	23(1)	22(1)	-1(1)	4(1)	-2(1)
N(1)	39(1)	46(2)	24(1)	-1(1)	3(1)	-17(1)
N(2)	36(1)	29(1)	31(1)	4(1)	16(1)	-7(1)
N(3)	42(2)	66(2)	42(2)	14(1)	-2(1)	-17(1)
N(4)	40(1)	34(1)	33(1)	-9(1)	14(1)	-5(1)
N(5)	43(1)	30(1)	26(1)	-3(1)	-2(1)	3(1)
N(6)	102(2)	67(2)	43(2)	5(2)	41(2)	-9(2)
N(7)	55(2)	42(2)	24(1)	6(1)	4(1)	12(1)
N(8)	42(2)	44(2)	23(1)	11(1)	-8(1)	-1(1)
N(9)	69(2)	102(3)	51(2)	16(2)	-6(2)	43(2)
N(10)	28(1)	30(1)	45(2)	-2(1)	4(1)	-5(1)
N(11)	43(2)	29(1)	28(1)	-4(1)	10(1)	-13(1)
N(12)	31(2)	59(2)	91(2)	-14(2)	17(2)	-6(1)
N(13)	39(1)	27(1)	23(1)	0(1)	8(1)	1(1)
N(14)	20(1)	31(1)	31(1)	-6(1)	2(1)	0(1)
N(15)	36(1)	60(2)	29(1)	5(1)	11(1)	-8(1)
N(16)	37(1)	31(1)	28(1)	4(1)	3(1)	5(1)
N(17)	54(2)	41(2)	19(1)	-1(1)	8(1)	14(1)
N(18)	118(2)	34(2)	45(2)	11(1)	9(2)	12(2)
P(1)	25(1)	30(1)	22(1)	-1(1)	3(1)	3(1)
P(2)	25(1)	22(1)	17(1)	1(1)	2(1)	0(1)
P(3)	25(1)	23(1)	19(1)	1(1)	4(1)	-1(1)
C(1)	24(1)	29(2)	25(1)	-5(1)	-3(1)	5(1)
C(2)	60(2)	41(2)	33(2)	-6(1)	16(2)	5(2)
C(3)	76(2)	30(2)	45(2)	-15(2)	13(2)	7(2)
C(4)	53(2)	28(2)	42(2)	2(1)	-8(2)	0(1)
C(5)	38(2)	39(2)	30(2)	1(1)	-4(1)	-6(1)
C(6)	35(2)	35(2)	29(2)	-9(1)	7(1)	-2(1)
C(7)	19(1)	29(2)	23(1)	-1(1)	3(1)	2(1)
C(8)	26(1)	27(2)	35(2)	0(1)	2(1)	2(1)
C(9)	36(2)	44(2)	25(2)	3(1)	-4(1)	-1(1)
C(10)	35(2)	48(2)	29(2)	-9(1)	2(1)	-8(1)
C(11)	34(2)	29(2)	45(2)	-7(1)	8(1)	-7(1)
C(12)	33(2)	31(2)	31(2)	4(1)	5(1)	1(1)
C(13)	22(1)	28(2)	21(1)	2(1)	5(1)	0(1)

C(14)	30(2)	33(2)	26(2)	3(1)	1(1)	3(1)
C(15)	37(2)	27(2)	39(2)	6(1)	14(1)	7(1)
C(16)	24(1)	43(2)	40(2)	21(1)	7(1)	9(1)
C(17)	26(2)	51(2)	26(2)	11(1)	1(1)	-8(1)
C(18)	25(1)	36(2)	25(2)	0(1)	7(1)	0(1)
C(19)	23(1)	37(2)	27(2)	-6(1)	6(1)	2(1)
C(20)	29(1)	29(2)	31(2)	-6(1)	6(1)	-1(1)
C(21)	44(2)	38(2)	29(2)	-4(1)	13(1)	-8(1)
C(22)	39(2)	47(2)	48(2)	-18(2)	24(2)	-13(1)
C(23)	28(2)	60(2)	60(2)	-7(2)	14(2)	6(2)
C(24)	35(2)	57(2)	45(2)	4(2)	10(1)	10(1)
C(25)	25(1)	25(2)	17(1)	2(1)	1(1)	2(1)
C(26)	29(2)	34(2)	30(2)	-5(1)	2(1)	3(1)
C(27)	26(2)	47(2)	41(2)	-8(2)	5(1)	11(1)
C(28)	26(2)	46(2)	44(2)	-3(2)	-2(1)	-2(1)
C(29)	37(2)	38(2)	45(2)	-14(1)	-1(1)	-6(1)
C(30)	27(2)	37(2)	39(2)	-10(1)	6(1)	0(1)
C(31)	29(1)	20(1)	16(1)	2(1)	4(1)	3(1)
C(32)	28(1)	30(2)	23(1)	2(1)	5(1)	4(1)
C(33)	45(2)	33(2)	19(1)	6(1)	3(1)	12(1)
C(34)	58(2)	23(2)	25(2)	4(1)	16(1)	1(1)
C(35)	39(2)	32(2)	30(2)	-1(1)	9(1)	-5(1)
C(36)	33(2)	29(2)	24(1)	5(1)	2(1)	2(1)
C(37)	22(1)	21(1)	23(1)	2(1)	3(1)	-1(1)
C(38)	27(1)	29(2)	21(1)	2(1)	2(1)	0(1)
C(39)	34(2)	32(2)	30(2)	-6(1)	8(1)	3(1)
C(40)	33(2)	24(2)	45(2)	3(1)	8(1)	4(1)
C(41)	44(2)	35(2)	33(2)	10(1)	3(1)	8(1)
C(42)	33(1)	32(2)	20(1)	3(1)	5(1)	5(1)
C(43)	21(1)	24(1)	18(1)	1(1)	1(1)	3(1)
C(44)	26(1)	30(2)	25(2)	1(1)	-1(1)	2(1)
C(45)	31(2)	31(2)	32(2)	-10(1)	-5(1)	2(1)
C(46)	30(2)	50(2)	19(2)	-11(1)	-3(1)	8(1)
C(47)	26(1)	47(2)	20(1)	3(1)	3(1)	6(1)
C(48)	25(1)	29(2)	25(2)	1(1)	3(1)	2(1)
C(49)	27(1)	20(1)	19(1)	1(1)	7(1)	-2(1)
C(50)	28(1)	39(2)	23(2)	-1(1)	1(1)	-6(1)
C(51)	31(2)	39(2)	33(2)	-6(1)	10(1)	-11(1)
C(52)	47(2)	25(2)	31(2)	2(1)	18(1)	-5(1)
C(53)	44(2)	31(2)	22(2)	6(1)	8(1)	8(1)

C(54)	25(1)	27(2)	25(2)	0(1)	7(1)	4(1)
C(55)	23(1)	27(2)	14(1)	0(1)	6(1)	-3(1)
C(56)	30(1)	24(2)	23(1)	1(1)	6(1)	-1(1)
C(57)	24(1)	43(2)	22(1)	2(1)	5(1)	1(1)
C(58)	28(2)	45(2)	22(2)	-4(1)	6(1)	-11(1)
C(59)	41(2)	28(2)	27(2)	-8(1)	9(1)	-12(1)
C(60)	31(1)	28(2)	24(1)	-2(1)	6(1)	0(1)
C(61)	22(1)	26(2)	24(1)	3(1)	1(1)	-1(1)
C(62)	30(1)	37(2)	29(2)	1(1)	6(1)	2(1)
C(63)	32(2)	39(2)	48(2)	1(2)	9(1)	8(1)
C(64)	35(2)	41(2)	58(2)	14(2)	-1(2)	13(1)
C(65)	46(2)	48(2)	36(2)	13(2)	-5(1)	7(2)
C(66)	35(2)	34(2)	30(2)	2(1)	1(1)	5(1)
C(67)	25(1)	23(1)	18(1)	-2(1)	1(1)	-1(1)
C(68)	36(2)	26(2)	31(2)	-2(1)	11(1)	-4(1)
C(69)	34(2)	39(2)	24(2)	-3(1)	8(1)	-4(1)
C(70)	41(2)	37(2)	27(2)	-14(1)	2(1)	-3(1)
C(71)	70(2)	27(2)	32(2)	-5(1)	7(2)	-10(2)
C(72)	50(2)	30(2)	19(1)	0(1)	8(1)	-8(1)

Table S23. Hydrogen coordinates (x 10^4) and isotropic displacement parameters (Å^{2}x 10^3) for C72H60InN18P3.

	x	y	z	U(eq)
H(2)	1402	2443	-251	53
H(3)	934	1462	-127	60
H(4)	144	1179	707	50
H(5)	-265	1879	1407	43
H(6)	163	2855	1281	39
H(8)	2097	3022	1572	35
H(9)	3012	3432	2439	43
H(10)	3275	4437	2505	45
H(11)	2606	5056	1712	43
H(12)	1689	4653	840	38
H(14)	-55	4375	1021	36
H(15)	-1664	4806	766	40
H(16)	-2597	4604	-172	42
H(17)	-1973	3939	-848	42
H(18)	-403	3480	-581	34
H(20)	978	4125	-743	35
H(21)	2117	4253	-1471	44
H(22)	3736	3825	-1326	52
H(23)	4209	3248	-466	58
H(24)	3087	3112	263	54
H(26)	3906	4945	5420	37
H(27)	5618	5178	5700	46
H(28)	6061	5998	6308	47
H(29)	4795	6563	6671	48
H(30)	3078	6329	6411	41
H(32)	3077	4762	6647	32
H(33)	2608	4036	7316	39
H(34)	901	3755	7287	41
H(35)	-346	4201	6599	40
H(36)	109	4918	5929	34
H(38)	1179	6103	6595	31
H(39)	192	6956	6597	38
H(40)	-383	7425	5685	40
H(41)	17	7044	4764	45

H(42)	1013	6200	4747	34
H(44)	1340	4309	5148	33
H(45)	1413	3867	4196	38
H(46)	1976	4405	3403	40
H(47)	2515	5371	3553	37
H(48)	2522	5807	4515	32
H(50)	4930	2909	1813	36
H(51)	4221	2323	2523	41
H(52)	5233	1990	3393	40
H(53)	6963	2224	3552	38
H(54)	7695	2802	2835	30
H(56)	8935	2902	2049	31
H(57)	10501	3342	2385	35
H(58)	10618	4359	2476	38
H(59)	9172	4944	2260	38
H(60)	7589	4510	1935	33
H(62)	5876	4234	2172	38
H(63)	4833	5004	1785	47
H(64)	4331	5066	741	54
H(65)	4847	4357	79	53
H(66)	5932	3592	459	40
H(68)	7706	3381	506	36
H(69)	8022	2703	-243	39
H(70)	7816	1702	-78	43
H(71)	7253	1377	824	51
H(72)	6844	2051	1555	39

Table S24. Crystal data and structure refinement for C72H60N18P3Tl.

Identification code	tlazidem	
Empirical formula	C72 H60 N18 P3 Tl	
Formula weight	1474.66	
Temperature	163(2) K	
Wavelength	0.71073 Å	
Crystal system	Monoclinic	
Space group	P2(1)/n	
Unit cell dimensions	a = 13.123(2) Å	α= 90°.
	b = 22.814(4) Å	β= 96.816(3)°.
	c = 22.038(3) Å	γ = 90°.
Volume	6551.4(18) $Å^3$	
Z	4	
Density (calculated)	1.495 Mg/m^3	
Absorption coefficient	2.598 mm^{-1}	
F(000)	2976	
Crystal size	0.30 x 0.18 x 0.09 mm^3	
Theta range for data collection	1.29 to 27.55°.	
Index ranges	-17<=h<=13, -29<=k<=27, -26<=l<=28	
Reflections collected	40444	
Independent reflections	14857 [R(int) = 0.0541]	
Completeness to theta = 27.55°	98.2 %	
Absorption correction	Multi-scan	
Transmission factors	min/max ratio: 0.665	
Refinement method	Full-matrix least-squares on F^2	
Data / restraints / parameters	14857 / 1 / 847	
Goodness-of-fit on F^2	1.051	
Final R indices [I>2sigma(I)]	R1 = 0.0424, wR2 = 0.0762	
R indices (all data)	R1 = 0.0710, wR2 = 0.0836	
Largest diff. peak and hole	1.561 and -0.811 $e.Å^{-3}$	

Table S25. Atomic coordinates (x 10^4) and equivalent isotropic displacement parameters ($Å^2$x 10^3) for C72H60N18P3Tl. U(eq) is defined as one third of the trace of the orthogonalized U^{ij} tensor.

	x	y	z	U(eq)
Tl(1)	6965(1)	3492(1)	7655(1)	25(1)
N(1)	6032(3)	4065(2)	6934(2)	47(1)
N(2)	5467(3)	4385(2)	7063(2)	38(1)
N(3)	4859(4)	4747(2)	7170(2)	82(2)
N(4)	8302(3)	4137(2)	7550(2)	40(1)
N(5)	8999(3)	4198(1)	7937(2)	31(1)
N(6)	9700(3)	4282(2)	8296(2)	54(1)
N(7)	7974(3)	2990(2)	8419(2)	33(1)
N(8)	7780(3)	2476(2)	8471(1)	38(1)
N(9)	7634(4)	1982(2)	8539(2)	70(1)
N(10)	5644(3)	2814(2)	7708(2)	37(1)
N(11)	4817(2)	3011(1)	7669(2)	36(1)
N(12)	3966(3)	3172(2)	7603(2)	69(1)
N(13)	6311(3)	4039(1)	8413(2)	31(1)
N(14)	6131(2)	3755(2)	8845(2)	29(1)
N(15)	5970(3)	3501(2)	9276(2)	41(1)
N(16)	7519(3)	2906(2)	6924(2)	37(1)
N(17)	7991(3)	3106(2)	6542(2)	36(1)
N(18)	8451(4)	3272(2)	6165(2)	69(1)
P(1)	2990(1)	426(1)	9322(1)	22(1)
P(2)	6130(1)	1475(1)	5417(1)	26(1)
P(3)	6946(1)	3300(1)	1664(1)	22(1)
C(1)	3357(3)	-96(2)	8778(2)	22(1)
C(2)	2605(3)	-356(2)	8361(2)	30(1)
C(3)	2897(4)	-784(2)	7971(2)	36(1)
C(4)	3908(4)	-946(2)	7986(2)	36(1)
C(5)	4655(3)	-687(2)	8394(2)	35(1)
C(6)	4378(3)	-260(2)	8786(2)	30(1)
C(7)	3059(3)	98(2)	10066(2)	22(1)
C(8)	3398(3)	-474(2)	10165(2)	27(1)
C(9)	3369(3)	-735(2)	10732(2)	32(1)
C(10)	3027(3)	-419(2)	11201(2)	34(1)
C(11)	2704(3)	153(2)	11117(2)	32(1)
C(12)	2698(3)	412(2)	10545(2)	26(1)
C(13)	3799(3)	1060(2)	9331(2)	21(1)

C(14)	4148(3)	1343(2)	9874(2)	30(1)
C(15)	4744(3)	1842(2)	9868(2)	38(1)
C(16)	4984(3)	2067(2)	9320(2)	34(1)
C(17)	4639(3)	1792(2)	8778(2)	32(1)
C(18)	4057(3)	1291(2)	8779(2)	26(1)
C(19)	1675(3)	622(2)	9113(2)	25(1)
C(20)	1412(3)	1096(2)	8730(2)	34(1)
C(21)	388(3)	1231(2)	8564(2)	41(1)
C(22)	-375(3)	902(2)	8784(2)	41(1)
C(23)	-116(3)	428(2)	9153(2)	40(1)
C(24)	898(3)	285(2)	9318(2)	33(1)
C(25)	6927(3)	1376(2)	4818(2)	32(1)
C(26)	6643(3)	1038(2)	4305(2)	30(1)
C(27)	7310(4)	966(2)	3874(2)	40(1)
C(28)	8271(4)	1223(2)	3950(2)	43(1)
C(29)	8557(4)	1567(2)	4456(2)	50(1)
C(30)	7896(3)	1642(2)	4894(2)	48(1)
C(31)	6801(3)	1189(2)	6106(2)	24(1)
C(32)	6952(3)	585(2)	6154(2)	32(1)
C(33)	7499(3)	349(2)	6669(2)	36(1)
C(34)	7898(3)	718(2)	7139(2)	39(1)
C(35)	7755(3)	1312(2)	7096(2)	36(1)
C(36)	7216(3)	1555(2)	6584(2)	31(1)
C(37)	5853(3)	2239(2)	5495(2)	27(1)
C(38)	5363(3)	2417(2)	5986(2)	35(1)
C(39)	5108(3)	2993(2)	6058(2)	34(1)
C(40)	5337(4)	3398(2)	5636(2)	44(1)
C(41)	5797(4)	3228(2)	5141(2)	51(1)
C(42)	6067(4)	2651(2)	5067(2)	45(1)
C(43)	4933(3)	1099(2)	5233(2)	25(1)
C(44)	4345(3)	1232(2)	4680(2)	30(1)
C(45)	3403(3)	965(2)	4532(2)	35(1)
C(46)	3040(3)	585(2)	4942(2)	35(1)
C(47)	3595(3)	461(2)	5492(2)	35(1)
C(48)	4548(3)	715(2)	5643(2)	28(1)
C(49)	7247(3)	2778(2)	1101(2)	23(1)
C(50)	7108(3)	2183(2)	1192(2)	34(1)
C(51)	7347(4)	1791(2)	753(2)	43(1)
C(52)	7686(3)	1979(2)	219(2)	37(1)
C(53)	7829(3)	2569(2)	133(2)	32(1)

C(54)	7628(3)	2967(2)	571(2)	30(1)
C(55)	8124(3)	3662(2)	1953(2)	23(1)
C(56)	9002(3)	3321(2)	2089(2)	25(1)
C(57)	9934(3)	3587(2)	2291(2)	30(1)
C(58)	9983(3)	4187(2)	2350(2)	34(1)
C(59)	9119(3)	4532(2)	2217(2)	33(1)
C(60)	8187(3)	4269(2)	2022(2)	27(1)
C(61)	6046(3)	3836(2)	1346(2)	26(1)
C(62)	5728(3)	3866(2)	722(2)	35(1)
C(63)	5080(4)	4313(2)	499(2)	48(1)
C(64)	4770(4)	4730(2)	879(2)	49(1)
C(65)	5053(3)	4700(2)	1497(2)	41(1)
C(66)	5684(3)	4251(2)	1732(2)	32(1)
C(67)	6398(3)	2909(2)	2254(2)	23(1)
C(68)	5362(3)	2768(2)	2162(2)	30(1)
C(69)	4940(3)	2423(2)	2590(2)	34(1)
C(70)	5539(3)	2222(2)	3098(2)	35(1)
C(71)	6565(3)	2365(2)	3195(2)	33(1)
C(72)	7006(3)	2707(2)	2771(2)	28(1)

Table S26. Bond lengths [Å] and angles [°] for C72H60N18P3Tl.

Tl(1)-N(16)	2.278(3)
Tl(1)-N(1)	2.295(4)
Tl(1)-N(7)	2.317(3)
Tl(1)-N(4)	2.322(3)
Tl(1)-N(13)	2.328(3)
Tl(1)-N(10)	2.338(3)
N(1)-N(2)	1.100(5)
N(2)-N(3)	1.193(6)
N(4)-N(5)	1.182(5)
N(5)-N(6)	1.156(5)
N(7)-N(8)	1.209(5)
N(8)-N(9)	1.155(5)
N(10)-N(11)	1.168(3)
N(11)-N(12)	1.169(3)
N(13)-N(14)	1.200(4)
N(14)-N(15)	1.152(5)
N(16)-N(17)	1.194(5)
N(17)-N(18)	1.146(5)
P(1)-C(19)	1.789(4)
P(1)-C(13)	1.793(4)
P(1)-C(7)	1.796(4)
P(1)-C(1)	1.796(4)
P(2)-C(31)	1.786(4)
P(2)-C(37)	1.792(4)
P(2)-C(25)	1.794(4)
P(2)-C(43)	1.794(4)
P(3)-C(61)	1.785(4)
P(3)-C(49)	1.796(4)
P(3)-C(67)	1.797(4)
P(3)-C(55)	1.801(4)
C(1)-C(6)	1.390(5)
C(1)-C(2)	1.398(5)
C(2)-C(3)	1.386(5)
C(3)-C(4)	1.373(6)
C(4)-C(5)	1.382(6)
C(5)-C(6)	1.381(5)
C(7)-C(8)	1.387(5)
C(7)-C(12)	1.404(5)

C(8)-C(9)	1.390(5)
C(9)-C(10)	1.379(6)
C(10)-C(11)	1.377(6)
C(11)-C(12)	1.391(5)
C(13)-C(14)	1.387(5)
C(13)-C(18)	1.404(5)
C(14)-C(15)	1.383(6)
C(15)-C(16)	1.381(6)
C(16)-C(17)	1.378(5)
C(17)-C(18)	1.375(5)
C(19)-C(20)	1.390(5)
C(19)-C(24)	1.395(5)
C(20)-C(21)	1.385(6)
C(21)-C(22)	1.383(6)
C(22)-C(23)	1.371(6)
C(23)-C(24)	1.376(6)
C(25)-C(26)	1.382(5)
C(25)-C(30)	1.401(6)
C(26)-C(27)	1.377(5)
C(27)-C(28)	1.382(6)
C(28)-C(29)	1.380(7)
C(29)-C(30)	1.382(6)
C(31)-C(32)	1.394(5)
C(31)-C(36)	1.402(5)
C(32)-C(33)	1.378(5)
C(33)-C(34)	1.387(6)
C(34)-C(35)	1.371(6)
C(35)-C(36)	1.375(5)
C(37)-C(42)	1.384(5)
C(37)-C(38)	1.385(5)
C(38)-C(39)	1.370(6)
C(39)-C(40)	1.370(6)
C(40)-C(41)	1.363(6)
C(41)-C(42)	1.378(6)
C(43)-C(48)	1.396(5)
C(43)-C(44)	1.396(5)
C(44)-C(45)	1.383(6)
C(45)-C(46)	1.375(6)
C(46)-C(47)	1.369(6)
C(47)-C(48)	1.383(5)

C(49)-C(50)	1.388(5)
C(49)-C(54)	1.392(5)
C(50)-C(51)	1.382(6)
C(51)-C(52)	1.375(6)
C(52)-C(53)	1.374(6)
C(53)-C(54)	1.374(5)
C(55)-C(56)	1.393(5)
C(55)-C(60)	1.395(5)
C(56)-C(57)	1.391(5)
C(57)-C(58)	1.376(5)
C(58)-C(59)	1.382(6)
C(59)-C(60)	1.384(5)
C(61)-C(62)	1.391(5)
C(61)-C(66)	1.392(5)
C(62)-C(63)	1.382(6)
C(63)-C(64)	1.360(6)
C(64)-C(65)	1.370(6)
C(65)-C(66)	1.378(6)
C(67)-C(68)	1.388(5)
C(67)-C(72)	1.389(5)
C(68)-C(69)	1.392(5)
C(69)-C(70)	1.369(6)
C(70)-C(71)	1.377(6)
C(71)-C(72)	1.394(5)

N(16)-Tl(1)-N(1)	91.92(14)
N(16)-Tl(1)-N(7)	91.22(12)
N(1)-Tl(1)-N(7)	174.90(14)
N(16)-Tl(1)-N(4)	89.61(13)
N(1)-Tl(1)-N(4)	85.29(14)
N(7)-Tl(1)-N(4)	90.71(13)
N(16)-Tl(1)-N(13)	175.86(12)
N(1)-Tl(1)-N(13)	88.81(13)
N(7)-Tl(1)-N(13)	88.35(12)
N(4)-Tl(1)-N(13)	94.51(13)
N(16)-Tl(1)-N(10)	87.01(13)
N(1)-Tl(1)-N(10)	94.23(14)
N(7)-Tl(1)-N(10)	89.95(13)
N(4)-Tl(1)-N(10)	176.57(13)
N(13)-Tl(1)-N(10)	88.88(13)

N(2)-N(1)-Tl(1)	121.3(3)
N(1)-N(2)-N(3)	176.2(5)
N(5)-N(4)-Tl(1)	122.1(3)
N(6)-N(5)-N(4)	176.1(4)
N(8)-N(7)-Tl(1)	116.1(3)
N(9)-N(8)-N(7)	176.9(5)
N(11)-N(10)-Tl(1)	115.4(3)
N(10)-N(11)-N(12)	174.8(5)
N(14)-N(13)-Tl(1)	113.8(3)
N(15)-N(14)-N(13)	177.2(4)
N(17)-N(16)-Tl(1)	120.7(3)
N(18)-N(17)-N(16)	176.8(5)
C(19)-P(1)-C(13)	110.73(18)
C(19)-P(1)-C(7)	106.35(17)
C(13)-P(1)-C(7)	111.12(17)
C(19)-P(1)-C(1)	108.72(17)
C(13)-P(1)-C(1)	109.71(17)
C(7)-P(1)-C(1)	110.14(17)
C(31)-P(2)-C(37)	111.08(18)
C(31)-P(2)-C(25)	108.03(19)
C(37)-P(2)-C(25)	109.54(19)
C(31)-P(2)-C(43)	110.31(18)
C(37)-P(2)-C(43)	107.74(18)
C(25)-P(2)-C(43)	110.13(19)
C(61)-P(3)-C(49)	111.89(18)
C(61)-P(3)-C(67)	108.72(18)
C(49)-P(3)-C(67)	108.12(17)
C(61)-P(3)-C(55)	108.92(18)
C(49)-P(3)-C(55)	107.38(18)
C(67)-P(3)-C(55)	111.85(17)
C(6)-C(1)-C(2)	120.0(4)
C(6)-C(1)-P(1)	120.3(3)
C(2)-C(1)-P(1)	119.7(3)
C(3)-C(2)-C(1)	118.7(4)
C(4)-C(3)-C(2)	120.9(4)
C(3)-C(4)-C(5)	120.6(4)
C(6)-C(5)-C(4)	119.3(4)
C(5)-C(6)-C(1)	120.5(4)
C(8)-C(7)-C(12)	119.5(3)
C(8)-C(7)-P(1)	121.1(3)

C(12)-C(7)-P(1)	119.3(3)
C(7)-C(8)-C(9)	120.1(4)
C(10)-C(9)-C(8)	119.8(4)
C(11)-C(10)-C(9)	121.1(4)
C(10)-C(11)-C(12)	119.6(4)
C(11)-C(12)-C(7)	119.9(4)
C(14)-C(13)-C(18)	118.9(3)
C(14)-C(13)-P(1)	121.3(3)
C(18)-C(13)-P(1)	119.7(3)
C(15)-C(14)-C(13)	120.3(4)
C(16)-C(15)-C(14)	120.2(4)
C(17)-C(16)-C(15)	120.1(4)
C(18)-C(17)-C(16)	120.2(4)
C(17)-C(18)-C(13)	120.3(4)
C(20)-C(19)-C(24)	119.1(4)
C(20)-C(19)-P(1)	120.9(3)
C(24)-C(19)-P(1)	120.0(3)
C(21)-C(20)-C(19)	119.8(4)
C(22)-C(21)-C(20)	120.4(4)
C(23)-C(22)-C(21)	119.8(4)
C(22)-C(23)-C(24)	120.5(4)
C(23)-C(24)-C(19)	120.3(4)
C(26)-C(25)-C(30)	119.5(4)
C(26)-C(25)-P(2)	123.2(3)
C(30)-C(25)-P(2)	117.2(3)
C(27)-C(26)-C(25)	119.9(4)
C(26)-C(27)-C(28)	120.8(4)
C(29)-C(28)-C(27)	119.7(4)
C(28)-C(29)-C(30)	120.1(4)
C(29)-C(30)-C(25)	120.0(5)
C(32)-C(31)-C(36)	119.5(4)
C(32)-C(31)-P(2)	118.5(3)
C(36)-C(31)-P(2)	121.9(3)
C(33)-C(32)-C(31)	120.2(4)
C(32)-C(33)-C(34)	119.4(4)
C(35)-C(34)-C(33)	120.9(4)
C(34)-C(35)-C(36)	120.4(4)
C(35)-C(36)-C(31)	119.5(4)
C(42)-C(37)-C(38)	118.8(4)
C(42)-C(37)-P(2)	122.5(3)

C(38)-C(37)-P(2)	118.6(3)
C(39)-C(38)-C(37)	121.1(4)
C(38)-C(39)-C(40)	119.4(4)
C(41)-C(40)-C(39)	120.3(4)
C(40)-C(41)-C(42)	120.8(4)
C(41)-C(42)-C(37)	119.5(4)
C(48)-C(43)-C(44)	119.8(4)
C(48)-C(43)-P(2)	121.9(3)
C(44)-C(43)-P(2)	118.2(3)
C(45)-C(44)-C(43)	119.7(4)
C(46)-C(45)-C(44)	119.5(4)
C(47)-C(46)-C(45)	121.6(4)
C(46)-C(47)-C(48)	119.8(4)
C(47)-C(48)-C(43)	119.6(4)
C(50)-C(49)-C(54)	119.3(4)
C(50)-C(49)-P(3)	120.4(3)
C(54)-C(49)-P(3)	120.3(3)
C(51)-C(50)-C(49)	119.3(4)
C(52)-C(51)-C(50)	121.3(4)
C(53)-C(52)-C(51)	119.1(4)
C(54)-C(53)-C(52)	120.7(4)
C(53)-C(54)-C(49)	120.2(4)
C(56)-C(55)-C(60)	119.7(4)
C(56)-C(55)-P(3)	118.2(3)
C(60)-C(55)-P(3)	122.1(3)
C(57)-C(56)-C(55)	119.9(4)
C(58)-C(57)-C(56)	119.6(4)
C(57)-C(58)-C(59)	121.2(4)
C(58)-C(59)-C(60)	119.5(4)
C(59)-C(60)-C(55)	120.2(4)
C(62)-C(61)-C(66)	119.0(4)
C(62)-C(61)-P(3)	121.9(3)
C(66)-C(61)-P(3)	119.0(3)
C(63)-C(62)-C(61)	119.2(4)
C(64)-C(63)-C(62)	120.9(4)
C(63)-C(64)-C(65)	120.7(4)
C(64)-C(65)-C(66)	119.4(4)
C(65)-C(66)-C(61)	120.6(4)
C(68)-C(67)-C(72)	120.0(4)
C(68)-C(67)-P(3)	118.6(3)

C(72)-C(67)-P(3)	121.2(3)
C(67)-C(68)-C(69)	119.6(4)
C(70)-C(69)-C(68)	120.5(4)
C(69)-C(70)-C(71)	120.3(4)
C(70)-C(71)-C(72)	120.2(4)
C(67)-C(72)-C(71)	119.4(4)

Table S27. Anisotropic displacement parameters ($Å^2 x\ 10^3$) for C72H60N18P3Tl. The anisotropic displacement factor exponent takes the form: $-2\pi^2[\ h^2\ a^{*2}U^{11} + ...\ + 2\ h\ k\ a^*\ b^*\ U^{12}\ ]$

	U^{11}	U^{22}	U^{33}	U^{23}	U^{13}	U^{12}
Tl(1)	29(1)	21(1)	25(1)	0(1)	5(1)	-2(1)
N(1)	61(3)	49(3)	30(2)	8(2)	4(2)	7(2)
N(2)	46(3)	39(3)	24(2)	9(2)	-9(2)	-7(2)
N(3)	83(4)	100(4)	59(3)	5(3)	-14(3)	43(3)
N(4)	46(2)	45(2)	28(2)	3(2)	6(2)	-21(2)
N(5)	39(2)	24(2)	31(2)	6(2)	17(2)	-5(2)
N(6)	42(3)	73(3)	45(3)	15(2)	-7(2)	-19(2)
N(7)	37(2)	30(2)	33(2)	3(2)	4(2)	3(2)
N(8)	51(3)	42(3)	22(2)	-4(2)	6(2)	13(2)
N(9)	120(4)	32(3)	56(3)	11(2)	6(3)	13(3)
N(10)	39(2)	24(2)	46(2)	2(2)	1(2)	-10(2)
N(11)	46(3)	26(2)	36(2)	-4(2)	10(2)	-13(2)
N(12)	41(3)	62(3)	106(4)	-14(3)	19(3)	-8(2)
N(13)	40(2)	24(2)	30(2)	0(2)	9(2)	5(2)
N(14)	20(2)	34(2)	34(2)	-7(2)	4(2)	-2(2)
N(15)	38(2)	53(3)	35(2)	3(2)	15(2)	-8(2)
N(16)	49(2)	26(2)	37(2)	-8(2)	11(2)	-5(2)
N(17)	52(3)	26(2)	30(2)	-2(2)	2(2)	4(2)
N(18)	106(4)	58(3)	48(3)	3(2)	35(3)	-13(3)
P(1)	25(1)	20(1)	20(1)	-2(1)	3(1)	-2(1)
P(2)	26(1)	28(1)	25(1)	2(1)	3(1)	-3(1)
P(3)	26(1)	20(1)	22(1)	1(1)	4(1)	-1(1)
C(1)	31(2)	18(2)	17(2)	0(2)	6(2)	0(2)
C(2)	37(3)	25(2)	28(2)	1(2)	3(2)	-7(2)
C(3)	49(3)	33(3)	26(2)	-4(2)	6(2)	-13(2)
C(4)	67(3)	18(2)	26(2)	-5(2)	15(2)	-1(2)
C(5)	42(3)	30(3)	34(2)	4(2)	16(2)	7(2)
C(6)	34(3)	30(2)	28(2)	-1(2)	8(2)	0(2)
C(7)	21(2)	23(2)	21(2)	-2(2)	0(2)	-1(2)
C(8)	28(2)	22(2)	29(2)	-2(2)	2(2)	-1(2)
C(9)	33(3)	28(2)	34(2)	8(2)	-3(2)	1(2)
C(10)	30(2)	47(3)	25(2)	9(2)	-1(2)	-5(2)
C(11)	26(2)	53(3)	17(2)	-5(2)	7(2)	-8(2)
C(12)	26(2)	27(2)	27(2)	0(2)	6(2)	-3(2)
C(13)	20(2)	20(2)	25(2)	-3(2)	5(2)	-1(2)

C(14)	36(3)	30(2)	25(2)	-4(2)	6(2)	-2(2)
C(15)	45(3)	31(3)	37(3)	-12(2)	4(2)	-10(2)
C(16)	37(3)	23(2)	43(3)	-1(2)	4(2)	-2(2)
C(17)	36(3)	27(2)	33(2)	9(2)	9(2)	0(2)
C(18)	29(2)	24(2)	23(2)	1(2)	5(2)	0(2)
C(19)	27(2)	28(2)	20(2)	-3(2)	1(2)	-4(2)
C(20)	28(2)	33(3)	39(3)	9(2)	4(2)	-1(2)
C(21)	36(3)	44(3)	41(3)	12(2)	-3(2)	4(2)
C(22)	29(3)	48(3)	45(3)	-3(2)	-3(2)	0(2)
C(23)	31(3)	47(3)	42(3)	9(2)	3(2)	-10(2)
C(24)	33(3)	30(3)	36(2)	7(2)	4(2)	-7(2)
C(25)	30(2)	35(3)	33(2)	1(2)	9(2)	0(2)
C(26)	31(2)	28(2)	31(2)	3(2)	9(2)	2(2)
C(27)	46(3)	40(3)	37(3)	5(2)	13(2)	9(2)
C(28)	43(3)	43(3)	48(3)	17(2)	25(2)	12(2)
C(29)	28(3)	59(4)	66(4)	11(3)	15(2)	-5(2)
C(30)	30(3)	61(4)	52(3)	-5(2)	7(2)	-13(2)
C(31)	26(2)	22(2)	24(2)	2(2)	3(2)	1(2)
C(32)	31(2)	32(3)	34(2)	-4(2)	6(2)	3(2)
C(33)	34(3)	27(3)	47(3)	4(2)	8(2)	8(2)
C(34)	34(3)	51(3)	33(2)	9(2)	5(2)	15(2)
C(35)	33(3)	37(3)	36(2)	-2(2)	-3(2)	2(2)
C(36)	32(2)	29(2)	31(2)	1(2)	3(2)	2(2)
C(37)	25(2)	29(2)	25(2)	1(2)	-3(2)	-7(2)
C(38)	36(3)	36(3)	33(2)	8(2)	6(2)	-1(2)
C(39)	40(3)	30(3)	31(2)	-2(2)	-4(2)	1(2)
C(40)	56(3)	25(3)	47(3)	5(2)	-11(2)	1(2)
C(41)	78(4)	28(3)	50(3)	14(2)	15(3)	-4(2)
C(42)	67(3)	37(3)	32(2)	5(2)	17(2)	-9(2)
C(43)	20(2)	28(2)	27(2)	-5(2)	6(2)	-2(2)
C(44)	31(2)	32(2)	27(2)	-1(2)	10(2)	6(2)
C(45)	27(2)	48(3)	28(2)	-8(2)	2(2)	8(2)
C(46)	25(2)	38(3)	44(3)	-22(2)	9(2)	-4(2)
C(47)	38(3)	28(3)	42(3)	-2(2)	13(2)	-8(2)
C(48)	33(2)	28(2)	24(2)	0(2)	6(2)	-2(2)
C(49)	22(2)	23(2)	23(2)	-1(2)	1(2)	0(2)
C(50)	47(3)	26(2)	28(2)	-2(2)	9(2)	-5(2)
C(51)	68(4)	19(2)	42(3)	-3(2)	7(2)	-7(2)
C(52)	49(3)	38(3)	22(2)	-9(2)	2(2)	-1(2)
C(53)	36(3)	35(3)	25(2)	-2(2)	10(2)	-3(2)

C(54)	35(3)	23(2)	33(2)	4(2)	10(2)	-6(2)
C(55)	25(2)	21(2)	23(2)	1(2)	7(2)	-3(2)
C(56)	30(2)	22(2)	24(2)	1(2)	5(2)	0(2)
C(57)	24(2)	40(3)	28(2)	1(2)	7(2)	-1(2)
C(58)	29(3)	50(3)	22(2)	-4(2)	2(2)	-11(2)
C(59)	41(3)	25(2)	34(2)	-5(2)	10(2)	-13(2)
C(60)	32(2)	22(2)	29(2)	1(2)	6(2)	1(2)
C(61)	24(2)	25(2)	31(2)	5(2)	6(2)	-1(2)
C(62)	38(3)	33(3)	33(2)	2(2)	2(2)	2(2)
C(63)	51(3)	52(3)	40(3)	14(2)	-4(2)	10(2)
C(64)	41(3)	43(3)	61(3)	17(3)	0(3)	15(2)
C(65)	28(3)	34(3)	62(3)	1(2)	13(2)	7(2)
C(66)	29(2)	37(3)	31(2)	1(2)	8(2)	3(2)
C(67)	29(2)	17(2)	24(2)	-3(2)	6(2)	-2(2)
C(68)	27(2)	39(3)	25(2)	-3(2)	4(2)	-4(2)
C(69)	33(3)	33(3)	38(3)	-8(2)	11(2)	-14(2)
C(70)	50(3)	22(2)	35(2)	2(2)	19(2)	-4(2)
C(71)	41(3)	34(3)	26(2)	5(2)	9(2)	9(2)
C(72)	29(2)	26(2)	29(2)	1(2)	8(2)	2(2)

Table S28. Hydrogen coordinates (x 10^4) and isotropic displacement parameters (Å^{2}x 10^3) for C72H60N18P3Tl.

	x	y	z	U(eq)
H(2)	1906	-241	8345	36
H(3)	2392	-968	7689	43
H(4)	4094	-1239	7713	44
H(5)	5353	-802	8403	42
H(6)	4889	-77	9065	36
H(8)	3652	-687	9844	32
H(9)	3583	-1130	10796	39
H(10)	3015	-598	11589	41
H(11)	2486	369	11447	38
H(12)	2449	800	10478	32
H(14)	3976	1193	10251	36
H(15)	4989	2031	10241	45
H(16)	5389	2412	9318	41
H(17)	4803	1949	8403	38
H(18)	3828	1101	8404	31
H(20)	1933	1327	8583	40
H(21)	207	1551	8298	49
H(22)	-1076	1004	8679	49
H(23)	-640	197	9297	48
H(24)	1069	-46	9572	39
H(26)	5987	856	4250	36
H(27)	7108	738	3520	48
H(28)	8733	1163	3654	52
H(29)	9210	1753	4505	60
H(30)	8099	1873	5246	57
H(32)	6677	335	5831	38
H(33)	7601	-62	6702	43
H(34)	8275	556	7494	47
H(35)	8030	1558	7423	43
H(36)	7126	1967	6554	37
H(38)	5200	2136	6277	42
H(39)	4776	3111	6399	41
H(40)	5175	3800	5687	53
H(41)	5932	3510	4845	62

H(42)	6398	2537	4724	53
H(44)	4590	1506	4407	35
H(45)	3009	1042	4150	41
H(46)	2389	406	4840	42
H(47)	3325	201	5770	42
H(48)	4939	628	6023	34
H(50)	6851	2047	1552	40
H(51)	7276	1382	821	52
H(52)	7819	1705	-87	44
H(53)	8069	2702	-232	38
H(54)	7749	3373	512	36
H(56)	8963	2907	2043	30
H(57)	10533	3356	2389	36
H(58)	10622	4368	2484	41
H(59)	9165	4946	2259	40
H(60)	7589	4503	1936	33
H(62)	5954	3582	453	42
H(63)	4848	4330	74	58
H(64)	4354	5046	714	59
H(65)	4816	4985	1761	49
H(66)	5873	4225	2160	39
H(68)	4944	2906	1810	36
H(69)	4231	2326	2528	41
H(70)	5246	1983	3385	41
H(71)	6974	2229	3552	40
H(72)	7715	2802	2835	33

Figure S1. Asymmetric unit in the crystal structure of $[PPh_4]_2[Ga(N_3)_5]$. Thermal ellipsoids are drawn at the 50% probability level.

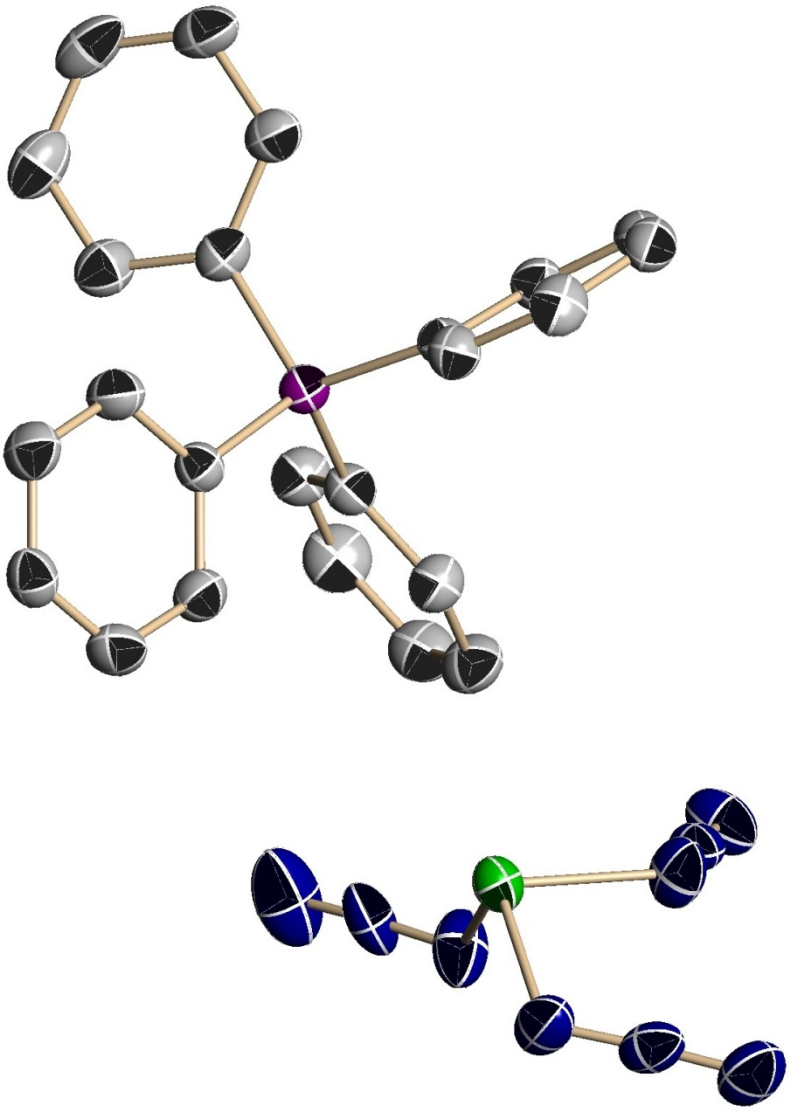

Figure S2. The unit cell of $[PPh_4]_2[Ga(N_3)_5]$. Thermal ellipsoids are drawn at the 50% probability level. The $[PPh_4]$ cations have been omitted.

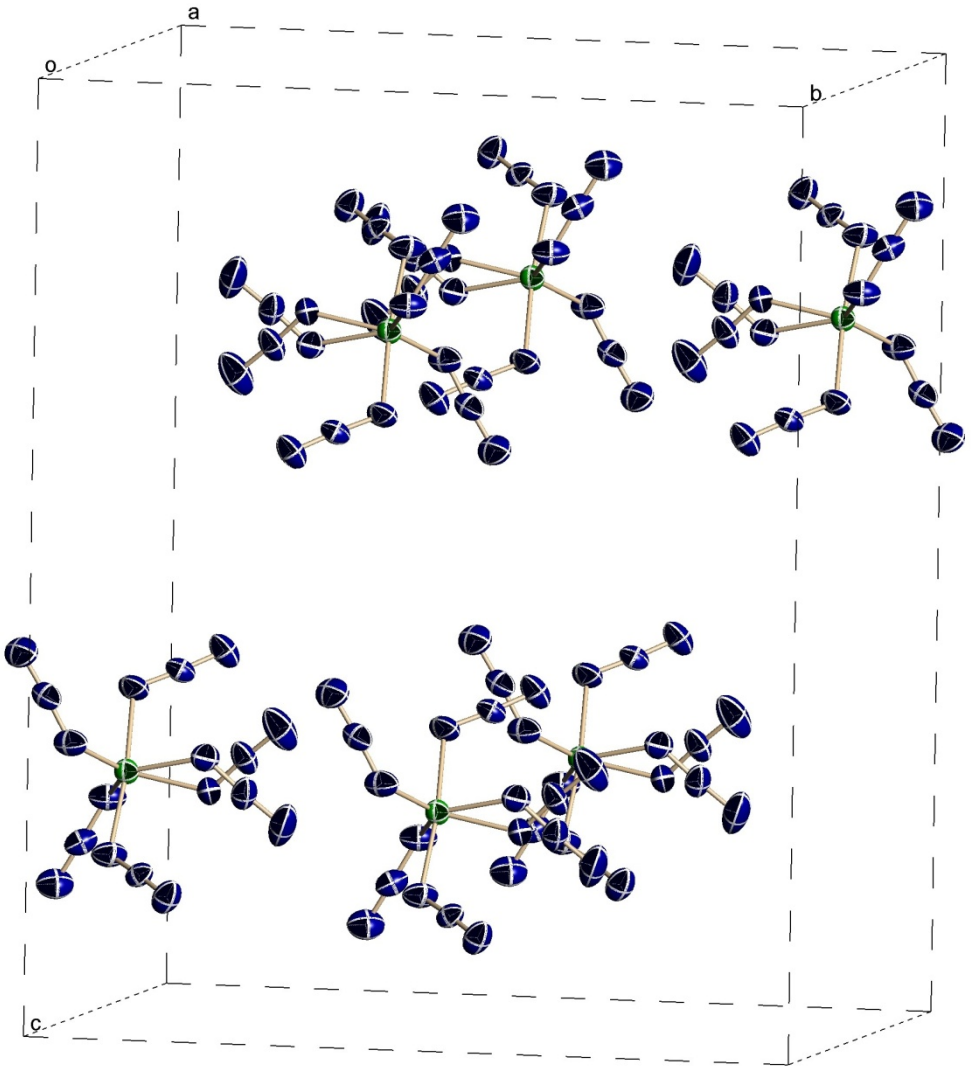

Figure S3. View along the a axis of the $[PPh_4]_2[Ga(N_3)_5]$ unit cell. Thermal ellipsoids are drawn at the 50% probability level. The $[PPh_4]$ cations have been omitted.

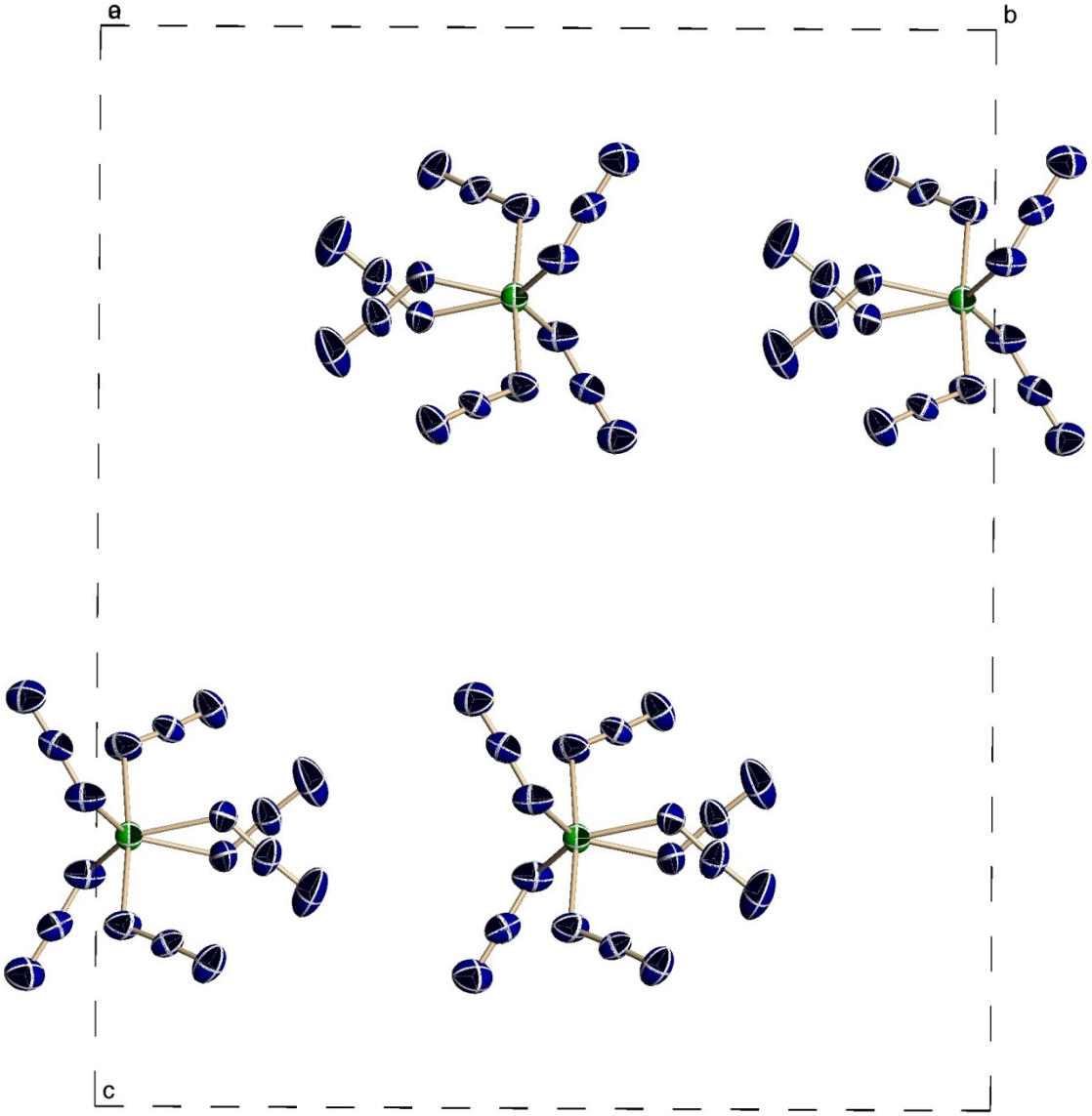

Figure S4. View along the b axis of the $[PPh_4]_2[Ga(N_3)_5]$ unit cell. Thermal ellipsoids are drawn at the 50% probability level. The $[PPh_4]$ cations have been omitted.

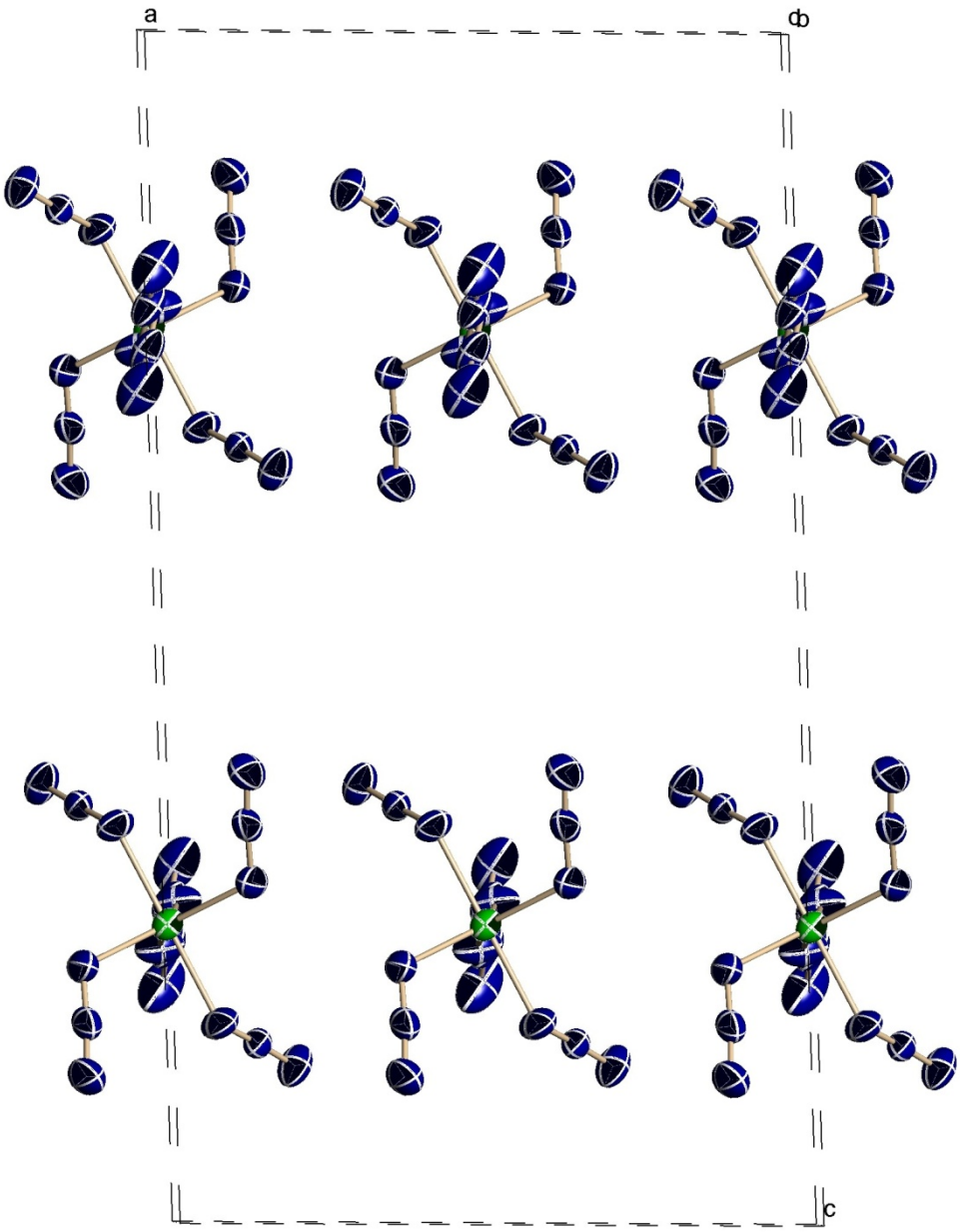

Figure S5. View along the b axis of the $[PPh_4]_2[Ga(N_3)_5]$ unit cell. Thermal ellipsoids are drawn at the 50% probability level. The $[PPh_4]$ cations have been omitted.

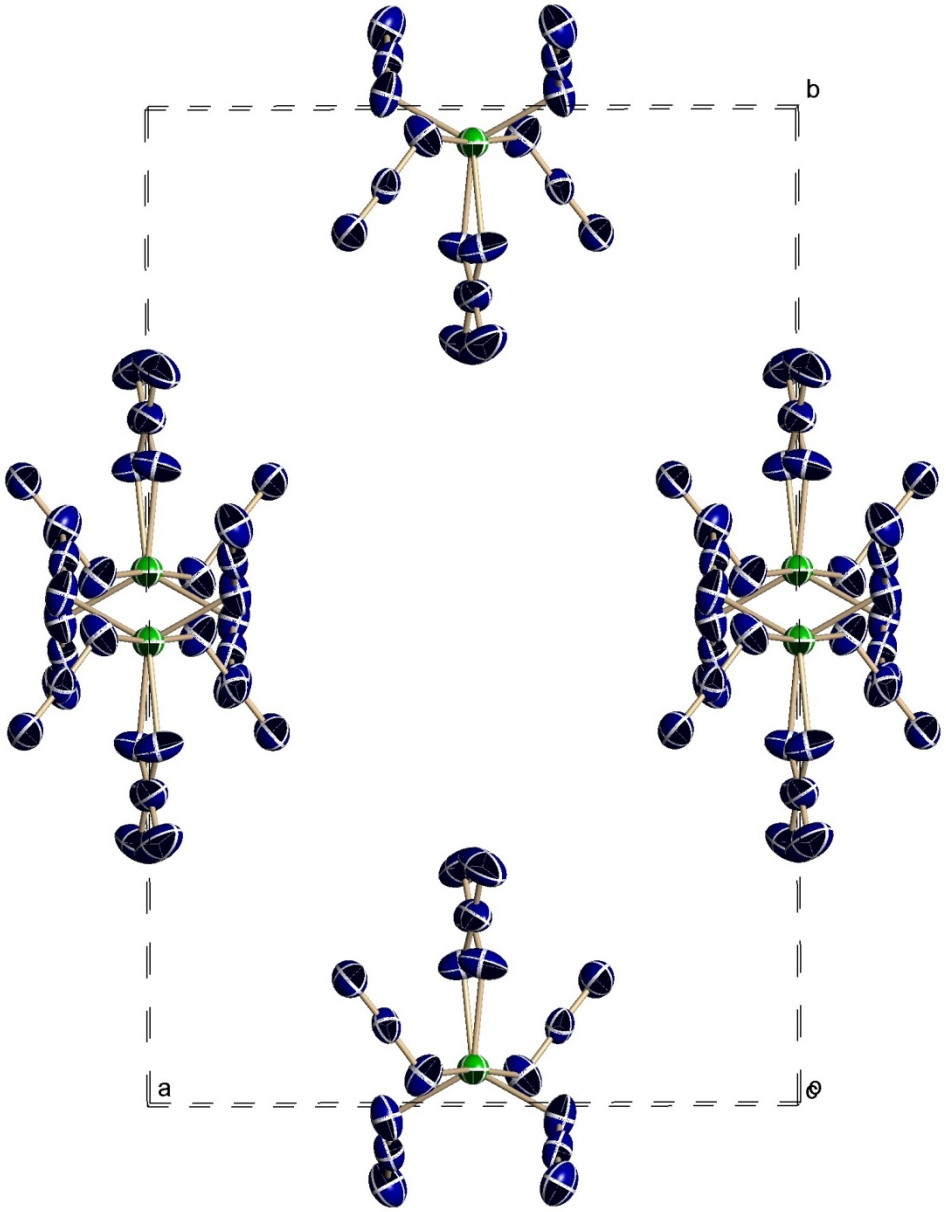

Figure S6. Asymmetric unit in the crystal structure of $[PPh_4]_3[In(N_3)_6]$. Thermal ellipsoids are drawn at the 50% probability level.

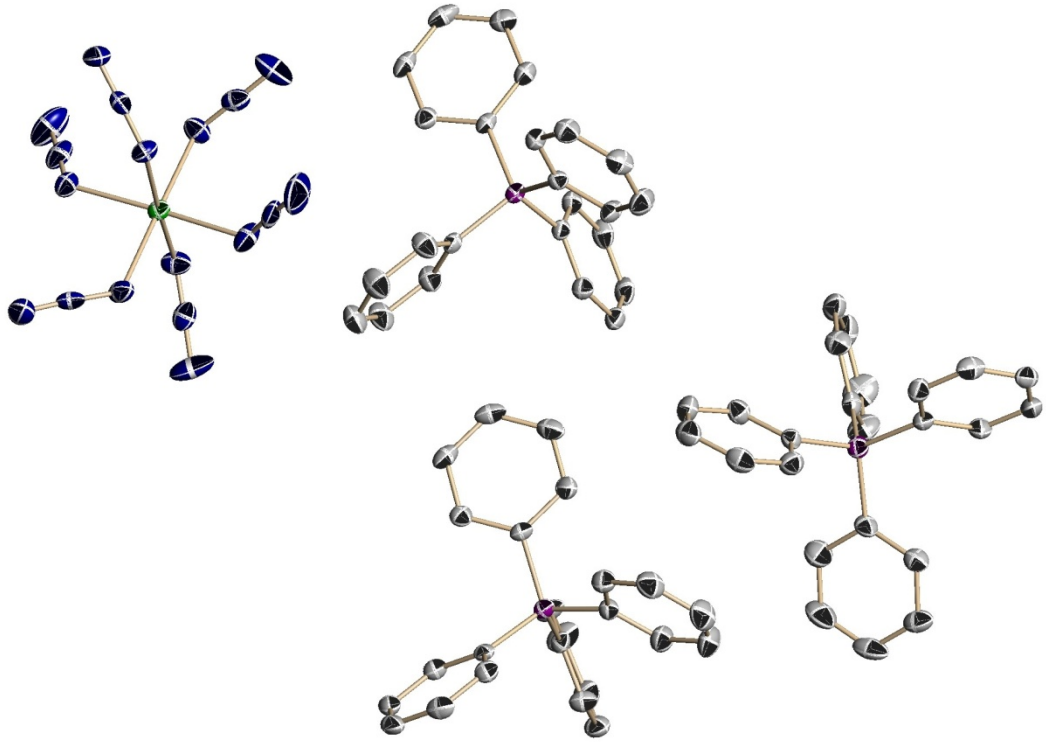

Figure S7. The unit cell of $[PPh_4]_3[In(N_3)_6]$. Thermal ellipsoids are drawn at the 50% probability level. The $[PPh_4]$ cations have been omitted.

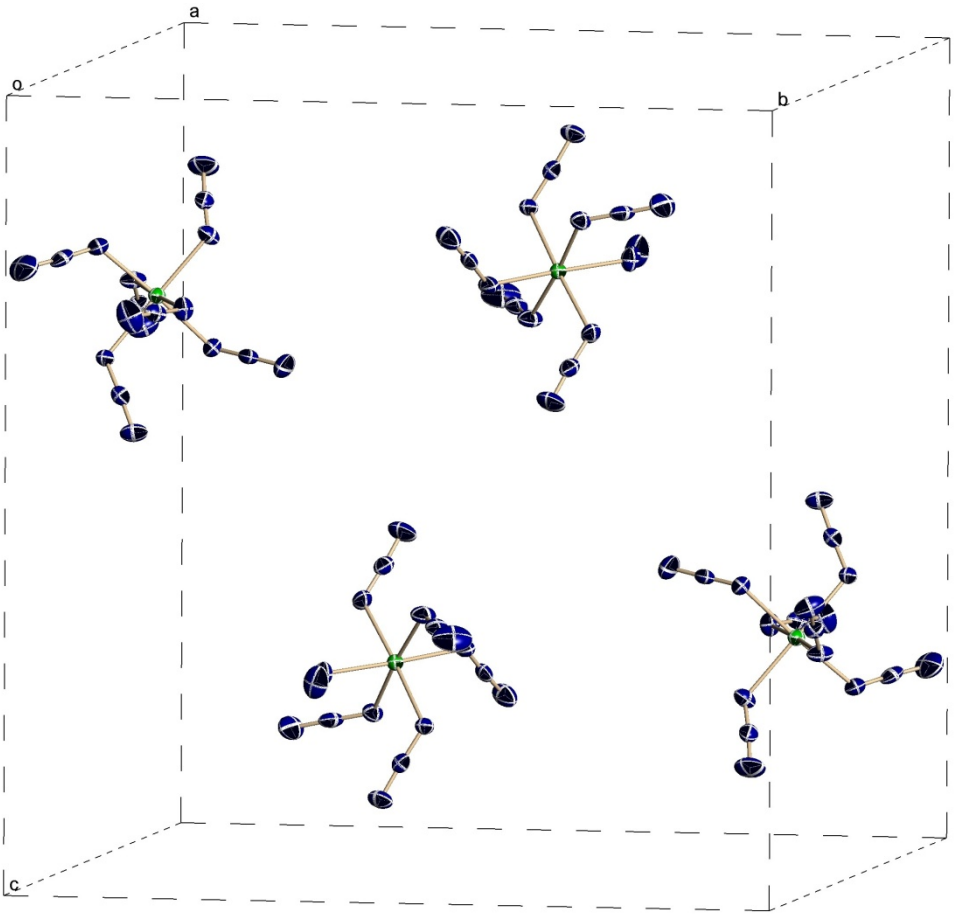

Figure S8. View along the a axis of the $[PPh_4]_3[In(N_3)_6]$ unit cell. Thermal ellipsoids are drawn at the 50% probability level. The $[PPh_4]$ cations have been omitted.

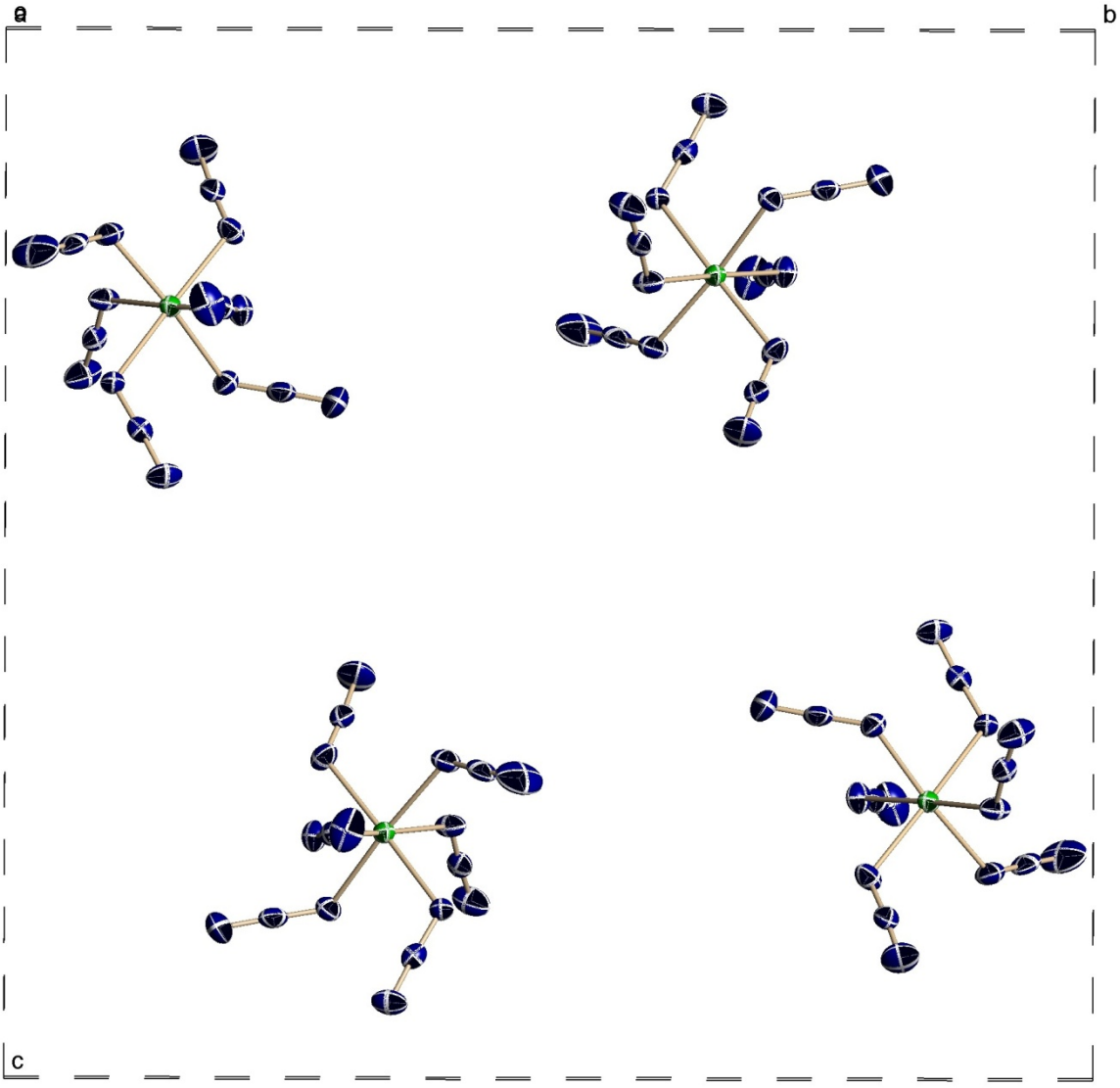

Figure S9. View along the b axis of the $[PPh_4]_3[In(N_3)_6]$ unit cell. Thermal ellipsoids are drawn at the 50% probability level. The $[PPh_4]$ cations have been omitted.

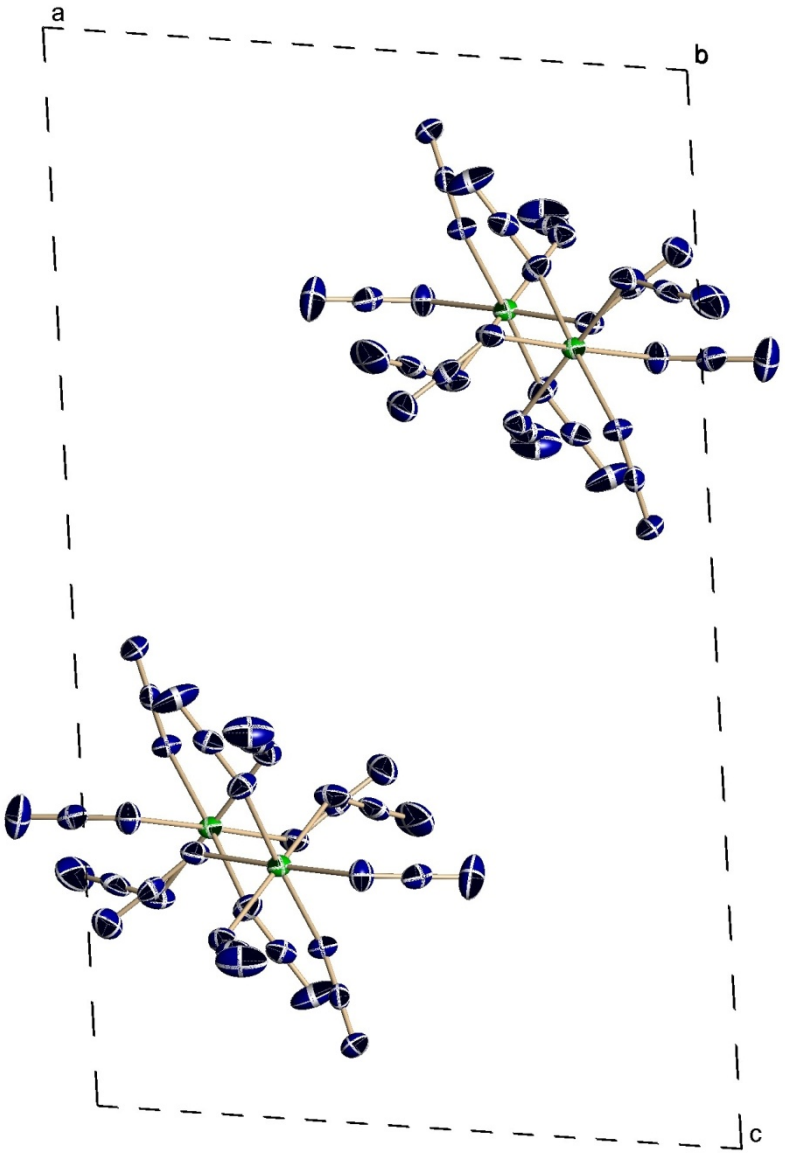

Figure S10. View along the c axis of the $[PPh_4]_3[In(N_3)_6]$ unit cell. Thermal ellipsoids are drawn at the 50% probability level. The $[PPh_4]$ cations have been omitted.

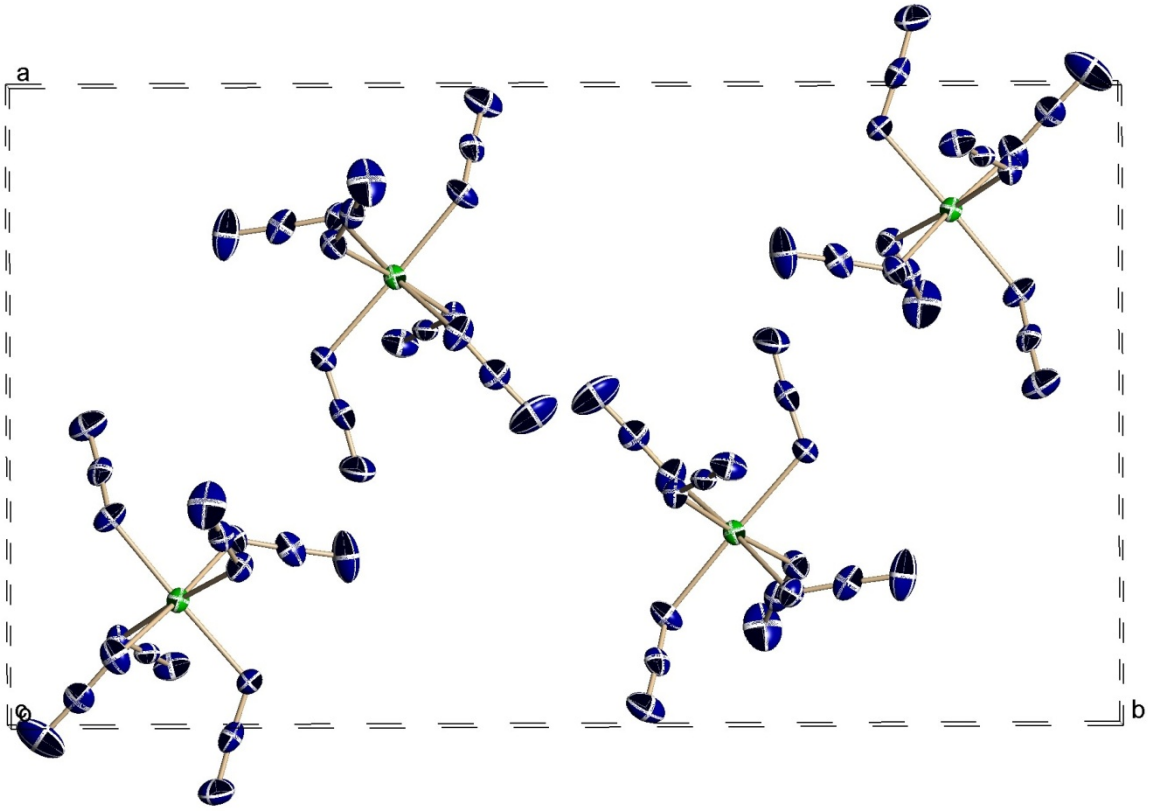

Figure S11. Asymmetric unit in the crystal structure of $[PPh_4]_3[Tl(N_3)_6]$. Thermal ellipsoids are drawn at the 50% probability level.

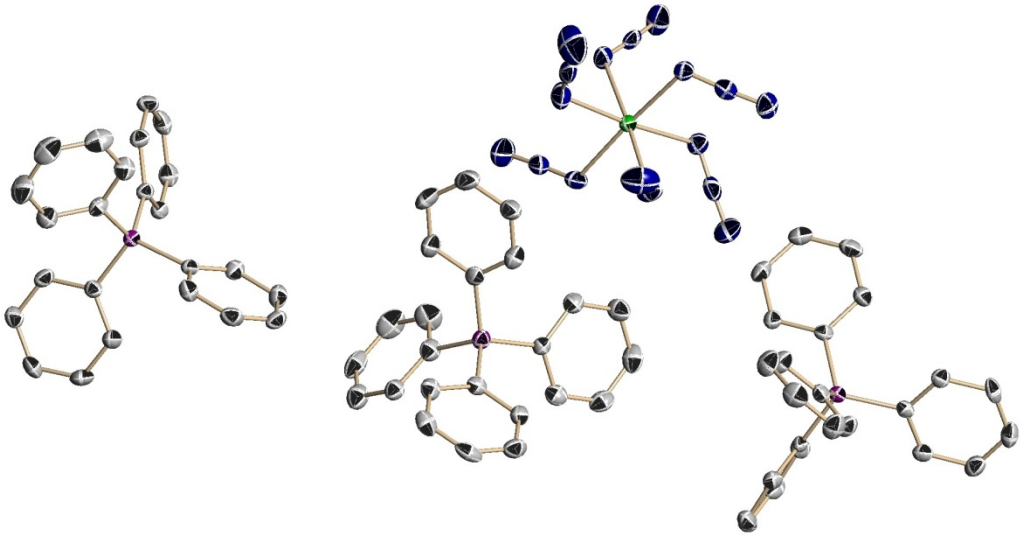

Figure S12. The unit cell of $[PPh_4]_3[Tl(N_3)_6]$. Thermal ellipsoids are drawn at the 50% probability level. The $[PPh_4]$ cations have been omitted.

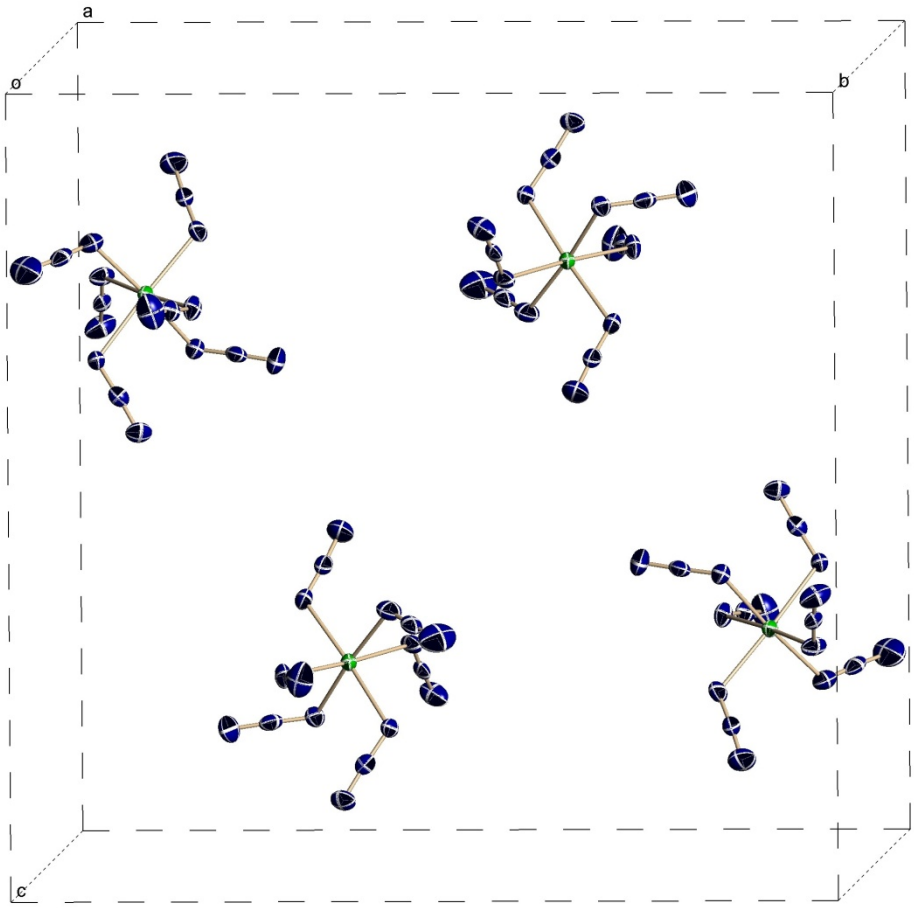

Figure S13. View along the a axis of the $[PPh_4]_3[Tl(N_3)_6]$ unit cell. Thermal ellipsoids are drawn at the 50% probability level. The $[PPh_4]$ cations have been omitted.

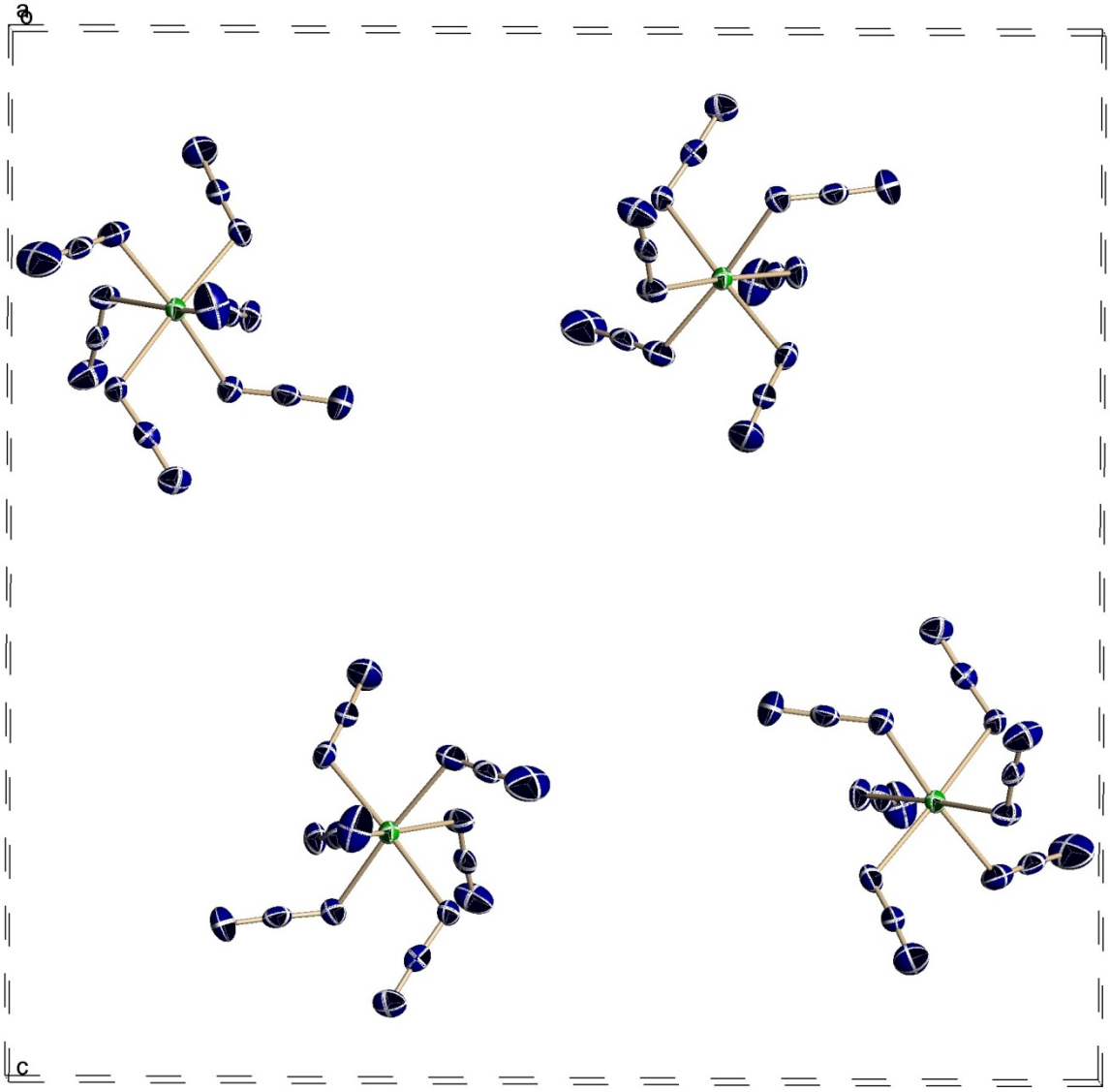

Figure S14. View along the b axis of the $[PPh_4]_3[Tl(N_3)_6]$ unit cell. Thermal ellipsoids are drawn at the 50% probability level. The $[PPh_4]$ cations have been omitted.

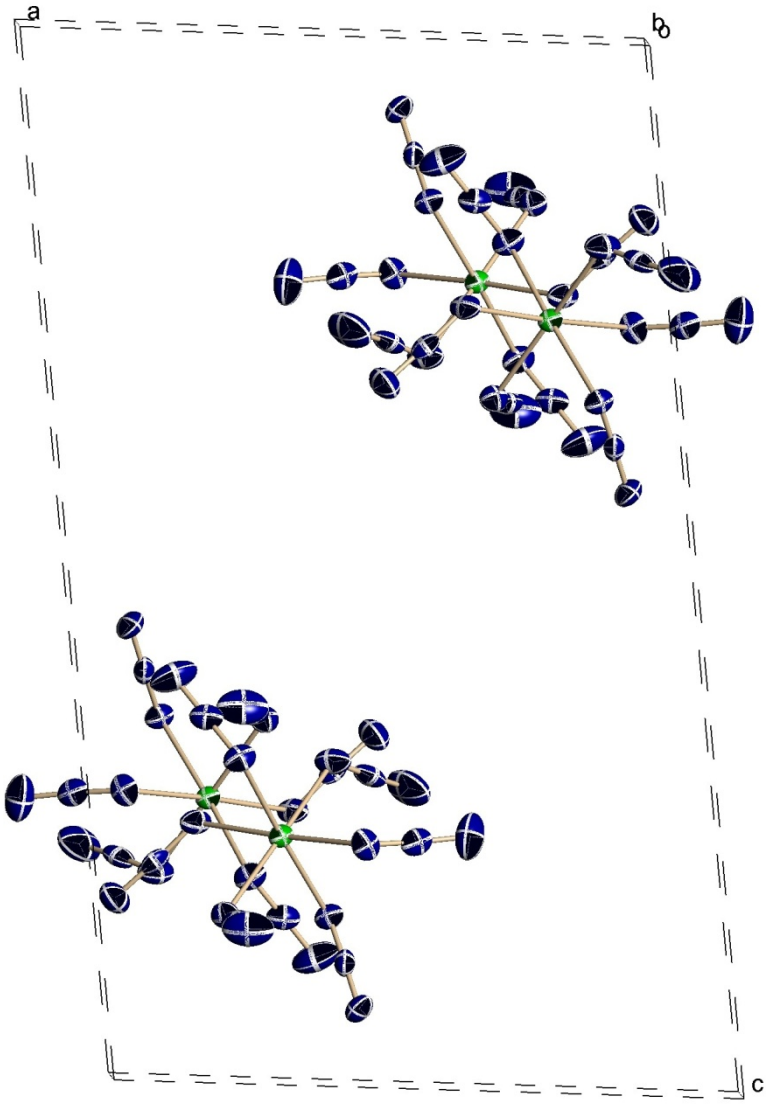

Figure S15. View along the c axis of the $[PPh_4]_3[Tl(N_3)_6]$ unit cell. Thermal ellipsoids are drawn at the 50% probability level. The $[PPh_4]$ cations have been omitted.

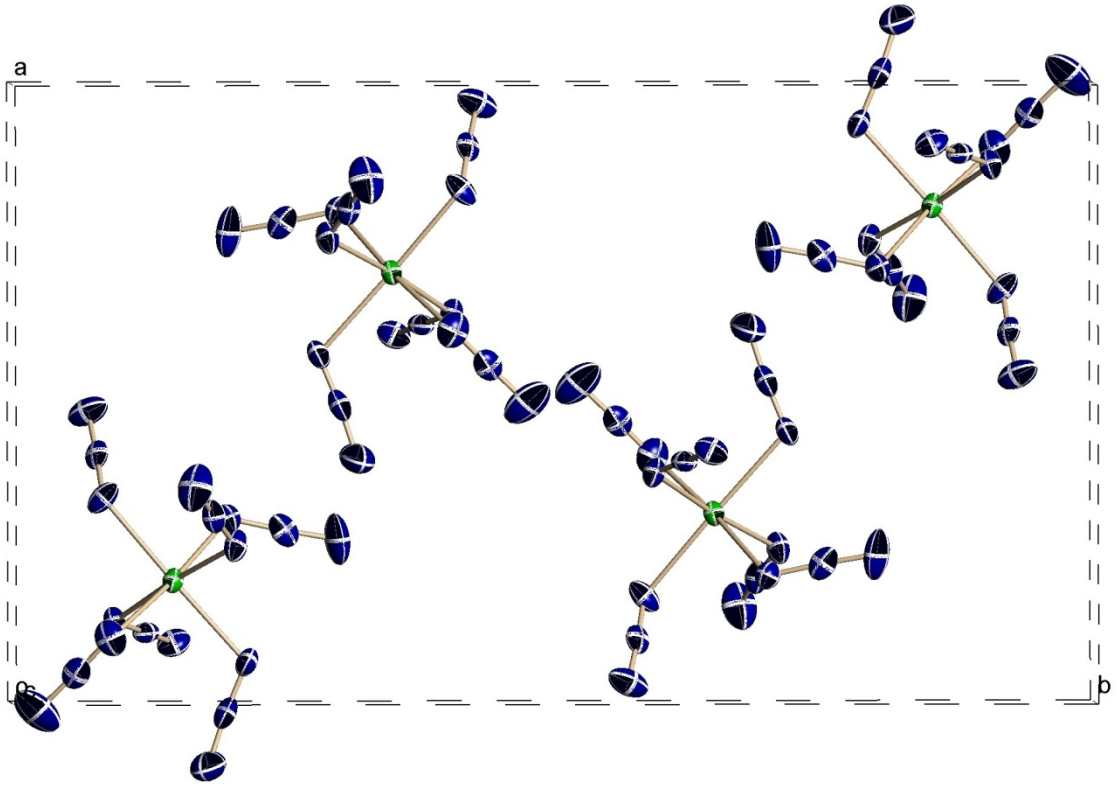

Figure S16. IR (top) and Raman (bottom) spectra of $Ga(N_3)_3$. The band marked with a dagger (†) is due to a residual amount of SO_2 solvent. Bands due to the FEP sample container are marked with an asterisk (*).

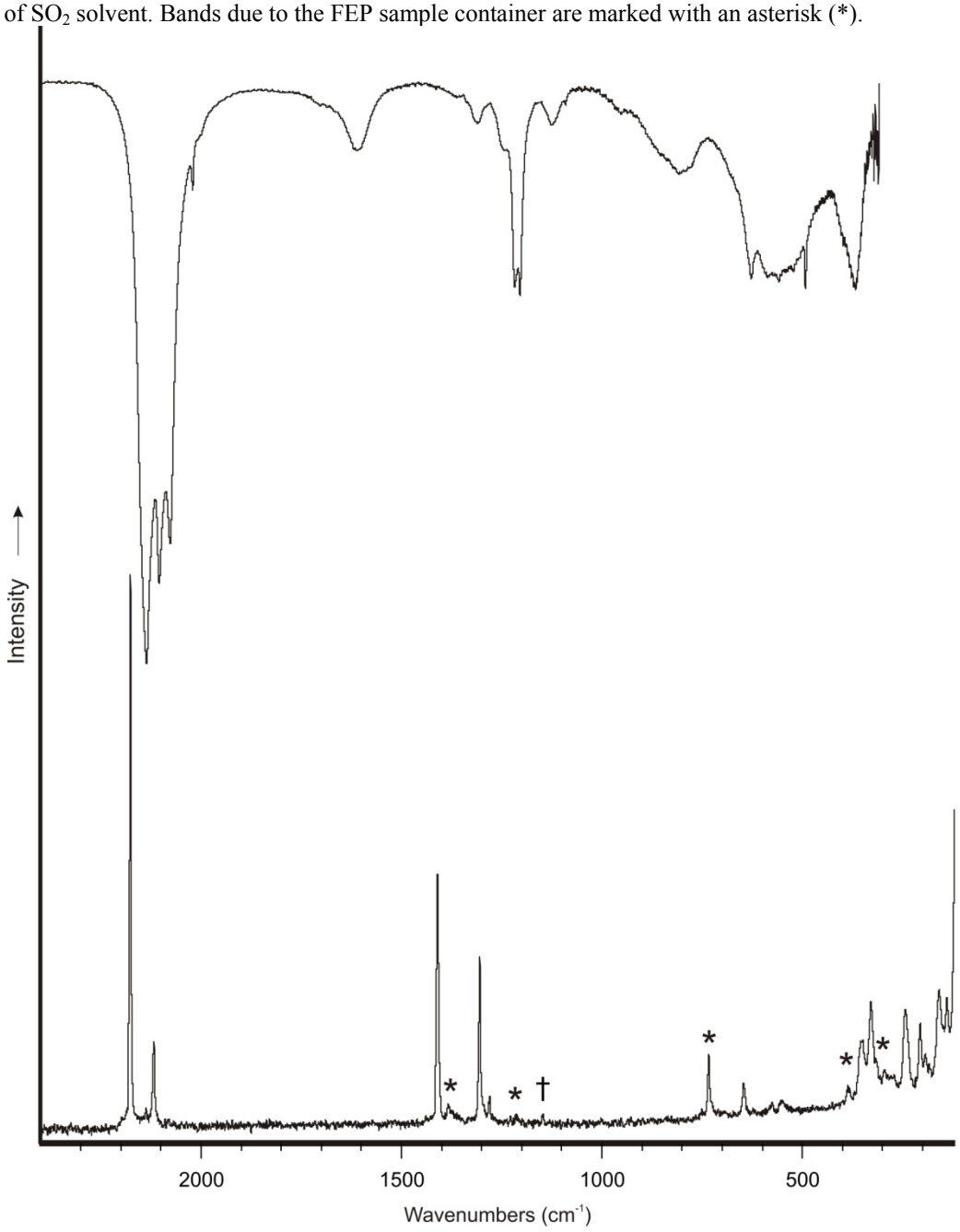

Figure S17. Raman spectrum of $In(N_3)_3$. The bands marked with a dagger (†) are due to a residual amount of SO_2 solvent. Bands due to the FEP sample container are marked with an asterisk (*).

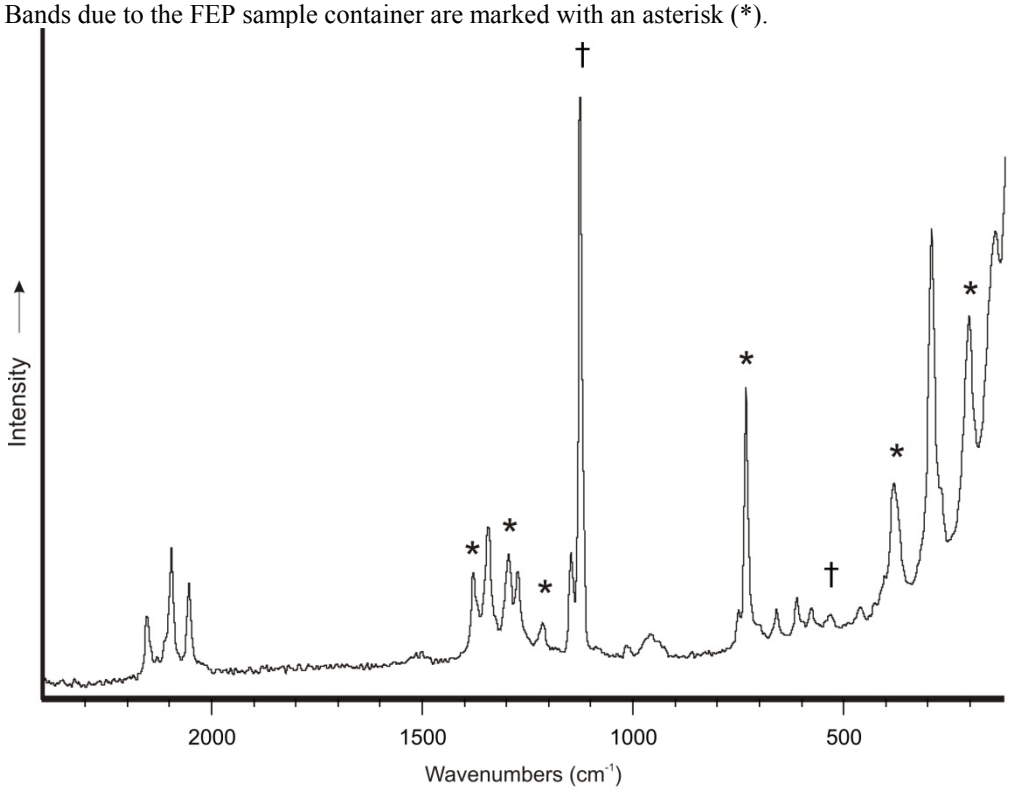

Figure S18. Raman spectrum of $Tl(N_3)_3$. The band marked with a dagger (†) is due to a residual amount of SO_2 solvent. Bands due to the FEP sample container are marked with an asterisk (*).

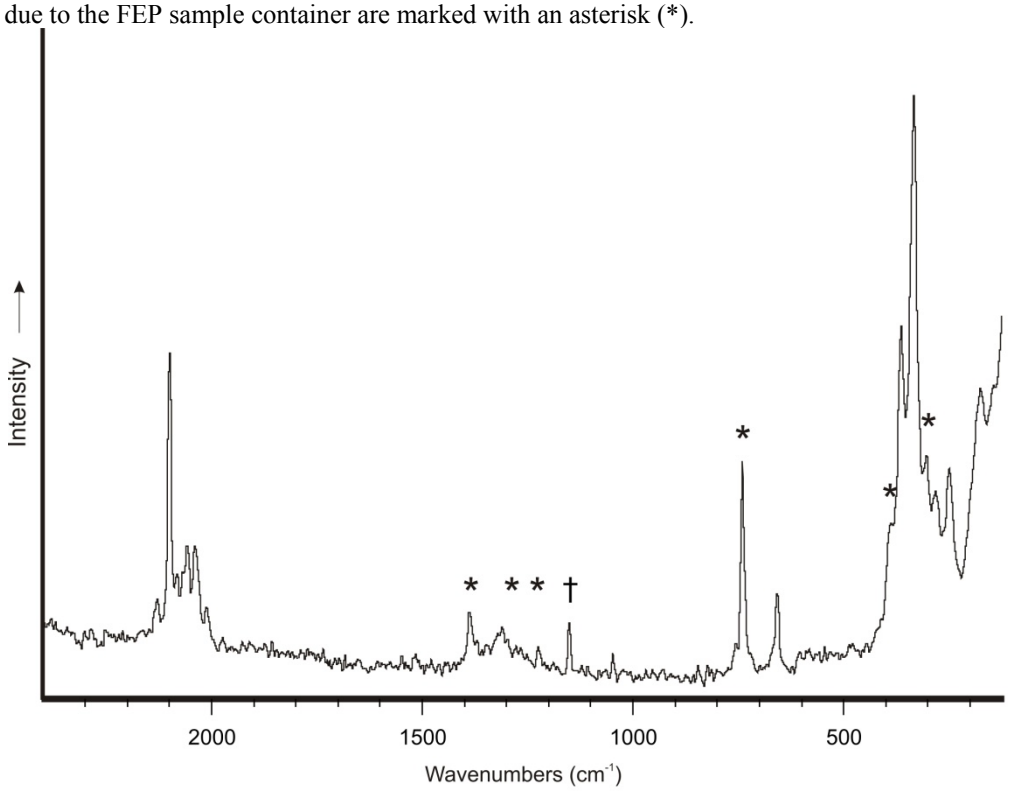

Figure S19. IR (top) and Raman (bottom) spectra of $Ga(N_3)_3 \cdot CH_3CN$. Bands marked with an asterisk (*) are due to the FEP sample container.

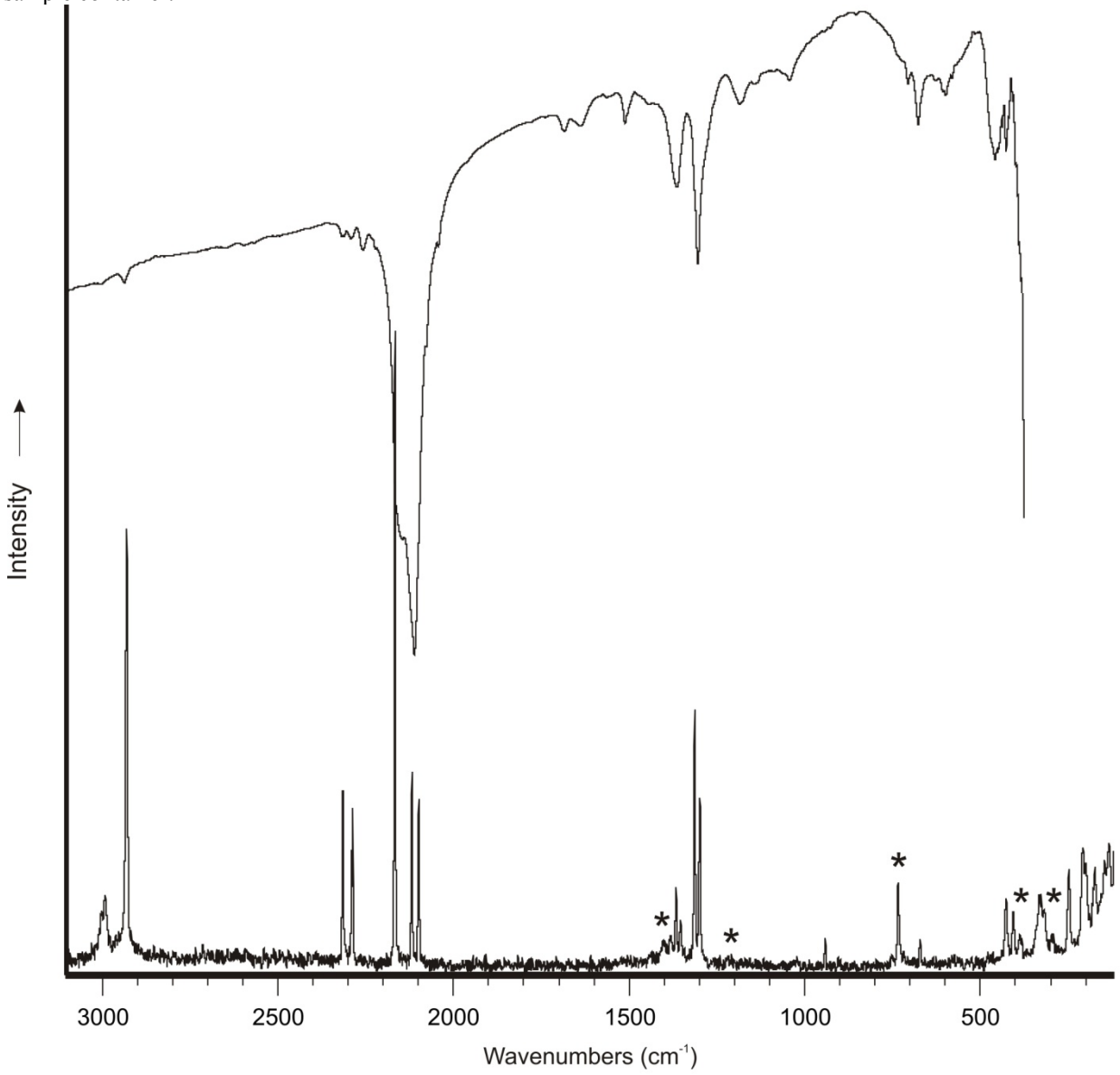

Figure S20. IR (top) and Raman (bottom) spectra of $In(N_3)_3 \cdot CH_3CN$. Bands marked with an asterisk (*) are due to the FEP sample container.

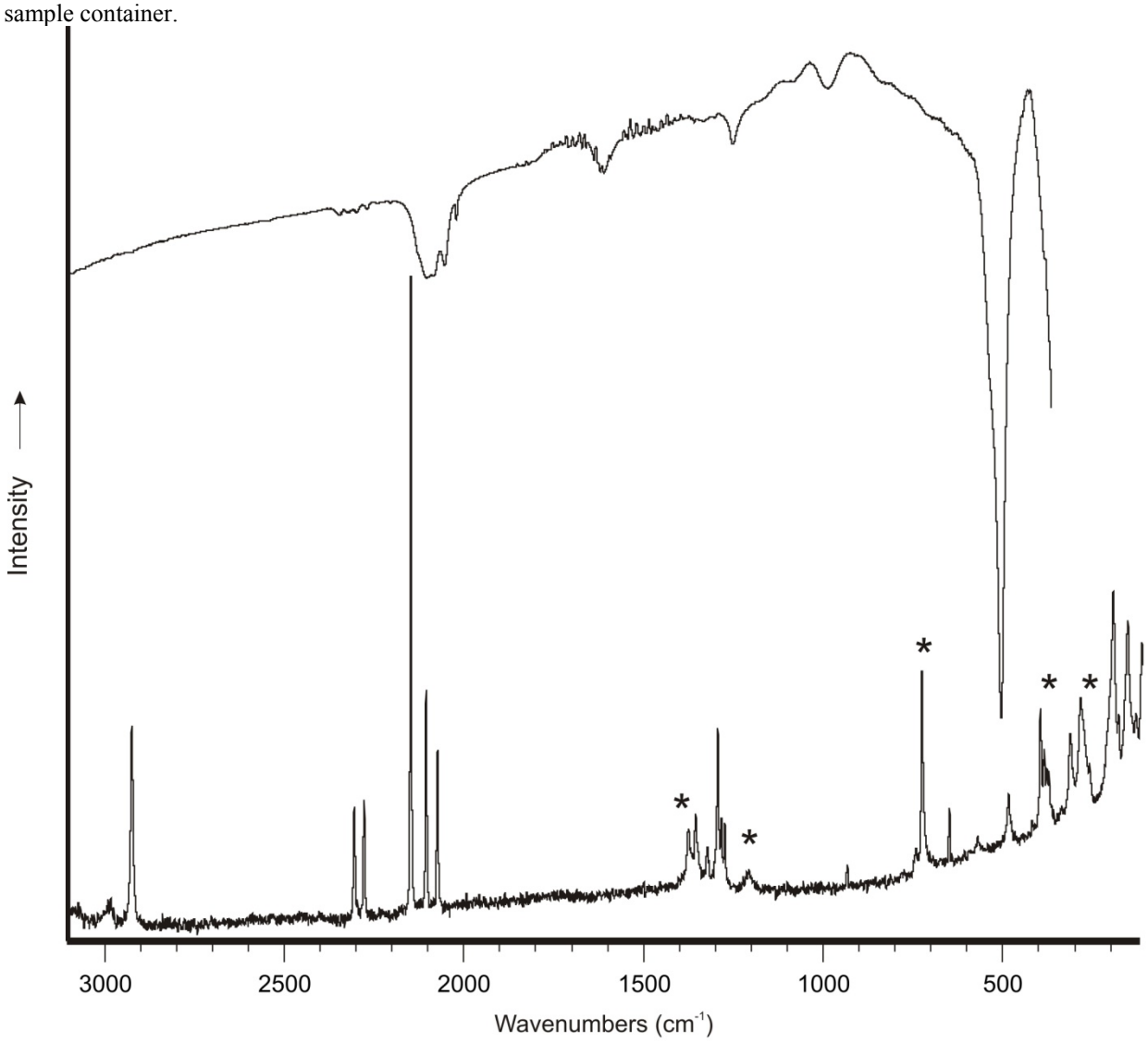

Figure S21. IR (top) and Raman (bottom) spectra of $Tl(N_3)_3 \cdot CH_3CN$. Bands marked with an asterisk (*) are due to the FEP sample container.

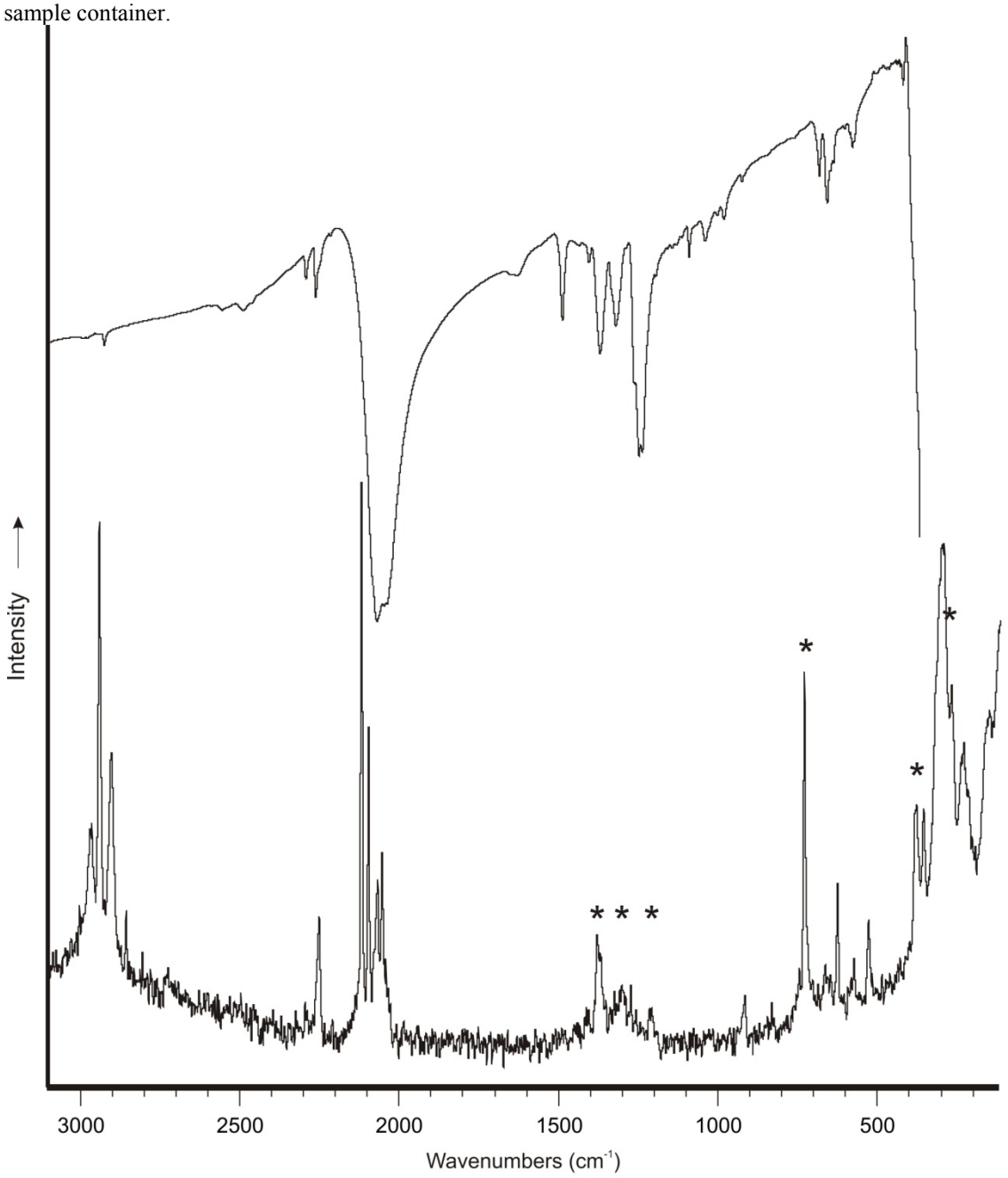

Figure S22. IR (top) and Raman (bottom) spectra of $[PPh_4]_2[Ga(N_3)_5]$. The band marked with a dagger (†) is due to an impurity of N_3^-. The bands of the $[Ga(N_3)_5]^{2-}$ anion are marked with an asterisk (*).

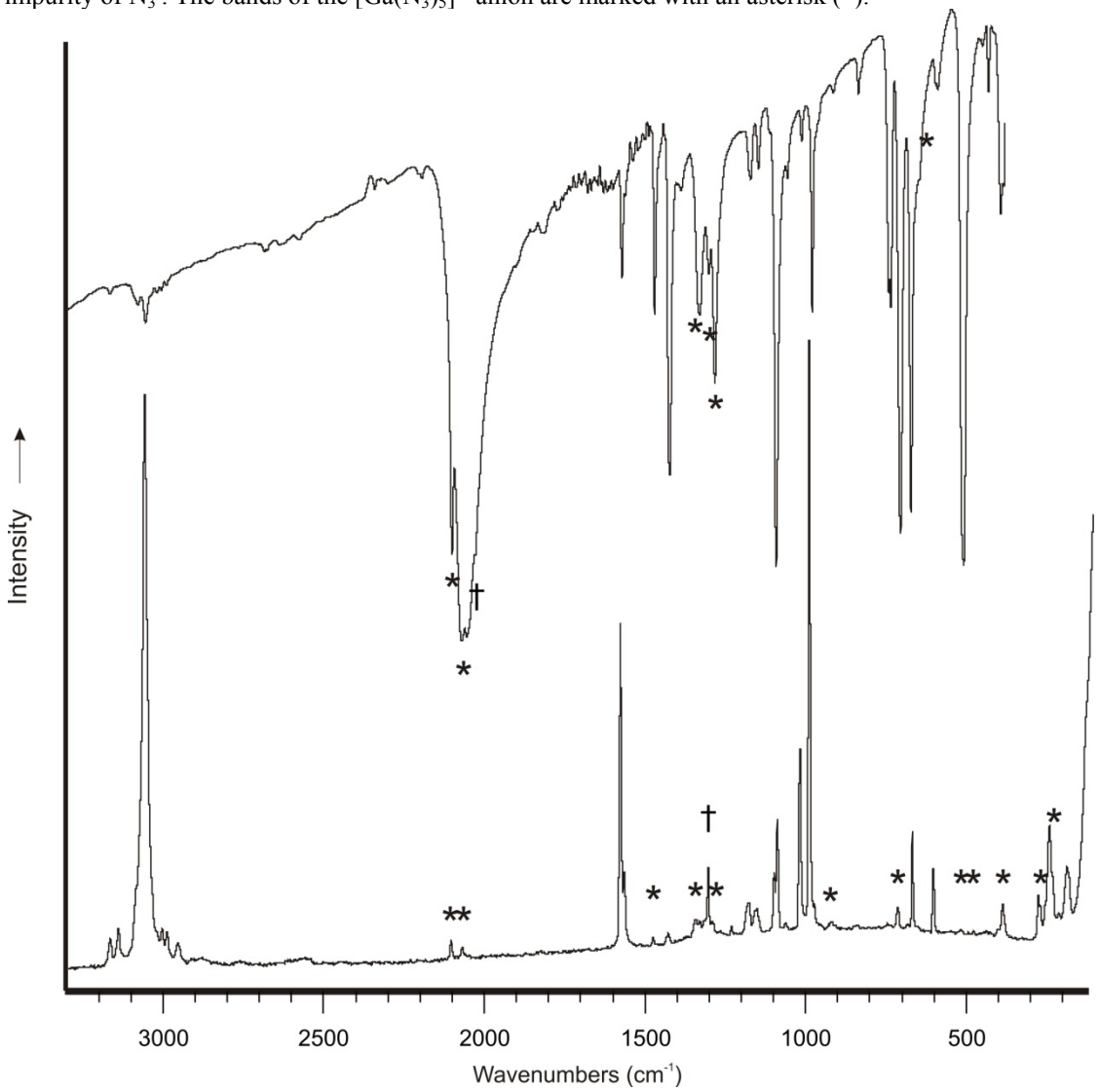

Figure S23. IR (top) and Raman (bottom) spectra of $[PPh_4]_3[In(N_3)_6]$. The band marked with a dagger (†) is due to an impurity of N_3^- and the one marked with a double dagger (‡) due to the FEP sample container. The bands of the $[In(N_3)_6]^{3-}$ anion are marked with an asterisk (*).

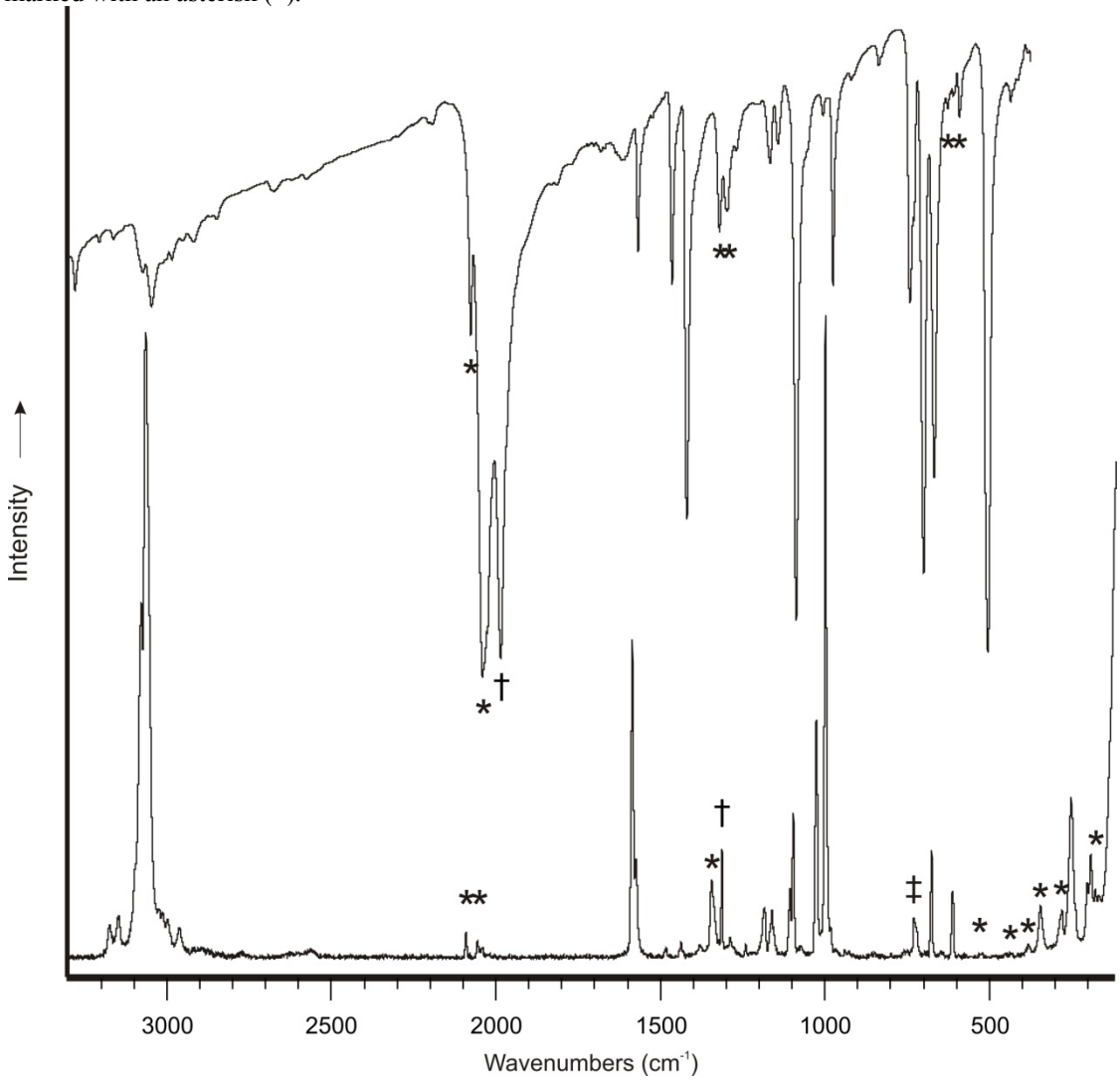

Figure S24. IR (top) and Raman (bottom) spectra of $[PPh_4]_3[Tl(N_3)_6]$. The band marked with a dagger (†) is due to an impurity of N_3^-. The bands of the $[Tl(N_3)_6]^{3-}$ anion are marked with an asterisk (*).